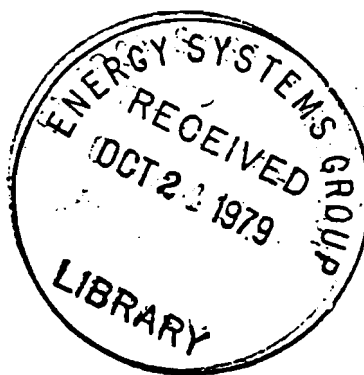


SRE FUEL ELEMENT DAMAGE

AEC Research and Development Report



ATOMICS INTERNATIONAL

A DIVISION OF NORTH AMERICAN AVIATION, INC.

LEGAL NOTICE

This report was prepared as an account of Government sponsored work. Neither the United States, nor the Commission, nor any person acting on behalf of the Commission:

A. Makes any warranty or representation, express or implied, with respect to the accuracy, completeness, or usefulness of the information contained in this report, or that the use of any information, apparatus, method, or process disclosed in this report may not infringe privately owned rights; or

B. Assumes any liabilities with respect to the use of, or for damages resulting from the use of information, apparatus, method, or process disclosed in this report.

As used in the above, "person acting on behalf of the Commission" includes any employee or contractor of the Commission to the extent that such employee or contractor prepares, handles or distributes, or provides access to, any information pursuant to his employment or contract with the Commission.

Price \$3.00
Available from the Office of Technical Services
Department of Commerce
Washington 25, D. C.

SRE FUEL ELEMENT DAMAGE

AN INTERIM REPORT

OF

THE ATOMICS INTERNATIONAL AD HOC COMMITTEE

R. L. ASHLEY

B. R. HAYWARD, JR.

R. J. BEELEY

T. L. GERSHUN

F. L. FILLMORE

~~**A. A. JARRETT**~~

W. J. HALLETT

J. G. LUNDHOLM, JR., CHAIRMAN

GENERAL EDITOR

A. A. JARRETT

(Nov 15, 1959)

ATOMICS INTERNATIONAL

**A DIVISION OF NORTH AMERICAN AVIATION, INC.
P.O. BOX 309 CANOGA PARK, CALIFORNIA**

**CONTRACT: AT(11-1)-GEN-8
ISSUED:**



DISTRIBUTION

This report has been distributed according to the category "Reactors-Power" as given in "Standard Distribution Lists for Unclassified Scientific and Technical Reports" TID-4500 (15th Ed.), August 1, 1959. Additional special distribution has been made. A total of 700 copies was printed.



CONTENTS

	Page
Abstract	xi
I. Introduction and Summary	I-1
II. The Sodium Reactor Experiment	II-A-1
A. Reactor System Design	II-A-1
1. Coolant	II-A-1
2. Moderator and Reflector Assemblies	II-A-3
3. Fuel Elements	II-A-6
4. Dummy Elements	II-A-8
5. Control Elements	II-A-8
a. Shim Regulating Elements	II-A-8
b. Safety Elements	II-A-9
6. Experimental Facilities	II-A-9
7. Reactor Vessel	II-A-9
8. Instrumentation	II-A-10
9. Shielding	II-A-11
10. Cooling System	II-A-12
a. Intermediate Heat Exchanger	II-A-14
b. Sodium Pumps	II-A-14
c. Auxiliaries	II-A-14
11. Fuel Handling	II-A-17
12. Fuel Storage Cells	II-A-17
13. Fuel Cleaning Facilities	II-A-21
14. SRE Hot Cells	II-A-21
15. Inert Gas System	II-A-21
16. Waste Disposal System	II-A-21
17. Emergency Electrical System	II-A-22
18. Reactor Building	II-A-22
19. Steam-Electric Facilities	II-A-23
B. Brief Operating History	II-B-1
1. Operating Data	II-B-1
2. Plant Performance	II-B-8
a. Fuel Element Data	II-B-8



CONTENTS

	Page
b. Sodium Components	II-B-8
c. Reactor Control and Instrumentation.	II-B-9
d. Reactor Physics Experiments	II-B-10
e. Reactor Auxiliaries	II-B-10
III. Chronology of Events	III-1
A. Run 8 (November 29, 1958 to January 29, 1959)	III-1
B. Run 9 (February 14, 1959 to February 26, 1959)	III-3
C. Run 10 (March 6, 1959 to March 7, 1959)	III-4
D. Run 11 (March 16, 1959 to April 6, 1959)	III-4
E. Run 12 (May 14, 1959 to May 24, 1959).	III-5
F. Run 13 (May 27, 1959 to June 3, 1959)	III-6
1. Initial Operation	III-6
2. Tetralin Leak	III-7
3. Wash Cell Incident.	III-7
4. Stripping Operation	III-8
G. Run 14 (July 12, 1959 to July 26, 1959).	III-8
1. Temperature Spread	III-8
2. High Air Activity	III-10
3. Reactor Excursion.	III-11
4. Pressure Effect on Reactivity	III-13
5. Operation on Airblast Heat Exchanger	III-13
6. Fuel Temperatures	III-16
7. Reactor Shutdown	III-17
H. Events Following the End of run 14	III-18
1. Fuel Examination	III-18
2. Fuel Handling Cask Operations	III-18
3. Fuel Canning	III-19
4. The Sodium System	III-23
5. Tests and Observations	III-23
6. Recovery Equipment	III-23

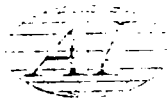
CONTENTS

	Page
7. Improved Fuel Washing Procedures	III-23
8. Preparation of Charts and Data	III-23
IV. Data and Evaluation	IV-A-1
A. Fuel Technology	IV-A-1
1. Uranium Metallurgy	IV-A-1
2. Fuel-Clad Compatibility	IV-A-2
3. Fuel Operating Limits	IV-A-5
4. Fuel Element History	IV-A-7
5. Fuel Element Central Temperatures	IV-A-10
6. Effects of Contamination During Run 14.	IV-A-16
a. Fuel Element Visual Examinations	IV-A-16
b. Cladding Analyses	IV-A-20
c. Wire Wrap Chemical Analysis	IV-A-28
d. Dimensions of Fuel Specimens	IV-A-28
e. Analyses of Foreign Material from Fuel Element	IV-A-28
f. Analytical Calculation of Cladding Temperatures	IV-A-29
7. Mechanisms of Cladding Failure	IV-A-32
B. Reactor Coolant Contamination	IV-B-1
1. Potential Contaminants	IV-B-1
a. Tetralin	IV-B-1
b. Oxygen	IV-B-3
2. Indications of Contamination During Runs 8 and 13	IV-B-4
3. Nitrogen Effects	IV-B-8
4. Indications of Contamination During Run 14	IV-B-10
a. Temperature Effects	IV-B-10
b. Tetralin Leakage	IV-B-11
5. Hydrogen Effects	IV-B-13
6. Carbon Effects	IV-B-13
7. Oxygen Effects	IV-B-14
8. Mechanisms of Restrictions of Coolant Passages	IV-B-14
C. Radiological Considerations	IV-C-1
1. Primary Sodium Activity	IV-C-1



CONTENTS

	Page
a. Activity Levels of Irradiated Sodium	IV-C-1
b. Analytical Methods	IV-C-1
c. Analyses	IV-C-2
d. Fission Products in NaK Bond	IV-C-5
e. Uranium and Plutonium	IV-C-7
f. Weight of Fission Products	IV-C-8
g. Conclusions	IV-C-8
2. Radioactivity from Primary System Components . . .	IV-C-9
a. Main Primary Gallery	IV-C-9
b. Main Primary Gallery Atmosphere	IV-C-11
c. Primary Cold Trap Radioactivity	IV-C-11
3. Reactor Cover Gas Activity	IV-C-12
4. Activity in Gaseous Storage Tanks	IV-C-15
5. Radioactivity in High Bay Area	IV-C-16
a. Airborne Activity	IV-C-16
b. Radiation Levels	IV-C-21
c. Reactor Building Contamination	IV-C-22
6. Stack Effluent Activity	IV-C-24
7. Environmental Contamination	IV-C-25
D. Reactor Physics	IV-D-1
1. Potential Mechanisms of Reactivity Changes . . .	IV-D-1
a. Dropping Part of a Fuel Cluster	IV-D-1
b. Doppler Coefficient	IV-D-1
c. Graphite Coefficient	IV-D-3
d. Void Coefficient	IV-D-3
e. Gas Bubbles in the Sodium	IV-D-4
f. Hydrogenous Plug in the Reactor Core	IV-D-4
g. Sodium in a Moderator Can	IV-D-4
h. Nitrogen Gas in Moderator Cans	IV-D-5



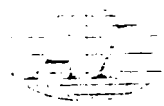
CONTENTS

	Page
2. Measured and Calculated Effects	IV-D-5
a. Xenon	IV-D-5
b. Temperature	IV-D-8
c. Cover Gas Pressure	IV-D-8
3. Run 13.	IV-D-8
4. Run 14.	IV-D-12
5. Power Excursion	IV-D-16
a. Reactivity	IV-D-16
b. Power Release	IV-D-20
V. Tentative Conclusions	V-1
A. Cause of Fuel Element Damage	V-1
B. Time of Element Failure	V-2
C. Effect of the High Temperature Runs	V-2
D. Reactivity Changes	V-3
E. Condition of Reactor and Primary System	V-3
F. Containment of Radioactivity	V-4
References	R-1



TABLES

	Page
III-1. Reactor Operating Conditions, Run 8	III-1
III-2. Reactor Operating Conditions, Run 14 (July 12, 1959) . .	III-9
III-3. Reactor Operating Conditions, Run 14 (July 13, 1959) . .	III-11
III-4. Primary Sodium Plugging Temperatures, Run 14. . . .	III-15
III-5. Damaged Fuel Elements	III-20
III-6. Fuel Element Status	III-21
III-7. Summary of Fuel Element Status	III-22
IV-A-1. Pertinent Properties of Uranium and Thorium	IV-A-1
IV-A-2. Eutectic Compositions of Uranium and Thorium	IV-A-4
IV-A-3. History of Fuel Elements in SRE During Run 14	IV-A-8
IV-A-4. Hot Cell Examinations of SRE Fuel	IV-A-13
IV-A-5. SRE Fuel Temperatures	IV-A-15
IV-A-6. Analyses of Materials from Element in Channel 55 . . .	IV-A-27
IV-A-7. Dimensions of Fuel Slugs from Element in Channel 12 . .	IV-A-29
IV-A-8. Moderator Temperature Measurements	IV-A-31
IV-B-1. Exposure Time for Carburization of Stainless Steel . . .	IV-B-2
IV-B-2. Fuel-Channel Exit-Temperature Spread	IV-B-6
IV-C-1. Radioisotopic Content of Primary Sodium Samples . . .	IV-C-3
IV-C-2. Decay of Sodium Sample 8	IV-C-4
IV-C-3. Isotopic Content of Sodium Sample 8	IV-C-4
IV-C-4. Calculated Release Fraction of Fission Products	IV-C-5
IV-C-5. Fission Product Activity in NaK	IV-C-6
IV-C-6. Radiation Levels in Gamma Facility	IV-C-10
IV-C-7. Radiation Levels from the Cold Trap	IV-C-12
IV-C-8. Activity History of the Reactor Cover Gas	IV-C-14
IV-C-9. Decay of Reactor Cover Gas Sample	IV-C-15
IV-C-10. Radioactive Concentrations in Gas Decay Tanks	IV-C-18
IV-C-11. Environmental Water Activity	IV-C-28
IV-C-12. Environmental Air Activity	IV-C-29
IV-D-1. Mechanisms of Reactivity Changes	IV-D-10



FIGURES

	Page
II-A-1 Cutaway View of SRE Reactor	II-A-2
II-A-2 Moderator Assembly	II-A-4
II-A-3 Moderator and Reflector Can Types	II-A-5
II-A-4 Typical Fuel Elements	II-A-6
II-A-5 Locations of Fuel Elements in the Core	II-A-7
II-A-6 Cooling System	II-A-13
II-A-7 Main Primary Sodium Pump	II-A-15
II-A-8 Pump Shaft Freeze Seal	II-A-15
II-A-9 Fuel Handling Cask	II-A-18
II-A-10 Cutaway View of Fuel Handling Cask	II-A-19
II-A-11 Moderator Handling Cask	II-A-20
II-B-1 Operating History of the SRE (FY 1957)	II-B-2
II-B-2 Operating History of the SRE (FY 1958)	II-B-3
II-B-3 Operating History of the SRE (FY 1959)	II-B-4
II-B-4 Operating History of the SRE (FY 1960)	II-B-5
II-B-5 Scram History of the SRE (FY 1957)	II-B-6
II-B-6 Scram History of the SRE (FY 1958)	II-B-6
II-B-7 Scram History of the SRE (FY 1959)	II-B-7
IV-A-1 Radiation Effects on SRE Fuel	IV-A-3
IV-A-2 Thermocouple Distribution in SRE Fuel	IV-A-6
IV-A-3 Temperature Distribution in SRE Fuel	IV-A-7
IV-A-4 Location of Damaged Elements in the Core	IV-A-9
IV-A-5 Temperature History of Element in Channel 55	IV-A-11
IV-A-6 Bottom of Damaged Element in Channel 55	IV-A-17
IV-A-7 Midsection of Damaged Element in Channel 55	IV-A-17
IV-A-8 Top of Damaged Element in Channel 55	IV-A-18
IV-A-9 Identification of Fuel Rods from Element in Channel 55	IV-A-19
IV-A-10 Small Piece of Cladding I from Element in Channel 55	IV-A-20
IV-A-11 Small Piece of Cladding II from Element in Channel 55	IV-A-21
IV-A-12 Location of Recovered Slugs in Channel 12	IV-A-23
IV-A-13 Edge of Cladding Rupture	IV-A-24
IV-A-14 Streaming Reaction I on Cladding from Element in Channel 12	IV-A-25



FIGURES

	Page
IV-A-15 Streaming Reaction II on Cladding from Element in Channel 12	IV-A-26
IV-A-16 End of Fuel Slug from Element in Channel 12	IV-A-30
IV-A-17 Temperature Profiles in Moderator and Fuel	IV-A-33
IV-B-1 Log Mean Temperature Difference and Power During Run 13	IV-B-8
IV-C-1 Radioactive Gas Decay Tank Activities	IV-C-17
IV-C-2 High Bay Area Airborne Activity	IV-C-20
IV-C-3 Environmental Monitoring Stations	IV-C-26
IV-C-4 Environmental Soil and Vegetation Activity	IV-C-27
IV-D-1 Reactivity Changes by Partition of Fuel Cluster	IV-D-2
IV-D-2 Reactivity Absorbed by Xenon after Shutdown	IV-D-6
IV-D-3 Reactivity Absorbed by Xenon after Step Changes in Power	IV-D-7
IV-D-4 Reactor Operating Conditions During Run 13	IV-D-9
IV-D-5a Reactor Operating Conditions During Run 14	IV-D-13
IV-D-5b Reactor Operating Conditions During Run 14	IV-D-14
IV-D-6 Machine Calculation I of the Power Excursion	IV-D-17
IV-D-7 Machine Calculation II of the Power Excursion	IV-D-18
IV-D-8 Machine Calculation III of the Power Excursion	IV-D-19

ABSTRACT

During the course of power run 14 on the Sodium Reactor Experiment (SRE) at low power, the temperature difference among various fuel channels was found to be undesirably high. Normal operating practices did not succeed in reducing this temperature difference to acceptable values and on July 26, 1959, the run was terminated. A series of fuel element inspections was begun to ascertain the cause of these circumstances, and several fuel elements were discovered to have suffered substantial damage. On July 29, 1959, an Ad Hoc Committee was appointed by Atomics International to assist in the analysis of the existing situation in the reactor and the determination of its origin.

During the three-month period since the termination of power run 14, there has been a very active program of investigation. The data accumulated during the operation of the SRE have been re-examined and evaluated. Metallurgical examination has been made of a few samples of the fuel and other components of the reactor where possible. Some chemical analysis has been made of the coolant and its contaminants. Radiochemical analyses have been made of the coolant and gaseous activity. Reactivity effects have been investigated. Some experimental programs have been initiated to examine mechanisms of damage and potential deleterious effects on the reactor system.

Tentative conclusions, based on data obtained to date by the current investigation into the causes of the fuel element damage, maybe summarized as follows: (1) The fuel cladding failed as a result of the formation of low-melting iron-uranium alloy which was produced because of partial blockage of some of the coolant passages and local overheating of the fuel elements. Coolant channel blockage was initiated by accumulation of the decomposition products of tetralin which had leaked into the primary system. Sodium oxide and sodium hydride may have contributed to this situation. (2) The high temperature runs on SRE bear no relation to the cladding failure of run 14. (3) While several possible explanations have been suggested for the reactivity changes incurred during run 14, no definitive conclusions are as yet available. (4) The extent of possible surface damage to the components of the primary system by carburization, nitriding or hydriding is not yet known. It is anticipated, however, that damage has been sustained by fuel cladding (known), moderator cans (probable), and the intermediate heat exchanger (just possible). (5) In spite of the cladding failure to at least 11 of the fuel elements, no radiological hazard was present to the reactor environs.

I. INTRODUCTION AND SUMMARY

During the course of power run 14 on the Sodium Reactor Experiment (SRE) at low power, the temperature difference among various fuel channels was found to be undesirably high. Normal operating practices did not succeed in reducing this temperature difference to acceptable values and on July 26, 1959, the run was terminated. A series of fuel element inspections was begun to ascertain the cause of these circumstances, and several fuel elements were discovered to have suffered substantial damage.

On July 29, 1959, an Ad Hoc Committee was appointed to:

- 1) Assist in the analysis of the existing situation in the reactor and the determination of its origin;
- 2) Review and advise on steps taken to remedy the situation and bring the reactor back into operation;
- 3) Recommend any necessary changes in operating procedures or the reactor system to prevent the occurrence of a similar situation.

This document is an interim Committee report on the origin, the nature, and the consequences of the damage to the SRE fuel, based on activities, data gathered, and evaluations performed to October 19, 1959.

For the reader who is not familiar with the SRE, the report begins with a brief description and operating history of the reactor.

The chronology of events begins in December 1958, because certain happenings at that time have a direct relation to similar events which occurred at the end of run 13 and during run 14. Most of the types of events which occurred during power run 14 had been observed, evaluated, and corrected by the SRE Operations Group during the previous two years of successful operation of the SRE. The Ad Hoc Committee has selected only those items for the chronology of events from the operating history of the SRE which are pertinent to an understanding of the fuel element damage which was observed at the termination of power run 14.

During the three-month period since the termination of power run 14, there has been a very active program of investigation. The data accumulated during the operation of the SRE have been re-examined and evaluated. Metallurgical



examination has been made of a few samples of the fuel and other components of the reactor where possible. Some chemical analysis has been made of the coolant and its contaminants. Radiochemical analyses have been made of the coolant and gaseous activity. Reactivity effects have been investigated. Some experimental programs have been initiated to examine mechanisms of damage and potential deleterious effects on the reactor system. It would be impractical to include in this report all of the data and information gathered and analyzed. Furthermore, removal of components from the reactor, data gathering and analysis, and experiments to evaluate effects and consequences are still in progress. Therefore, the Committee has selected only a portion of the data accumulated to this time for this report.

Tentative conclusions, based on data obtained to date by the current investigation into the causes of the fuel element damage, may be summarized as follows:

- 1) The fuel cladding failed as a result of the formation of low-melting iron-uranium alloy which was produced because of partial blockage of some of the coolant passages and local overheating of the fuel elements. Coolant channel blockage was initiated by accumulation of the decomposition products of tetralin which had leaked into the primary system. Sodium oxide and sodium hydride may have contributed to this situation.
- 2) The high temperature runs on SRE bear no relation to the cladding failure of run 14.
- 3) While several possible explanations have been suggested for the reactivity changes incurred during run 14, no definitive conclusions are as yet available.
- 4) The extent of possible surface damage to the components of the primary system by carburization, nitriding or hydriding is not yet known. It is anticipated, however, that damage has been sustained by fuel cladding (known), moderator cans (probable), and the intermediate heat exchanger (just possible).
- 5) In spite of the cladding failure to at least 11 of the fuel elements, no radiological hazard was present to the reactor environs.

The investigation into the causes and effects of the fuel element damage in the SRE is still underway. At the present time all of the fuel has been removed from the core with the exception of two elements which are stuck in their process channels* and the lower sections of ten parted elements. Examinations are continuing into the condition of the primary system, the sodium coolant, and the metallurgical state of the parted fuel elements, moderator cans, and other components of the reactor system.

* Unless otherwise noted, "channel" refers to reactor core channel. Storage channels are always noted as such in this report. When space demands in tables and figures, core channels are identified only by "R-"; thus, R-57 would be core channel 57.

II. THE SODIUM REACTOR EXPERIMENT

A. REACTOR SYSTEM DESIGN

The following brief description of the SRE is intended only to provide the necessary background for this report. Additional details may be found in reference 1.

The SRE was designed and constructed by Atomics International, a division of North American Aviation, Inc., as part of a joint program with the Atomic Energy Commission to develop a sodium-cooled, graphite moderated, thermal power reactor for civilian application. The Southern California Edison Company installed and is operating the steam electric power generating plant utilizing heat from the SRE.

The SRE is a thermal reactor designed as a flexible developmental facility. The reactor was built as a development tool with emphasis on investigation of fuel materials. The sodium systems incorporate the use of conventional equipment to the maximum; e. g. the sodium pumps are modified hot oil pumps.

The reactor, Figure II-A-1, is cooled by liquid sodium in the primary loop. Induced Na^{24} activity in the primary loops introduces the need for an intermediate heat exchanger in which reactor heat is transferred to the secondary loop containing nonradioactive sodium. The secondary system can dissipate reactor heat either in an airblast heat exchanger or in the steam generator of the Southern California Edison Company's installation. The steam generator is normally used.

1. Coolant

Reactor coolant flow is single pass, with sodium flowing up through the core and collecting above it in a top pool. Over the top pool helium, as a blanket gas is maintained at approximately 3 psig. This pressure prevents cavitation in the suction of circulating pumps which draw heated sodium from the reactor top pool and force it through the heat transfer apparatus. The system pressure drop is about 15 psi at rated flow of 1080 gpm.

High-temperature characteristics of sodium are exploited by utilizing a ΔT of about 450°F across the reactor and heat exchangers. The design outlet temperature is 960°F.

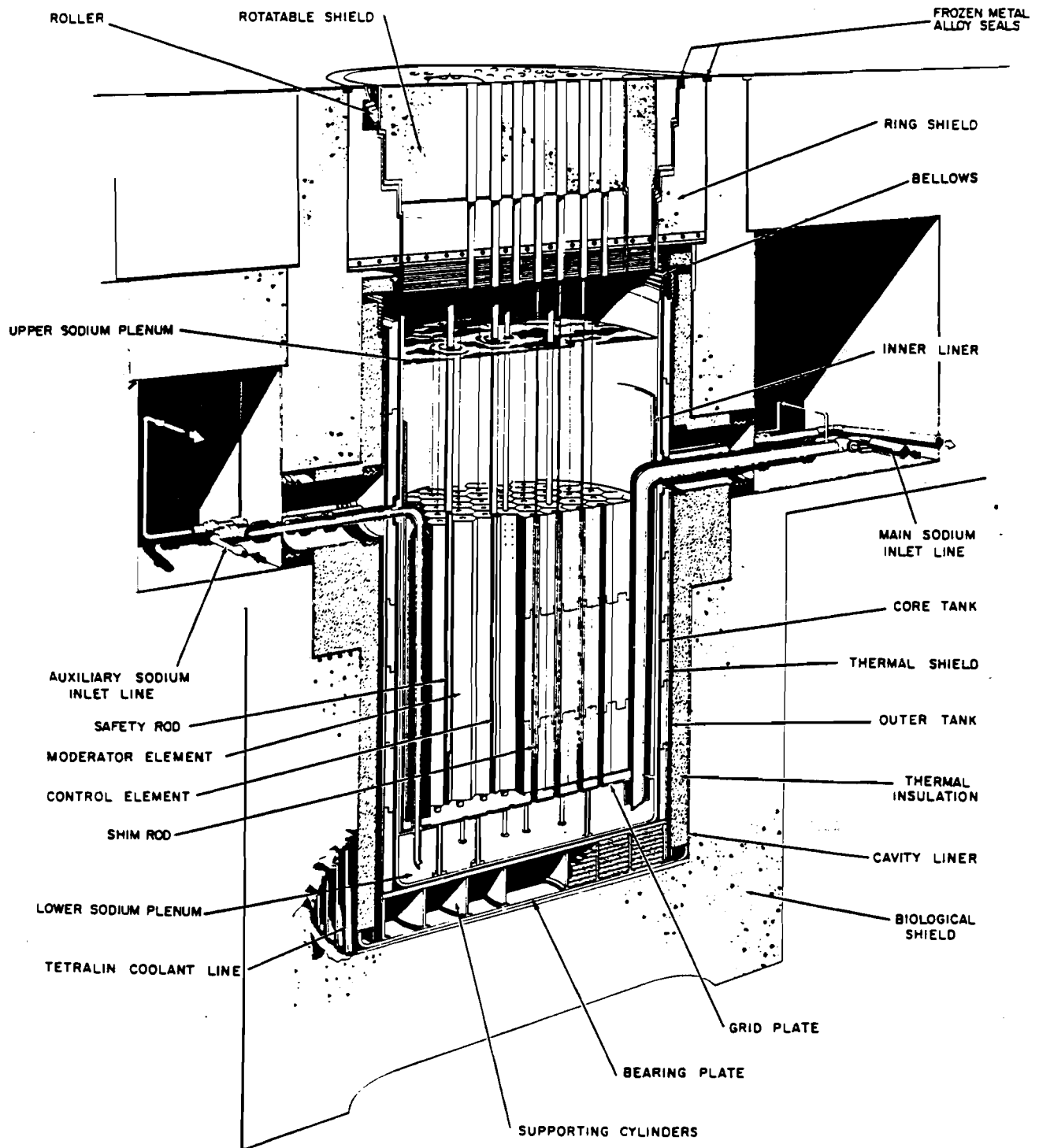


Figure II-A-1. Cutaway View of SRE Reactor



2. Moderator and Reflector Assemblies

The moderator is National Carbon Co. grade TSP graphite in hexagonal prisms measuring about 11 in. across flats. Each prism, 10 ft high, is made up of three logs stacked vertically, machined as a unit, and keyed together with cylindrical graphite plugs, as shown in Figure II-A-2.

Preventing contact with the sodium coolant is the principal problem associated with the use of graphite. Free contact would result in the absorption of sodium into void spaces in the graphite, which constitute approximately 27% of its volume. This volume of sodium in the moderator would constitute an important neutron poison. The graphite cladding is formed of zirconium sheet fabricated into individual can assemblies, as shown in Figure II-A-2. A 0.035-in.-thick sheet is used on the side panels of each hexagonal graphite column, and 0.10-in.-thick zirconium stock is used for the bottom and top can heads. The distance across the flats of each can assembly is slightly less than the 11-in. center-to-center spacing of the triangular fuel lattice. This reduction is sufficient to provide an average gap between cans of approximately 0.170 in. during normal operation. The gap forms a thin flat channel through which sodium may flow to remove heat generated within the graphite. The can is dimpled to maintain clearance.

Each moderator/reflector assembly is bolted by zirconium studs to a supporting pedestal at the base of the can, and to a spacer plate at the top. Pedestals and spacer plates are fabricated from type 405 stainless steel to minimize thermal expansion problems. The pedestal supports the can and locates it in the lattice by fitting into an accurately located hole provided in the grid plate. The bottom of the pedestal is formed as a section of a sphere which mates with a conical taper in the grid plate hole to form a seal. This seal was designed to prevent excessive leakage into the plenum formed between the top of the grid plate and the bottom of the moderator cans.

Each moderator can pedestal has a circular channel along its axis which permits flow of sodium from the main lower plenum up through the coolant tube in the moderator can assembly. The top spacer plate serves as a lifting fixture for the entire assembly and as a means of lateral support for the cans. Spacer plates on adjacent cans nest together and are maintained in place by a crimping

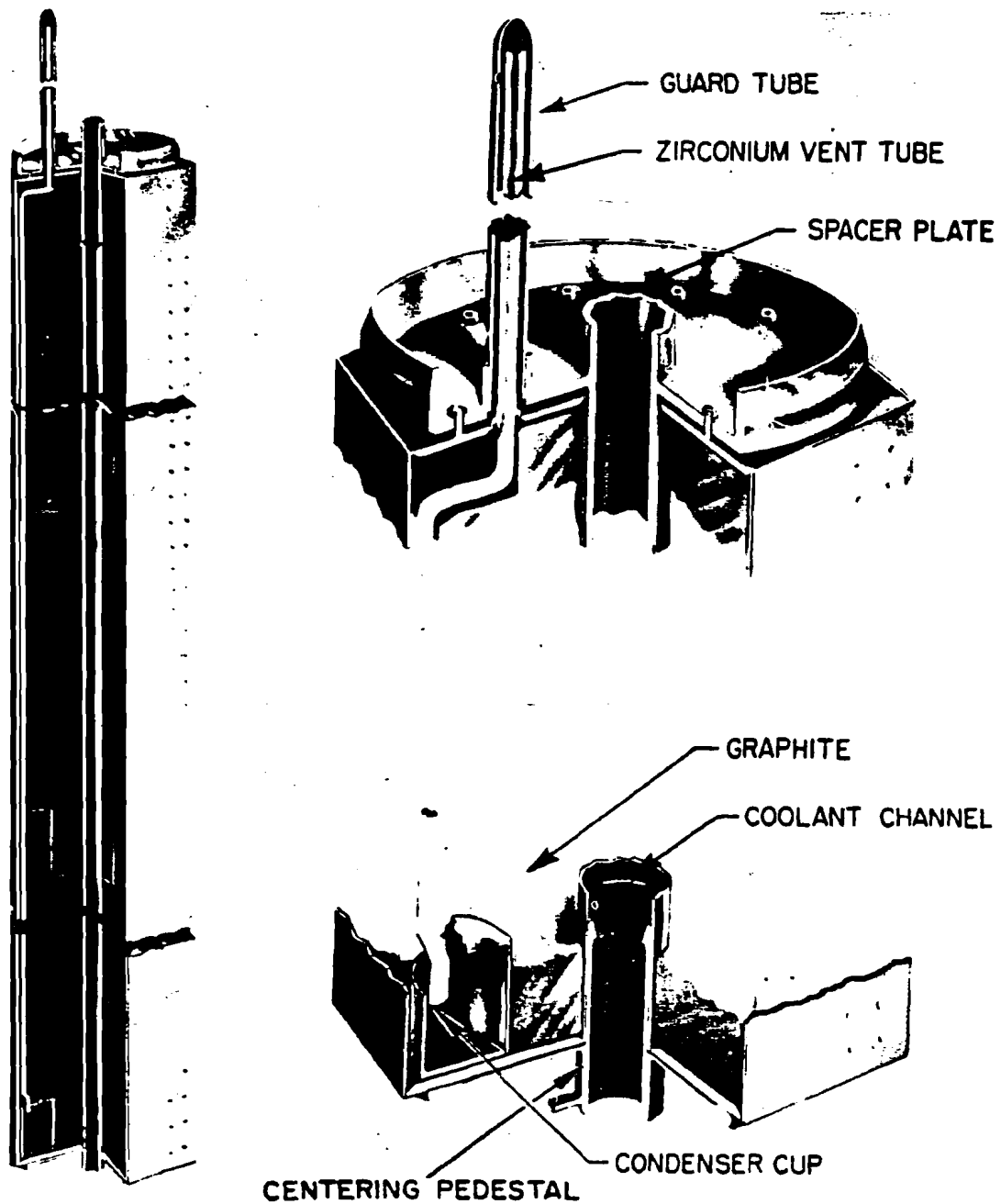


Figure II-A-2. Moderator Assembly

band around the periphery of the outer ring of cans. Each moderator can assembly in the core region is penetrated along its vertical axis by a zirconium tube of 2.80-in. ID and 0.035-in. wall thickness, welded to the bottom and top heads. Each tube normally contains a fuel element.

Some of the moderator cans were modified from the hexagonal cross section to provide a groove at one, two, or three corners for the full length of the column. These grooves, when the cans are installed, form 3-1/2-in. -diam channels at the adjacent corners of three cans and provide space for control rods, safety rods, and special reactor accessory elements, such as the source element and a liquid-level measuring device.

Reflector assemblies are generally similar to moderator assemblies except that no axial channels have been provided, and the outermost rows of reflector assemblies are canned in type 304 stainless steel sheet rather than zirconium. The types of cans are indicated in Figure II-A-3. There are a total of 119 cans in all.

The extent of outgassing from the graphite under radiation and temperature conditions expected in the reactor core was unknown when moderator can design was commenced. Consequently, it was considered necessary that provisions be made for venting the moderator/reflector assembly in order that gas

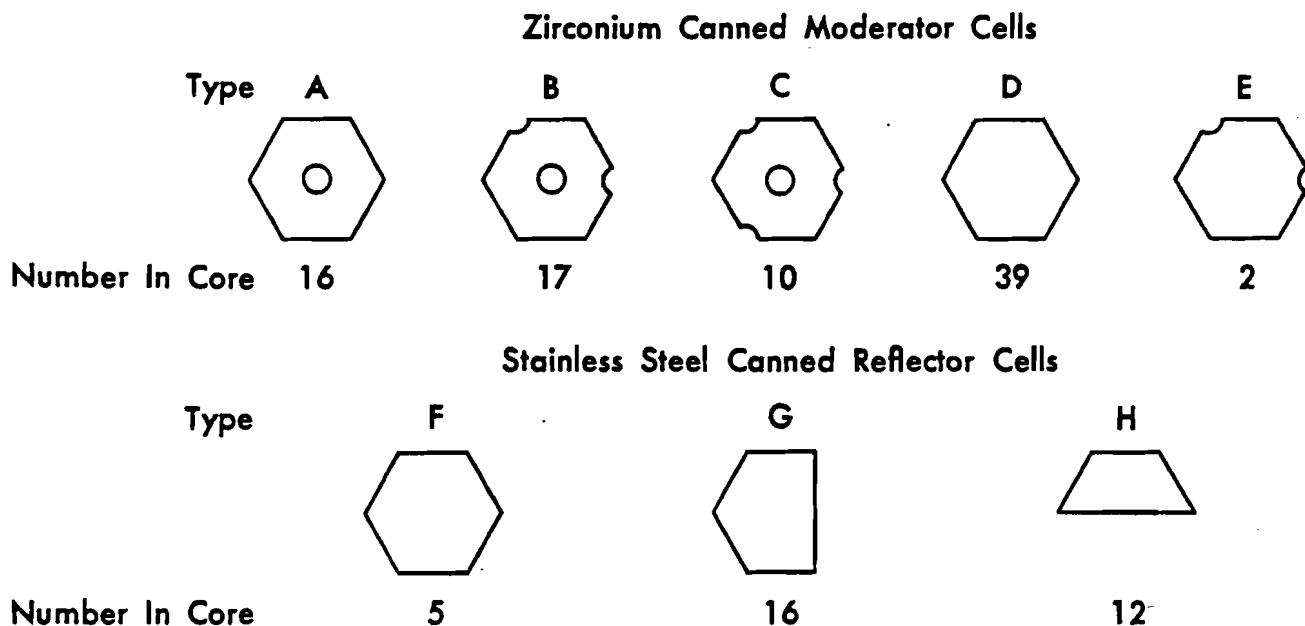


Figure II-A-3. Moderator and Reflector Can Types



buildup would not bulge the cladding and distort the coolant channels. A "snorkel" tube was attached to each can, running internally to the bottom of the moderator/reflector assembly and terminating just above a 2-1/2-in.-deep by 2-7/8-in.-diam stainless steel cup. The purpose of the cup is to accumulate any condensed sodium vapor which may pass down the snorkel tube. This 1/4-in.-diam zirconium snorkel tube projects above the can about 7 ft, so that it terminates in the gas atmosphere above the top pool. That portion of the tube which projects above the moderator can is protected by a 3/4-in. stainless steel guard tube.

3. Fuel Elements

The fuel elements, Figure II-A-4 are fabricated in clusters of 7 rods, each consisting of a 6-ft-high column of uranium slugs in a thin-walled (0.010-in.) stainless steel jacket tube. The 12 slugs are 0.75 in. in diameter and 6 in. long. They are thermally bonded to the jacket by a 0.010-in. NaK annulus. Above the column of slugs is a space containing helium. This gas-filled space allows

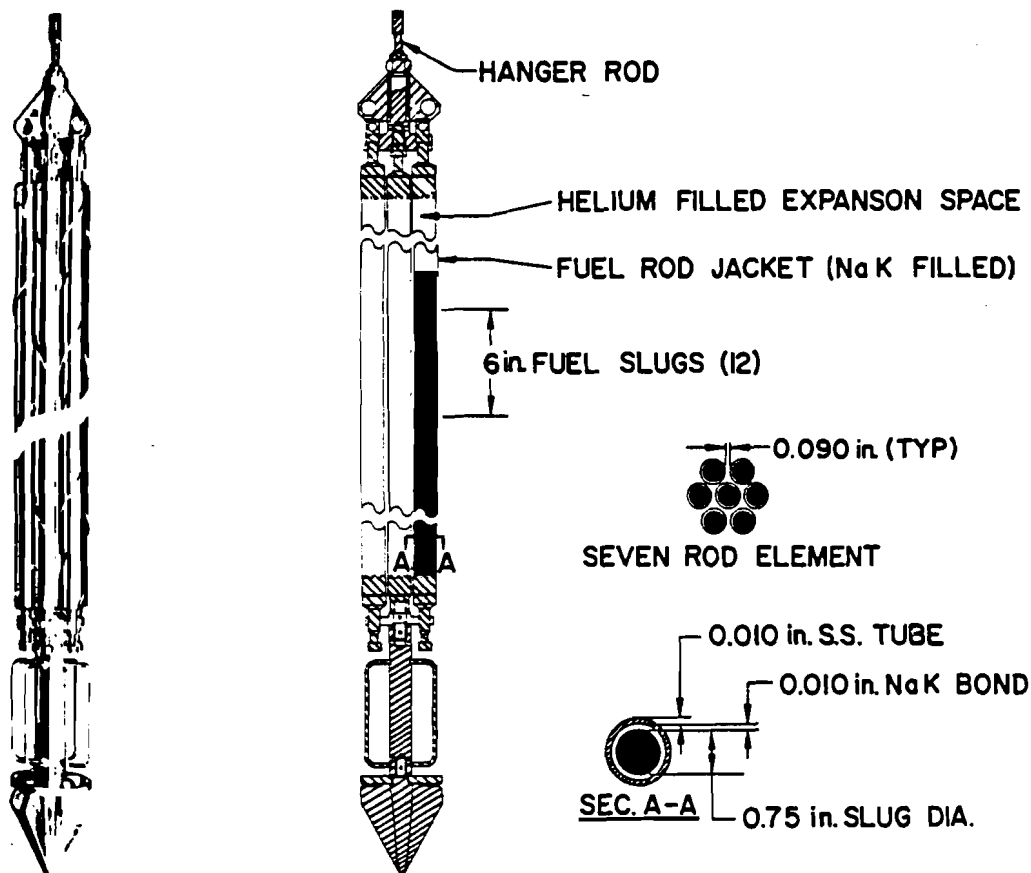


Figure II-A-4 Typical Fuel Element



expansion of the bonding NaK and serves as a reservoir for any fission gases not retained by the fuel slugs. The six outside rods of the cluster are spirally wrapped with stainless steel wire; this prevents the fuel rods from touching each other or the process channel within the moderator can. A location guide and replaceable orifice plate for controlling sodium flow are fastened to the bottom of the cluster assembly.

The cluster is supported by a hanger tube attached to a stepped shield plug. The shield plug rests in the rotatable top shield when the fuel element is inserted in its process channel. The hanger tube is designed to serve as a holddown for the moderator cans if they should, for any reason, tend to rise in the core. The tube has twelve 3/4-in.-diam drain holes cut in the wall and six 5/8 in.-diam holes in the end plate to insure sodium drainage when the element is lifted out. A thermocouple indicates the temperature of the sodium at the outlet from the fuel channel, the lead wires passing up the center of the hanger tube. The locations of fuel elements in the core are shown in Figure II-A-5.

During normal operation, there is a pressure drop of about 2.5 psi

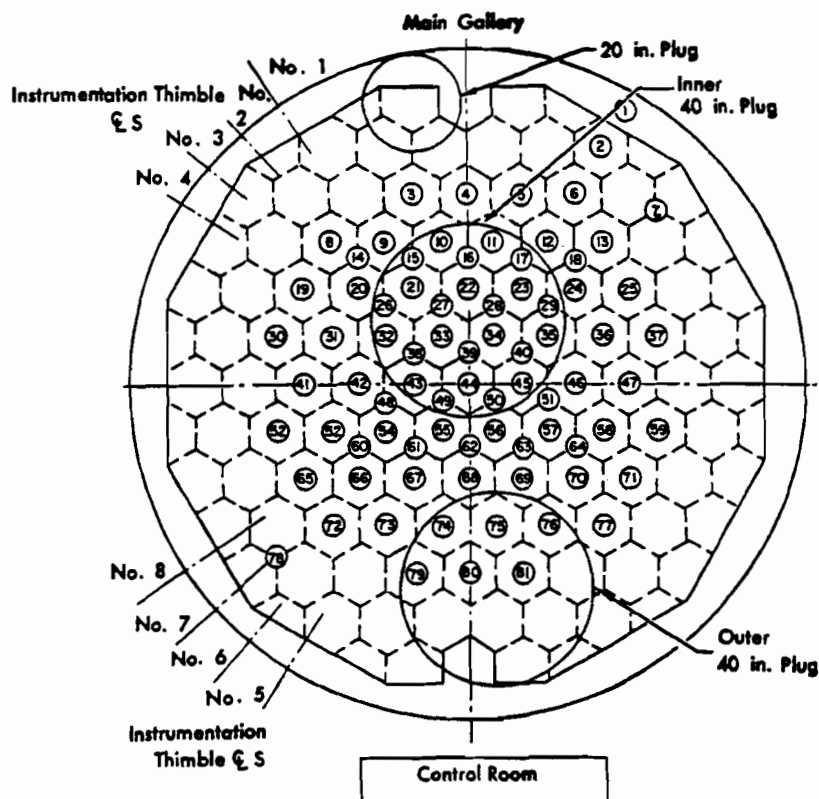


Figure II-A-5. Locations of Fuel Elements in the Core



across the central fuel element and 1.5 psi across its orifice plate. The design flow past the central fuel element is 17,500 lb/hr of sodium, at a velocity of 5 ft/sec. Outer fuel clusters are orificed to pass lesser amounts of sodium, in accordance with radial power generation distribution within the core. This maintains approximately equal temperatures of the sodium discharge from each process channel into the top sodium pool.

4. Dummy Elements

Spare channels are occupied by graphite-filled zirconium thimbles called "dummy" elements. These elements increase the density of the moderator and serve to displace sodium from unused channels. The graphite is the same as that used in the moderator elements. The zirconium thimble has a 0.035-in. wall and loosely fits the diameter of the channel. The lower end is weighted with a stainless steel plug which forms a ball and socket seal in the grid plate opening. The upper end has a hanger rod similar to that used for the fuel elements except that it includes a slip joint to permit thermal expansion. A 5/16-in. tube, sealed at its extreme end, extends up from the top of the element to act as a gas reservoir.

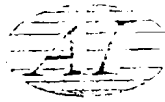
5. Control Elements

a. Shim-Regulating Elements

There are four rods or elements, capable of regulating a total of 7.0% reactivity. Each element is contained in a stainless steel thimble assembly extending from the top surface of the rotatable top shield plug to a point just below the active section of the core. This assembly prevents contact between flowing sodium and the poison element, which is operated within the thimble. The poison column of the element is made up of a series of 18 cylinders of boron-nickel alloy suspended on a pull tube. The boron concentration in the alloy is approximately 2% by weight. This poison column is essentially black to thermal neutrons.

The rods, partially inserted in the core much of the time the reactor is critical, are cooled by conduction through an atmosphere of helium at 16 psig introduced into the top of the thimbles.

Rod motion is obtained by a ball-nut screw arrangement in which the pull tube is attached to the nut, and a drive mechanism above the top shield turns



the screw. The nut is prevented from rotating by guides moving in flutes machined on the inside of the heavy wall portion of the thimble above the core. Rods have dual speed drives that produce 0.29-ft/min motion for shim action and 3.75-ft/min motion for regulating action. To avoid removal of a large amount of negative reactivity at any single time, the high speed drives are mechanically limited to a travel range without resetting of ± 7 in. The motion-limiting stops can be reset if travel through a different range of insertion is required. These rods cannot be disengaged or dropped for scram purposes.

b. Safety Elements

Four safety rods or elements may also be inserted into the core. These elements can control approximately 5.1% reactivity. They are contained in thimbles similar to those of the shim elements. However, safety elements are operated only by a high-speed drive of 3.75 ft/min for withdrawal. They have a hold magnet which can release the rod at any time during withdrawal from the core or when in the fully withdrawn position. When the magnet is disengaged by a scram signal, the poison rod assembly falls within the thimble by gravity. The safety rods, not normally inserted in the core during operation, are maintained in a helium atmosphere.

6. Experimental Facilities

Six corner channels in the reactor core are available for experimental purposes. Of small diameter, (3-1/2 in.) they extend from the top of the core to the lower sodium plenum and can be used for the full 6-ft height of the active core. Removable plugs in the top shield provide access.

Three central-channel locations in reflector assemblies are also available, at successively greater radii from the core center. Center channel openings are similar to those of the corner channels.

7. Reactor Vessel

The reactor core, Figure II-A-1, consisting of the moderator assembly, fuel rods, and control and safety rods discussed above, is situated below floor level within a stainless steel core tank, 19 ft deep and 11 ft in diameter. A



stainless steel liner, supported near midpoint by brackets on the core tank, provides a 2-1/2-in. sodium annulus at the inner surface of the tank. The liner, open at both ends and pierced by the coolant circulating pipes, projects above the upper sodium pool. This liner minimizes transient thermal stresses in the core tank wall by providing a stagnant sodium layer which reduces the effect of mismatches in the temperature of the flowing sodium.

Surrounding the core tank is a thermal shield composed of a vertical stack of seven low-carbon steel rings with interlocking joints. Immediately outside the thermal shield rings is the outer tank, also fabricated of low carbon steel. This tank provides containment of sodium if a leak develops in the core tank. Both the core tank and the outer tank have bellows attached between the tops of the tanks and the shield structure directly above them. These bellows allow vertical thermal expansion of the tanks and serve as seals for the inert gas atmosphere maintained between the tanks.

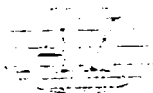
A cavity liner of low carbon steel surrounds the outer tank. The annulus between the cavity liner and the outer tank is filled with a 1-ft layer of calcined diatomaceous silica and asbestos thermal insulation under an inert atmosphere. This cavity liner, which prevents ground water from permeating the thermal insulation, is cooled by circulating tetralin through steel pipes located outside the liner. The concrete shield surrounds the cavity liner.

Four concentric cylinders of low carbon steel support the flat bottom of the outer tank. These cylinders rest on circular bearing plates attached to the bottom of the cavity liner by anchor bolts which extend into the concrete foundation.

8. Instrumentation

The SRE nuclear control and safety instrumentation consists of eight channels, two for startup, two period circuits, two power channels, and two safety channels. The reactor thermal power is determined by signals from coolant delta T and coolant flow instrumentation.

The main shutdown interlock circuit system receives shutdown signals from the following instrumentation: neutron flux level, pile period, high channel



temperature, moderator delta T, secondary cold leg temperature, loss of coolant flow, power failure, earthquake, and manual functions. Upon activation of the shutdown system, the four safety rods are released from holding magnets and drop by gravity into the reactor core. Setback is obtained by driving the shim-regulating rods into the core.

Each fuel element is equipped with a thermocouple located in the process channel near the bottom of the hanger rod. These thermocouples measure the outlet sodium temperatures of each fuel channel directly. The temperatures are continuously scanned and recorded on multipoint recorders in the control room. In addition to the above, six standard fuel elements and four which contain experimental fuel materials, have thermocouples in the center of the fuel slugs at various elevations in the active core and measure directly the fuel temperature. Other thermocouples located in dummy elements measure moderator coolant temperature. There are thermocouples to measure the core inlet and outlet sodium temperature and at various locations in piping and apparatus throughout the plant.

9. Shielding

A 4-ft-thick, reinforced-concrete pad poured on a limestone base supports the cavity liner. An annular cylinder of reinforced concrete about 3 ft thick surrounds the cavity liner.

The top biological shield which terminates at floor level, is made of magnetite iron ore aggregate set in concrete. It is a ring-shaped shield supported on a ledge at the top of the cavity liner. The 70-ton ring shield has three steps to prevent radiation streaming. A circular rotatable shield is supported on these steps and a gas seal between the rotatable shield and the ring shield is made by a lip and trough arrangement filled with a low-melting alloy. Both the ring shield and the rotatable shield are of dense concrete (3.7 gm/cm^3), 5-1/2 ft thick.

The rotatable top shield is a stainless steel shell filled with magnetite iron ore and dense concrete grout. It weighs approximately 82 tons when all internal plugs are in place. Eighty-one small plugs, two 40-in.-diam plugs, and one 20-in.-diam plug extend through the shield. The large plugs are located so that removal of any graphite assembly from the core tank may be



achieved when the shield is rotated to a proper position. The small plugs provide access to the core for fuel rods, control and safety rod thimbles, neutron sources, and experimental assemblies. Attached to the underside of the concrete in the top shield is a plate of low carbon steel. The lower surface of this plate is in contact with a layer of lead in which coolant tubes are embedded. Immediately below the lead is a stainless steel seal plate. The periphery of this seal plate is welded to the steel side shell of the rotatable shield. Suspended horizontally from the bottom seal plate are a stack of thin, stainless steel plates, separated from each other by about 1/2 in., which serve as a thermal radiation shield. Each plug in the top shield is stepped to prevent radiation streaming, and is filled with concrete and aggregate or lead to provide the same degree of shielding as the rotatable shield.

Eight 1-3/4 in. ID radial tubes embedded in the concrete outside the reactor extend from floor level downward ending just within the cavity liner and below the core center. These tubes contain the neutron detectors.

10. Cooling System

The primary and secondary systems each have two separate circulating loops, a main loop designed for transferring 20,000 kw of heat and an auxiliary loop for transferring 1000 kw of heat, Figure II-A-6. The auxiliary loops are for removal of afterglow heat in the event of outage of the main loops.

Sodium flows through 6-in. stainless steel pipe in the main primary and secondary circuits at a velocity of 13 ft/sec. Pressure drop is 15 psi in the primary circuit and 42 psi in the secondary circuit. The auxiliary sodium velocity is 30 gpm, 3 ft/sec through 2-in. stainless steel piping with a total pressure drop of 1 psi in the primary loop and 2 psi in the secondary loop. An airblast heat exchanger is the only means for dissipating heat in the auxiliary secondary loop, while the main secondary loop is provided with both an airblast heat exchanger and a steam generator.

Inlet lines from the main and auxiliary primary coolant loops enter the core tank above the graphite assemblies and extend vertically downward in double-walled, stainless steel pipes into a plenum between the bottom of the core tank and the grid plate. An inert atmosphere is maintained between the walls of the double-walled pipe to prevent excessive heat transfer.

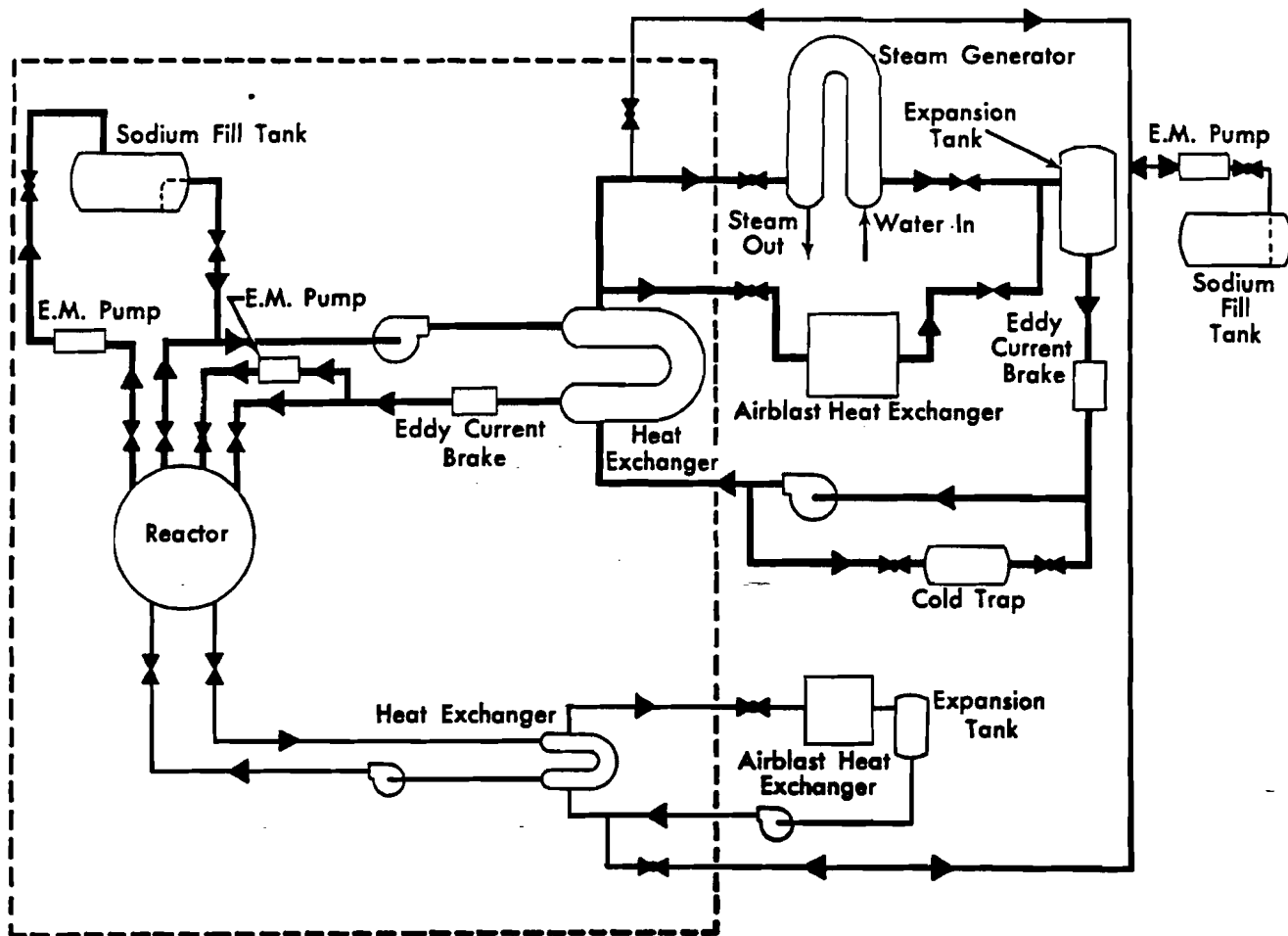


Figure II-A-6. Cooling System

At full power, the sodium at a temperature of 500°F passes from the lower plenum up through the fuel channels, absorbing heat from the fuel elements, and discharges into the upper pool about 6 ft deep at a mixed mean temperature of 950°F. Separate outlet pipes for the main and auxiliary primary loops are located in the core tank above the graphite assemblies. Moderator coolant flow is controlled by a reversible EM pump. The main source of the moderator coolant flow is leakage through the lower grid. If the leakage is not of the required rate, flow can be added to or subtracted from the grid plate leakage by the moderator coolant pump. After several power runs, the leakage was found to be about right for moderator cooling. During power run 14 the EM pump was out of the system and the moderator coolant line was capped-off.



The coolant pipes extending from the core tank are double-walled for a distance of about 6 ft, with an inert atmosphere in the annulus between pipes. This prevents gross leakage of sodium if the inner pipe containing sodium should fail. The inlet and outlet pipes are located to prevent uncovering of the fuel elements in the event of a major break in the piping. Bellows are provided around the pipe nozzles at the interface between the cavity liner and the piping gallery to permit thermal expansion of the piping while maintaining a seal for the inert atmosphere within the tank annulus.

a. Intermediate Heat Exchanger

The main and auxiliary intermediate heat exchangers are counterflow, sodium-to-sodium, shell-and-tube heat exchangers. The main intermediate heat exchanger is a U-shaped shell and tube design mounted horizontally, with a slight pitch for gravity draining. It contains 316 single-wall seamless (type 304, 3/4-in. OD by 0.058-in. wall) tubes with a total surface area of 1155 ft². The tubes terminate in a tube sheet at each end. Primary sodium flows in the tubes. The secondary sodium is in the shell. The unit was designed to exchange 20 Mw of heat with a log mean temperature difference of 60°F at a flow of 485,000 lb/hr.

b. Sodium Pumps

Sodium pumps are modified hot oil process pumps similar to those used in refinery services. Principal modifications are vertical mounting and the addition of frozen sodium seals at the pump casing and the pump shaft, Figure II-A-7. The conventional stuffing box around the shaft is replaced with a narrow, cooled annulus that provides a continuously shearing film of frozen sodium to seal the impeller space within the pump, Figure II-A-8. This "freeze seal" is cooled with tetralin. Main primary and secondary pumps are driven by electric motors. The main primary pump can deliver 1480 gpm against a 60-ft sodium head. The main secondary pump can deliver 1240 gpm against a 140-ft sodium head. Low-power electric motors serve the two auxiliary pumps. All pumps are controlled in the reactor control room.

c. Auxiliaries

Piping and vessels containing sodium are heated by rod and strip heaters. These heaters provide system preheating and keep sodium molten

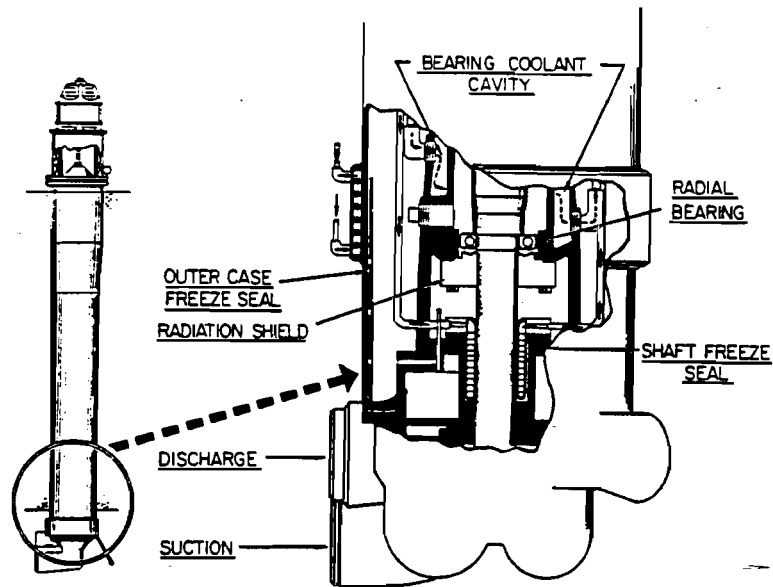


Figure II-A-7. Main Primary Sodium Pump

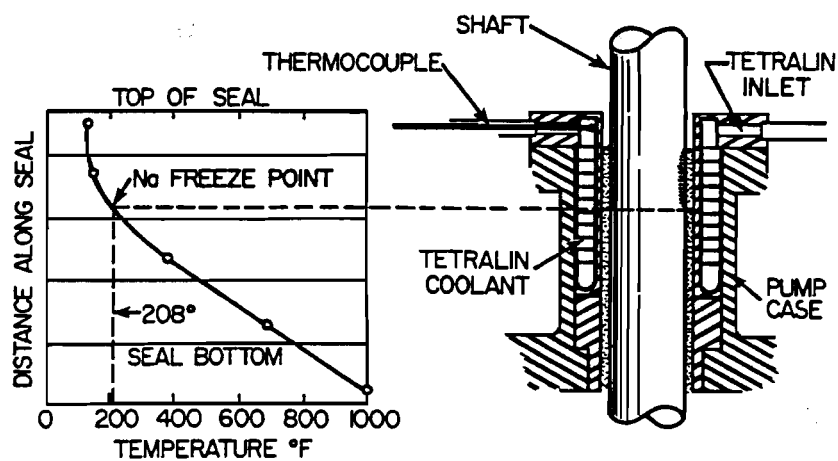


Figure II-A-8. Pump Shaft Freeze Seal



while filling and when reactor heat is not being generated. Thermocouples are attached to piping and vessels to indicate temperatures. Control of heaters, to maintain uniform temperatures, is effected by switch gear located in the reactor building. Temperature readout instruments and automatic controls are located as close as feasible to the associated switch gear. Sodium leak-detecting cable is attached to the underside of piping and vessels and leads to instruments located in the control room. Thermal insulation is strapped to all sodium containing surfaces. Electrical terminals projecting through the insulation are protected by metal tubes plugged with thermal insulation.

Hot and cold traps maintain sodium oxide content at specified low levels in the sodium cooling systems. The main primary loop has two circulating, disposable filter hot traps which can be used alternately and one circulating cold trap. The hot traps are maintained at about 1200°F by electric heaters and employ the principle of gettering on a large area of zirconium foil. Regenerative heat exchangers attached to the hot traps reduce the heat loss in this system. The main secondary coolant loop also contains a circulating cold trap. The auxiliary secondary loop is fitted with a tetralin-cooled diffusion cold trap.

One-in. pipes, welded into the inlet and discharge lines of the main intermediate heat exchanger, carry sodium to two vertical stand pipes. This permits insertion of material samples from the reactor room floor into the stand pipes, one normally containing flowing sodium at 500°F and the other containing flowing sodium at 950°F. The outlets from these two stand pipes are connected to the flowing sodium streams through stress-relieving nozzles. Samples of construction materials are inserted into this facility (Materials Evaluation Facility) to study corrosion and mass transfer effects in radioactive flowing sodium under reactor conditions.

Component cooling in the SRE is accomplished by a circulating liquid-tetralin system. The tetralin is circulated from a reservoir by two parallel electrically driven process pumps. The heated tetralin is cooled in two evaporative cooler units operated in parallel. Total cooling load can be maintained by either evaporative cooler. In the event of complete electrical failure, coolant may be circulated by a remote-starting gasoline engine attached to one of the tetralin pumps.

11. Fuel Handling

To remove any element from the reactor core it is necessary to use the shielded cask designed for this purpose, Figure II-A-9. It is carried on the 75-ton crane bridge and may be moved as required within the reactor room. To remove an element from the SRE, the fuel-handling cask is located over the fuel element shield plug after electrical and thermocouple connectors and the retaining ring with its gasket have been removed from the plug. A pneumatic mechanism within the cask (see Figure II-A-10) forces a cylinder vertically downward to make an O-ring seal at the top of the plug casing. Following this, a large lead shield skirt is pneumatically lowered to the surface of the shield. A gas lock at the lower end of the cask, where the seal has been made to the casing, is then evacuated and helium is admitted to match the pressure existing in the core tank. A latch mechanism is lowered until it engages the top of the plug of the element to be removed. The direction of the motion is then reversed to raise the plug and attached element into the cask. A mechanism then rotates the entire lifting assembly to bring a new element into position. The procedure is then reversed to lower the new element into place, disengage the latch, retract the lifting mechanism into the cask, close the opening between the lock and cask body, flush and admit air into the lock, raise the shielding skirt, and break the seal made by the lock at the casing. The cask is then free to transport the irradiated element to the cleaning or storage facilities or the hot cell at the other end of the reactor room.

A second cask, designed to remove moderator cans, is also available (Figure II-A-11). This cask can also be modified to remove fuel elements from the core or to transport core components to facilities outside the SRE.

12. Fuel Storage Cells

There are 99 fuel storage cells located in the west end of the reactor building. The cells are steel tubes, 4 in. in diam and 21 ft 6 in. in length, recessed below floor level with access at floor level. The access is designed to form a seal with the O-ring on the fuel plugs or control rod thimbles. Three of these cells are isolated from the others, and are designated for new fuel storage. The remaining 96 form a rectangular lattice 6 cells wide and 16 cells long. Eighty of these are cooled by tetralin circulating through a pipe welded to the

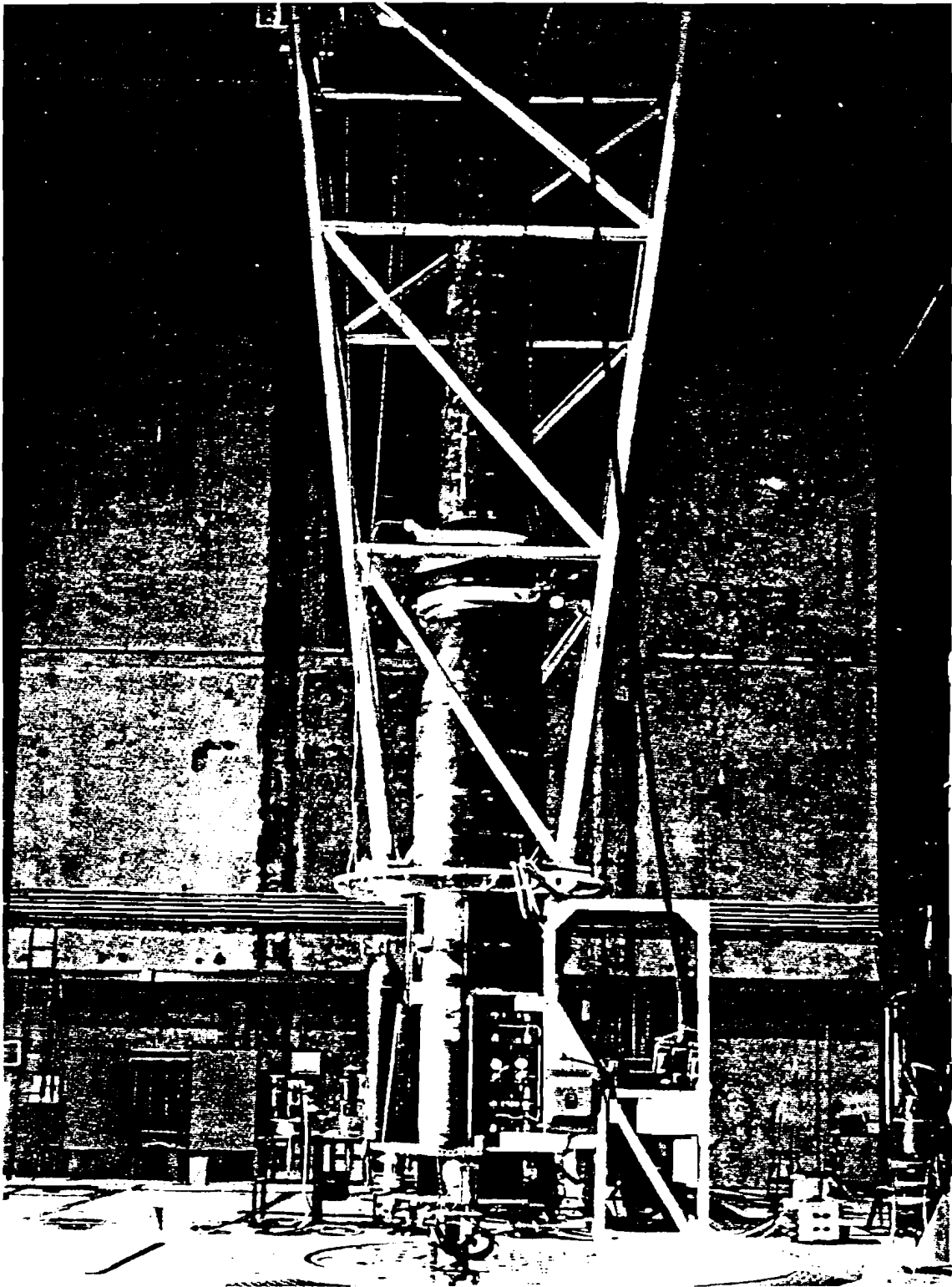
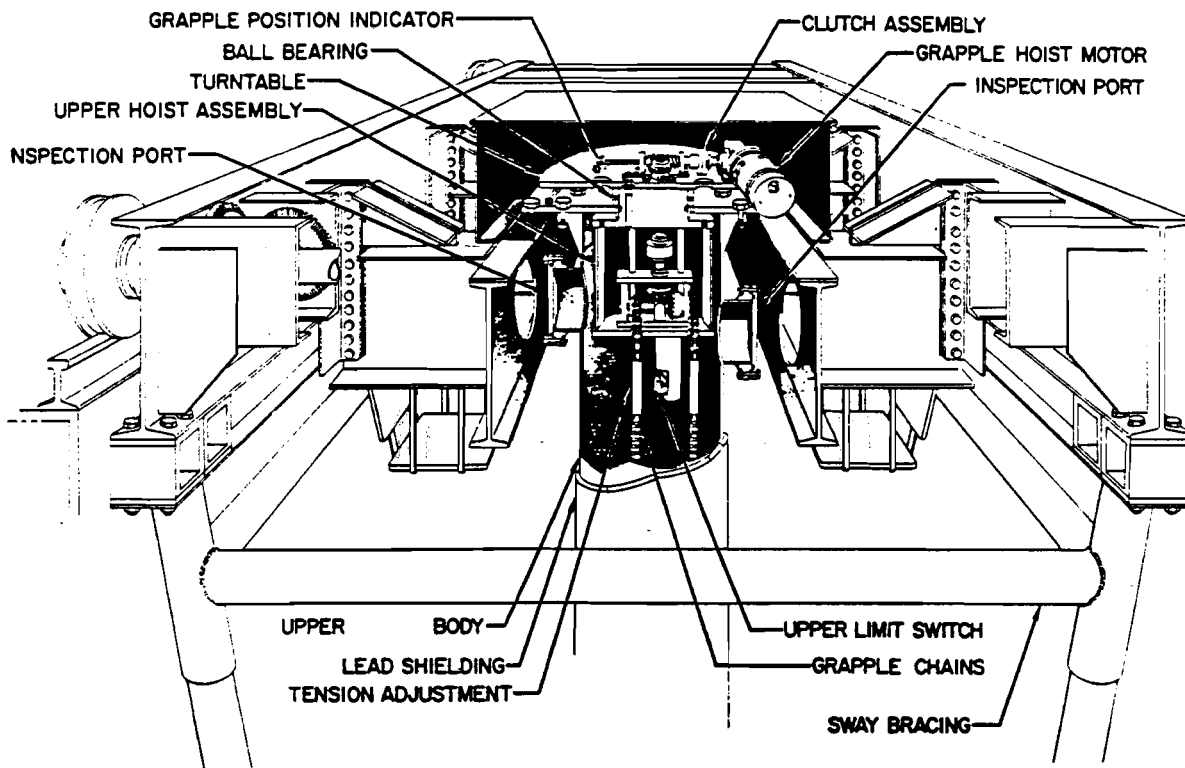
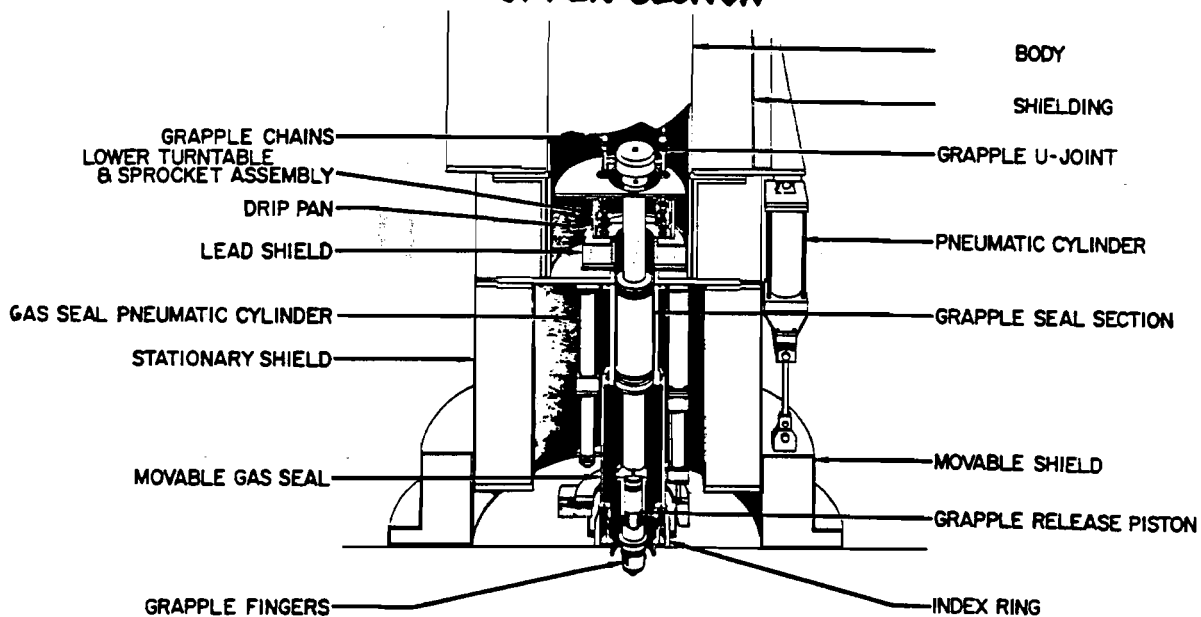


Figure II-A-9. Fuel Handling Cask



UPPER SECTION



LOWER SECTION

Figure II-A-10. Cutaway View of Fuel Handling Cask

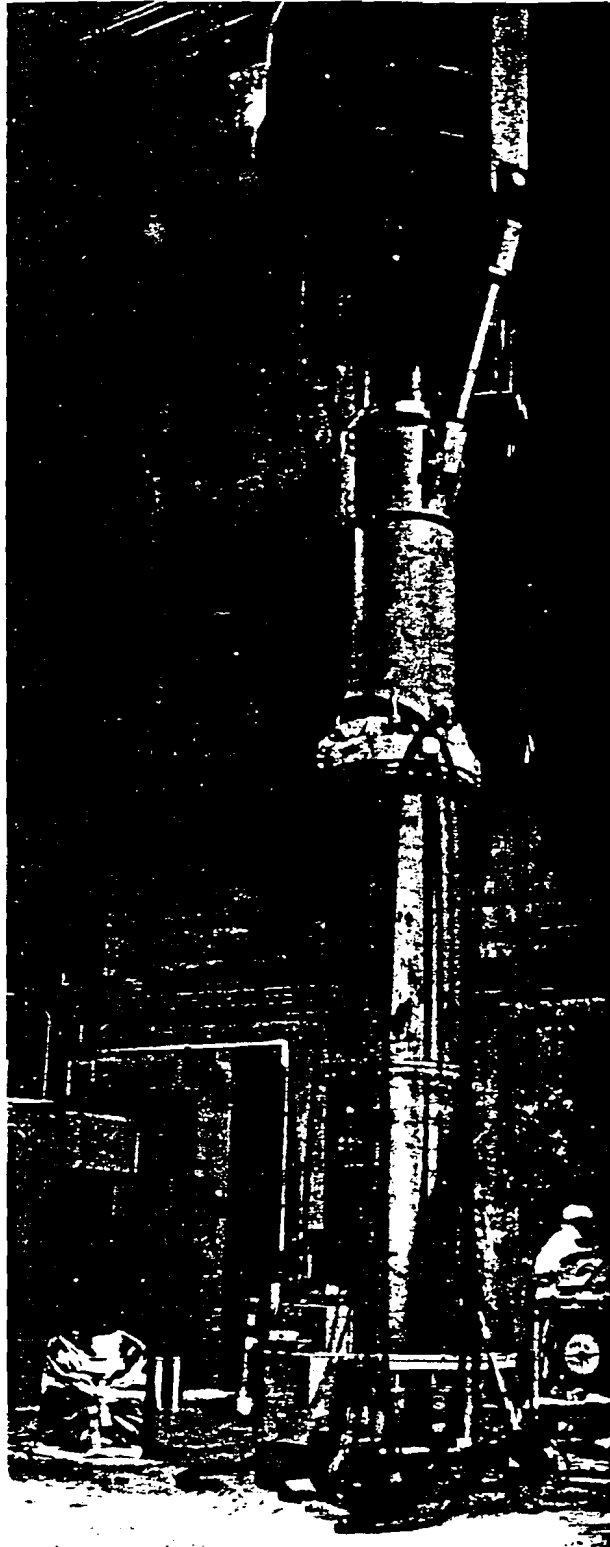
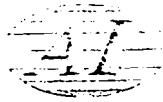


Figure II-A-11. Moderator Handling Cask



outside of the tube. An inert atmosphere is established in the cells by an auxiliary cask designed for this purpose.

13. Fuel Cleaning Facilities

Three cleaning cells are located adjacent to the fuel storage cells. They are designed to wash sodium from the fuel elements, control rod thimbles, etc., with water under an inert atmosphere. Gas liberated from the sodium-water reaction is passed to the radioactive-gas vent system. Wash water from the cells is passed to the liquid-waste system.

14. SRE Hot Cells

The SRE hot cells are located in a basement area of the reactor building. The cells are designed to afford limited examination facilities for the evaluation of fuel elements. The physical location of the cells allows direct transfer of fuel from the reactor to the cells via the fuel handling cask. This feature dictated that the cells be below the level of the reactor building floor, with the transfer point within reach of the main crane.

15. Inert Gas System

An inert gas system, which supplied both helium and nitrogen to the SRE installation, furnishes nonreactive gas blankets for contact with sodium. Helium is used as the reactor sodium-pool cover gas, and nitrogen is supplied to regions (not normally containing sodium) into which radioactive sodium might leak. Individual regulators control helium and nitrogen pressures to appropriate values. These systems are protected by relief valves and flow is monitored by in-line flow meters. Helium is used also in the fuel handling cask, cleaning and storage facilities, seals for sodium pumps and valves, core tank, and all system components with a free sodium surface. Nitrogen is used to maintain a low-oxygen atmosphere in the primary piping galleries and in the cavity containing reactor thermal insulation.

16. Waste Disposal System

Operation of the SRE may generate both gaseous and liquid radioactive wastes. Vent lines are connected to the systems containing potentially radioactive gases. These gases are discharged from the building vent line to a stack on the roof of the reactor building. Gases are continuously monitored, and if



activity rises above a preset level, the gases are automatically diverted to one of four shielded storage tanks. Compressors and controls are located in a shielded vault some distance from the reactor building. Radioactivity in gases normally stems from sodium vapor and impurities in cover gases exposed to a neutron field.

Liquid wastes, generated primarily from washing reactor components that have been in contact with primary coolant, are normally directed to a sump from which they are pumped into one of a series of holdup tanks for sampling. Highly radioactive waste are transferred from the holdup tank into shielded storage tanks. Low activity wastes go to portable, disposable, containers. Controls and valves for the liquid-waste system are manipulated entirely outside of the shielding barriers.

17. Emergency Electrical System

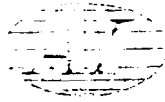
There are several sources of emergency power for the SRE if normal electric power fails. The emergency load, which approaches 50 kw, is required to maintain operation of the instrumentation and heat removal equipment.

Two sets of battery-motor alternators are provided to supply continuous emergency power and are powered by lead-acid storage batteries rated for one hour at full discharge. In addition, there is a 100-kw diesel-driven alternator that starts automatically on failure of the main electric power.

Operation of the tetralin cooling system is vital to the plant because pump and valve freeze seals depend on this coolant system for their integrity. Therefore, a remote-starting gasoline engine is connected to one of the tetralin pumps by belting, ensuring coolant circulation if all of the previously noted standby systems fail to operate.

18. Reactor Building

The reactor building is not designed as a containment pressure vessel, since the maximum credible accident would not release enough gas volume to require pressure containment. It is designed, however, to retain gases at about atmospheric pressure, and to reduce diffusion leakage of potentially contaminated gas. Aside from this, the building is designed simply to provide reactor shelter, office space, and support for a 75-ton bridge crane.

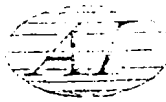


The building is of preformed tiltup concrete slabs, and the exterior shell is fireproof throughout. Nonradioactive sodium systems as well as shielded concrete vaults for primary fill tanks and service systems that are not in constant use are outside the reactor building.

Electricity is supplied by a substation capable of furnishing 1000 kw of electric power. Water, for other than drinking purposes, is supplied from local wells.

19. Steam-Electric Facilities

The steam plant is a conventional steam electric installation. A 7500-kw turbine-generator is supplied with steam from a once-through, liquid-metal to water steam-generator, providing a plant capacity in excess of rated reactor output. With the exception of the steam generator, the high-purity water conditioning system necessary for the steam generator and the interconnections between the reactor and the steam plant, all components are conventional.



B. BRIEF OPERATING HISTORY

This section of the report outlines the operating history of the SRE (see Figures II-B-1 through II-B-7). Details of the difficulties which developed during power run 14 are presented in section III.

1. Operating Data

Construction of the SRE was initiated in April 1955, and the first dry critical experiment performed in March 1957.

The reactor was first critical with sodium in the core on April 25, 1957. The turbine equipment of the Southern California Edison Co. was first operated, at low power, on July 12, 1957. During the following 10 months, a series of corrections and modifications were made to the system. The most important of these was the installation of eddy-current brakes on the main primary and secondary coolant loops to reduce thermal stress following a reactor scram.

During FY 1958 (July 1957 through June 1958) the reactor was used to generate electricity during July 12 to 14, July 25, 26, November 9 to 20, 1957, and May 21 to 28, 1958. Power levels were up to 21 Mwt and 5.8 Mwe. The total thermal energy generated in FY 1958 was 218 Mwd; the total electricity developed was 569,910 kwh. A large part of the reactor down time was consumed in reactor physics experiments.

During FY 1959 (July 1958 through June 1959) the reactor logged a total of 2191 Mwd of power operation, bringing the total to 2409 Mwd and the total electricity developed to over 15×10^6 kwh. The reactor was critical for 179 days of the year, of which 144 were at significant power levels; the remainder were at low power for experimental purposes. The last 260 Mwd of operation was accumulated at a reactor outlet temperature of 1000°F or higher, generating steam at 900°F and 600 psig. For a short period of time the reactor was operated with a peak outlet temperature of 1065°F generating steam at 1000°F. This performance exceeded the design specification (960°F outlet sodium) and demonstrated the capability of sodium-graphite reactor systems to achieve modern steam temperatures.

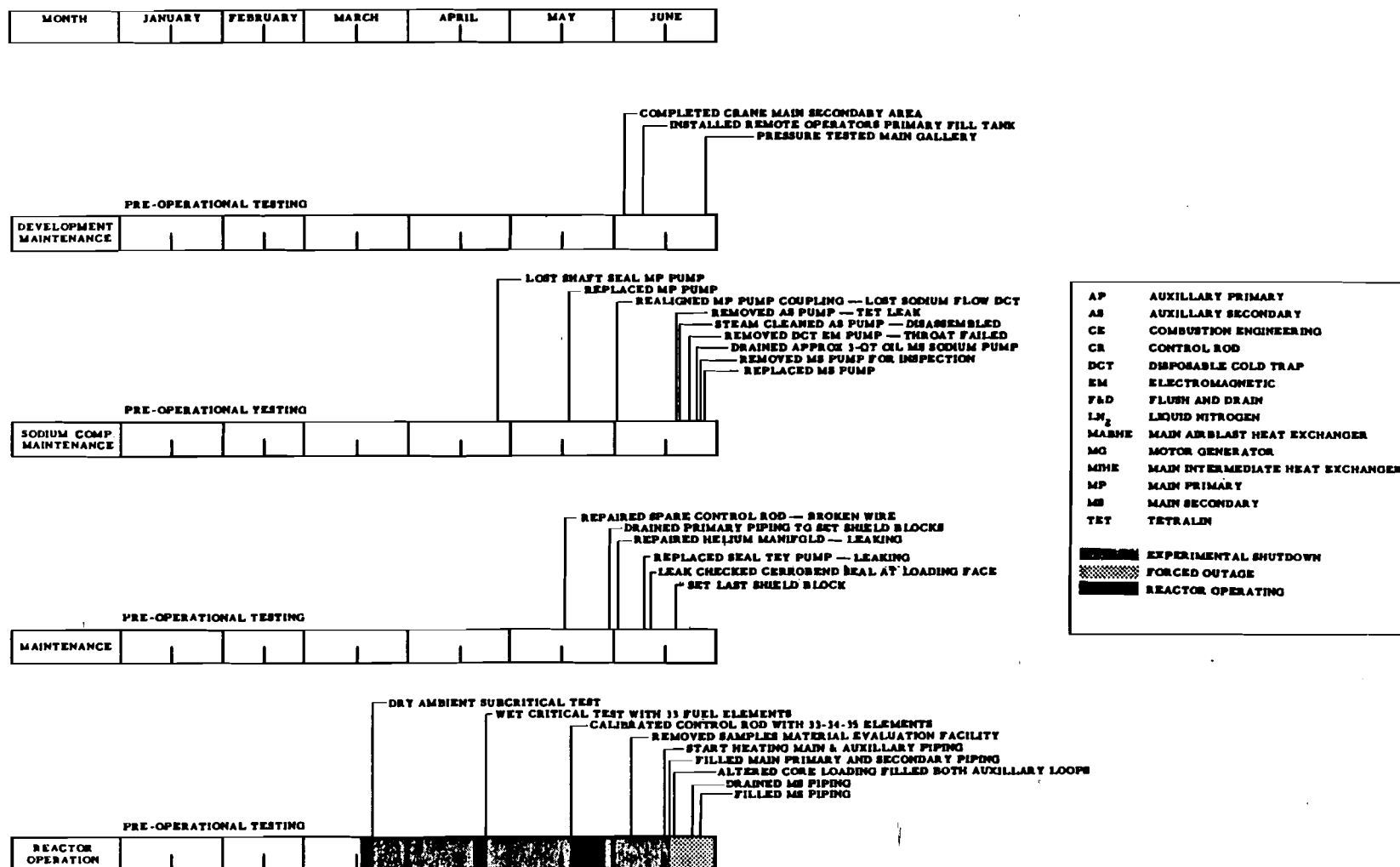


Figure II-B-1. Operating History of the SRE (FY 1957)

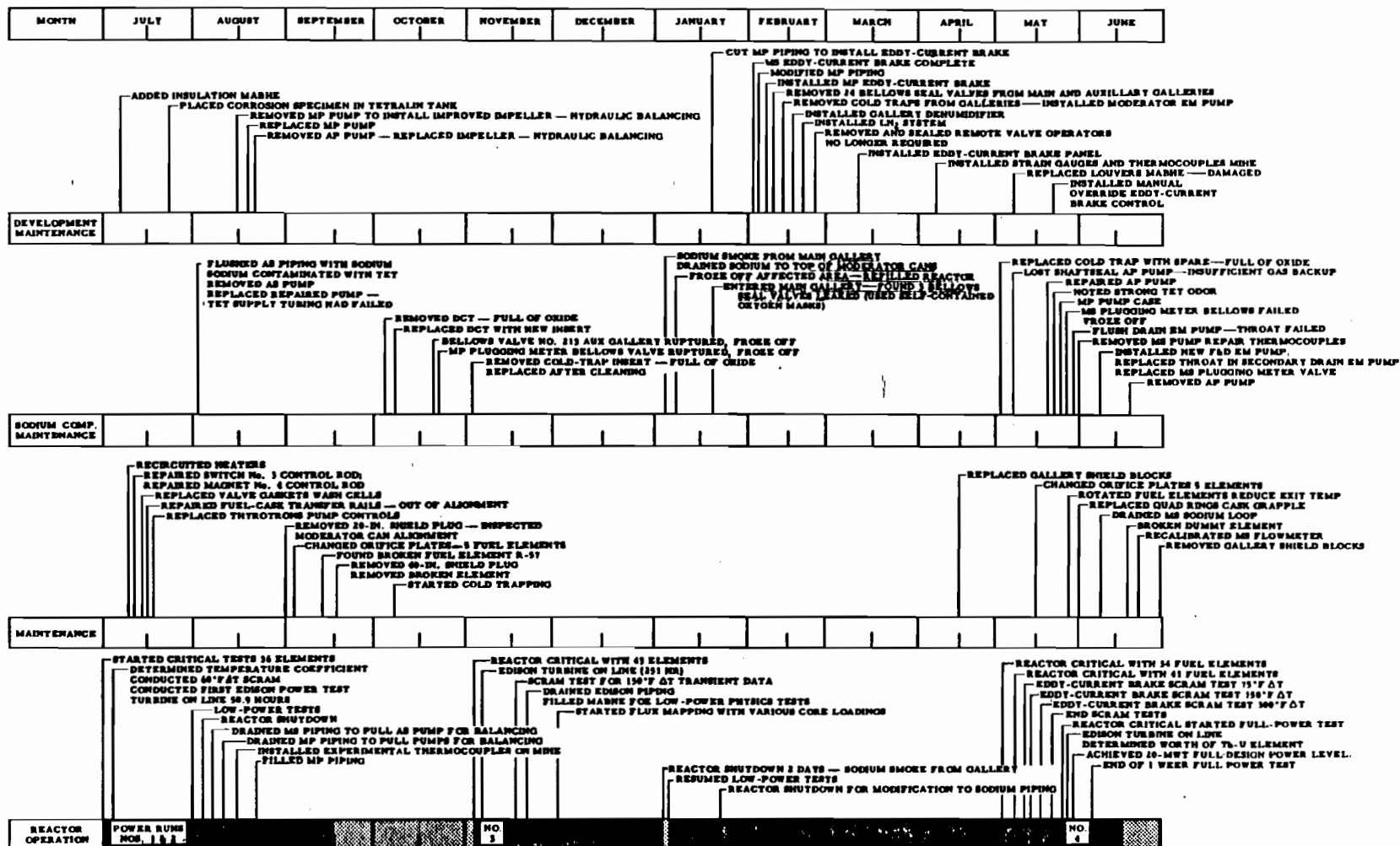


Figure II-B-2. Operating History of the SRE (FY 1958)

Figure II-B-3. Operating History of the SRE (FY 1959)

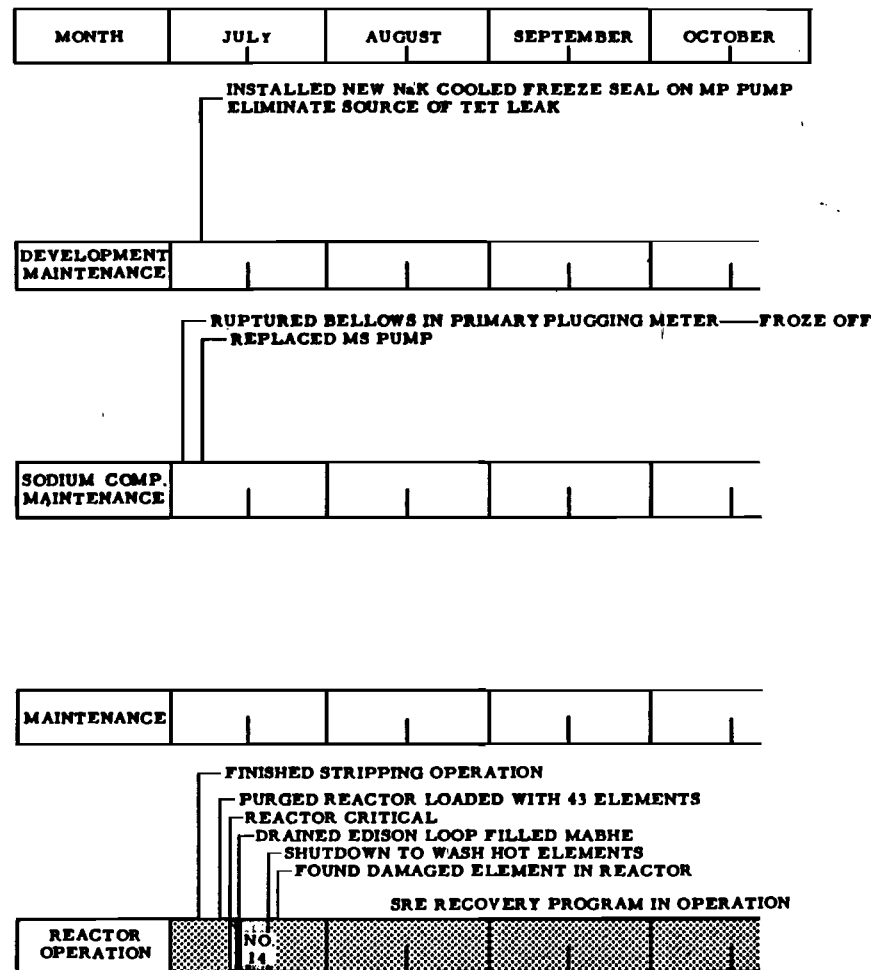


Figure II-B-4. Operating History of the SRE (FY 1960)

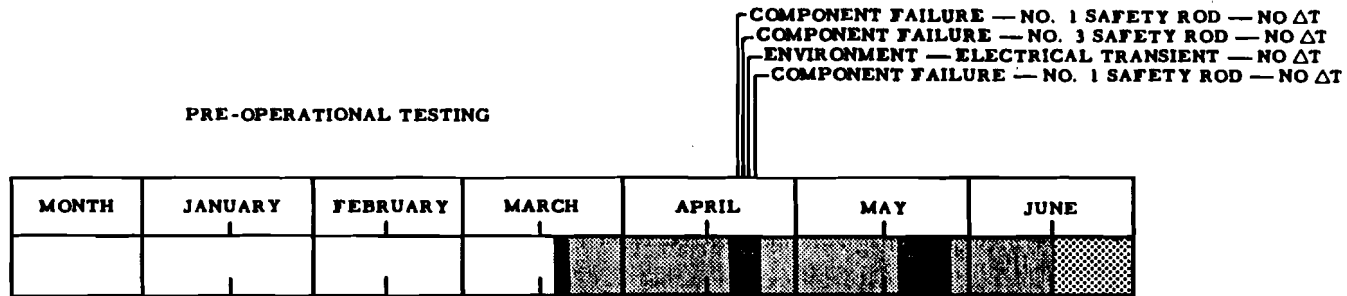


Figure II-B-5. Scram History of the SRE (FY 1957)

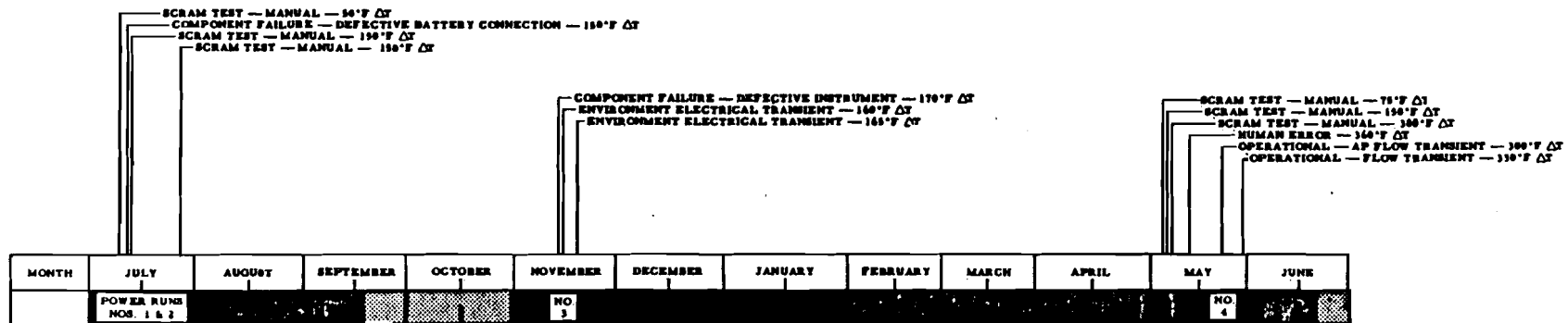


Figure II-B-6. Scram History of the SRE (FY 1958)

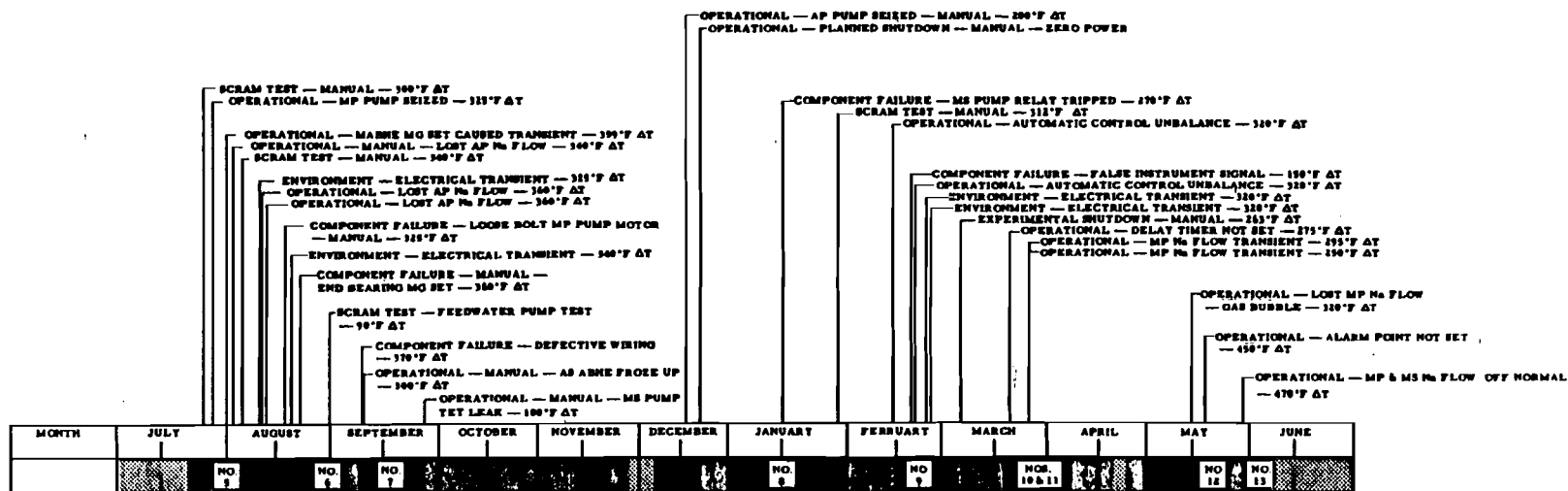


Figure II-B-7. Scram History of the SRE (FY 1959)



2. Plant Performance

a. Fuel Element Data

Operation of the SRE demonstrated that unalloyed uranium metal is an unsatisfactory fuel material for a high-temperature reactor because of a tendency to swell. Fuel rods irradiated to about 1000/Mwd/T and examined in the SRE hot cell showed an increase in diameter of 3 to 4 mils. The fuel rod was manufactured with a NaK annulus (between fuel slug and stainless-steel canning jacket) of 0.010 in. (0.020 in. on the diameter). This annulus had been occupied by the swelling uranium and the can (0.010-in. wall thickness) slightly distended.

The design maximum fuel temperature of 1220°F was never reached before run 14. Thermocouples in the uranium slugs indicated a maximum temperature of about 1100°F with a sodium outlet temperature of 1000°F. Not all of the slugs (3612 in reactor) were temperature monitored. It has been estimated that flux variations might have produced a maximum hot spot temperature of 1150°F at some point where there was no thermocouple.

The generally unsatisfactory performance of this experimental fuel material led to fabrication of a Th-U alloy loading, which is now available for use. Run 14, in which the fuel element damage occurred, was the last scheduled run for the first core loading. Use of the Th-U loading was awaiting only approval of the supplementary Hazards Report, which has now been received.²

b. Sodium Components

The sodium systems have generally performed well, demonstrating the feasibility of quite conventional components and fabrication techniques for use with this coolant. Two of the components, the sodium pumps and the intermediate (sodium-to-sodium) heat exchanger, have, however, caused difficulty in the SRE operations. The major difficulty with the pumps has been with the tetralin-cooled freeze seals which have leaked tetralin on three occasions. The intermediate heat exchanger has been found to be poorly baffled and stratification of the sodium on the shell side has resulted in a larger log mean temperature difference across the exchanger than was anticipated (90°F rather than the design value of 60°F at full power).

Thermal convection flow of sodium proved to be greater than desirable as indicated by analog computer studies and in-plant tests. Eddy current brakes were installed to avoid a sudden temperature decrease at the top (outlet) of the reactor following a reactor scram. This temperature transient would have induced undesirably large stresses in the outlet nozzle during a scram from full power; full power operation was therefore deferred until flow control was installed.

Several of the small, bellows-seal valves in the sodium service system failed and had to be replaced. Failures occurred at the bellows and apparently were due to extrusion of frozen sodium from adjacent piping during melting operations. The freeze-stem valves in the system have operated with 100% reliability.

Modification and maintenance of the sodium system have been accomplished with ease and safety. Piping can be cut and welded by first freezing the contained sodium. There have been no sodium fires during any operation involving cutting or welding piping containing frozen sodium. The cold traps and hot traps have performed well in removing sodium oxide; no difficulty was experienced in maintaining the oxide concentration below 10 ppm. The "once-through" steam generator has been highly reliable and has demonstrated its ability to operate in excess of design performance (900°F sodium inlet temperature, 825°F steam.) Steam at 1000°F was produced for about 1 hr at reduced power during run 12.

The reactor and sodium systems have demonstrated excellent flexibility. The ability of the reactor to change power levels quickly was demonstrated by changing from one-half to full power in 2-1/2 min. Sodium and steam temperatures changed less than 20°F in this test.

c. Reactor Control and Instrumentation

Performance of the control and safety rods in the SRE has been excellent. Examination of one control rod after an exposure of 2140 Mwd showed variations from nominal dimensions of less than 6 mils on the diameter. The major difficulty with the instrumentation has been a series of spurious scrams caused by fluctuations in voltage from the power supply.



One instrument failure of importance occurred. This was during run 14 and is described in section III. The cause of failure was readily corrected.

d. Reactor Physics Experiments

The most important physics experiments on the SRE have been in the area of kinetics. The SRE has proved to be an unusually stable reactor. During a 144-hr period of steady-state operation in full power, integrating timers on the automatic control system recorded only 3.5 min of control-rod movement. Extensive experiments with the pile oscillator have demonstrated the reactor stability at all power levels and at all frequencies. The ratio of the prompt neutron lifetime to the effective delayed neutron fraction in the SRE was measured to be 75 ± 7.5 msec, from which a prompt neutron lifetime of 0.525 ± 0.035 msec was obtained. A considerable amount of reactor time has been consumed in additional experiments such as control and safety rod calibrations, measurement of the radial power distribution, determination of temperature coefficients and danger coefficient measurements on experimental fuel elements.

e. Reactor Auxiliaries

Containment has been readily accomplished even during the cladding failure incurred during run 14. The washing of fuel elements to remove radioactive sodium has generally been successful, although some difficulties have been encountered as discussed in section III. A total of 387 fuel washings was successfully accomplished in the course of fuel element examinations. The fuel handling cask was used to effect fuel element transfers from the core on approximately 2000 occasions. It was not properly designed, however, to handle the broken elements found after run 14, and the moderator cask modified for handling fuel is currently in use.

In summary, the SRE has proved to be easy to operate once the minor difficulties with the new sodium systems were overcome. The reactor has exceeded its design performance and has successfully demonstrated the capabilities of the SGR concept.



III. CHRONOLOGY OF EVENTS

This section presents the background information necessary to an understanding of the present condition of the reactor and how it came about. It was decided to start this account at the beginning of run 8 because conditions existed at that time which were similar to those which existed during run 14 when the damage to the reactor fuel occurred. A discussion of the activities following the end of run 14 is given so as to bring the chronological story up to date. An evaluation of the events that occurred and their possible relation to the fuel damage will be given in section IV.

A. RUN 8 (November 29, 1958 to January 29, 1959)

Prior to run 8, there was an extended shutdown lasting about two months. During this time considerable repairs and modifications were made to the primary sodium system. While this work went on, the primary sodium was pumped back and forth several times between the primary loop and the primary fill tank which was known to contain a large amount of sodium oxide. This resulted in the introduction of a substantial amount of oxide into the primary sodium. Eighteen fuel elements were examined in the SRE hot cell and reinstalled in the reactor.

At the beginning of run 8 a large spread in the fuel-channel exit temperatures existed, and the plugging temperature was high. Extreme reactor operating conditions at that time are shown in Table III-1.

TABLE III-1

REACTOR OPERATING CONDITIONS, RUN 8
(0800 November 29, 1958)

Power (Mw)	3.6
Inlet Temperature (°F)	458
Outlet Temperature (°F)	565
Flow (gpm)	900
Fuel Channel Exit Temperature (°F)	
Minimum	415
Maximum	800

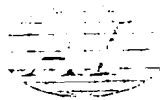


With the reactor power at about 3.6 Mw, there was a spread of 385°F between the highest and lowest fuel-channel outlet temperature in the reactor; under normal conditions at 20-Mw power, the maximum spread is usually less than 100°F. This unusually high temperature spread was attributed to oxide plugging in the process tubes since the oxide content of the sodium, determined from the sodium plugging temperature, was high at the start of run 8.

The reactor was shut down to reduce the oxide content of the sodium by cold trapping. On December 12, fuel elements from channels 9 and 10 which had been running excessively hot were washed. Both had black material on them before washing. Washing the fuel elements was found to be the most successful method for reducing the temperature spread. Reactor operation continued intermittently at low powers of 1 to 2 Mw until December 18. Some improvement in the fuel-channel exit-temperature spread occurred merely by running the reactor at elevated temperatures. This increases the rate at which oxides pass into solution. It was observed that moving a fuel element up and down about 1 in. or less in its process tube (jiggling) frequently had a beneficial effect on sodium outlet temperature for that channel. Movement of the element apparently caused foreign matter to dislodge from the element, particularly from the orifice plate.

On December 18, reactor power was increased to 12 Mw. In order to raise the power to this level without introducing an excessive spread in the fuel-channel exit temperatures, it was necessary to increase the primary sodium flowrate to 1400 gpm. Normally the flowrate is about 1100 gpm with the reactor operating at 20 Mw. On the next day the power was increased to 14 Mw, and operation continued at that level for several days. At 1800 on December 23, the reactor was shut down to inspect fuel elements.

Before resuming operation on December 27, 15 fuel elements were washed, and more cold trapping was done. A power level of 20 Mw was achieved on December 28 with the sodium flowrate at 1460 gpm. The practice of jiggling hot elements up and down to dislodge foreign matter was continued. The spread in the fuel-channel exit temperatures continued to improve as operation continued at various power levels until the end of run 8 on January 29, 1959.



On January 7, a sample of the core cover gas was bubbled through cyclohexane and the solution analyzed. Napthalene was identified, indicating that tetralin had entered the primary sodium at some earlier time. Prior to this analysis the presence of tetralin in the primary system was not suspected. The only known tetralin leak prior to this occurred in June 1958 when a crack was found in the bearing housing casting of the main primary pump. It is not known if any tetralin had entered the primary sodium at that time.

Run 8 was terminated because the desired exposure of 600 Mwd was attained. No reactivity anomalies were observed during this run. During the ensuing shutdown, more fuel elements were washed and more cold trapping was done. The sodium was cold trapped down to less than 5-ppm oxygen content.

B. RUN 9 (February 14, 1959 to February 26, 1959)

On February 16, reactor power of 20 Mw was achieved. However, some difficulties were still being experienced with the fuel-channel exit temperatures. Therefore, the reactor was shut down on February 18 to wash some fuel elements that had been running hot and to further cold trap the primary sodium. The fuel from reactor channels 10, 20, 36, and 42 was washed and replaced in the reactor.

Reactor operations were resumed on February 20. An examination of the records of the shim-rod positions (made after run 14) indicated that an increase in reactivity of 1/2% had occurred. Such an increase is expected because of the xenon decay during a shutdown of this length. However, a preliminary calculation of this effect indicated an expected increase in the reactivity of about 1%. It is believed that this discrepancy is due to approximations made in calculations of the xenon correction. Similar discrepancies are noted in later runs. The record shows that this discrepancy had disappeared by February 22 and that the reactivity remained normal during the remainder of this run.

After operation was resumed on February 20, the reactor power was maintained between 20 and 21 Mw. The condition of the fuel-channel exit temperatures continued to improve. There were two reactor scrams caused by excessive temperature drop across a moderator can (moderator delta T) and several scrams caused by power line transients. The reactor has a long history of scrams due to the latter effect.



Run 9 was terminated after the desired exposure of 125 Mwd was achieved. During the ensuing shutdown, the fuel element in reactor channel 56 was examined in the SRE hot cell. This examination was made as a part of the reactor fuels program and included micrometer measurements of fuel rod diameters. The orifice plate had a thin black deposit. The fuel element was washed and replaced in the reactor.

C. RUN 10 (March 6, 1959 to March 7, 1959)

This run was made for the purpose of making a temperature test on a UO_2 fuel element. No unusual circumstances were noted, and the fuel-channel exit temperature spread continued to improve. After completion of the test, the run was terminated after an exposure of 3 Mwd. During the ensuing shutdown a thimble was replaced in the reactor. An examination of the records of shim rod position (made after run 14) shows that at the start of run 11 a loss in reactivity of 1/4% had occurred. This loss may have been due to the thimble change.

D. RUN 11 (March 16, 1959 to April 6, 1959)

The reactor was operated at reduced power of 2 to 4 Mw until March 20. Some difficulties with the fuel-channel exit-temperatures spread were still being experienced. From March 20 until March 23 the reactor power was slowly increased to 20 Mw. Operation was continued at this level until March 27 when several reactor scrams occurred. These were caused by fluctuations in the main primary sodium flow, which occurred because helium had gotten into the primary sodium and helium bubbles caused cavitation of the pump. The helium is believed to have come from a leak in the Materials Evaluation Facility. The reactor was returned to 18-Mw power on March 28.

Examination of records of the shim-rod positions (made after run 14) indicated that a gain in reactivity of about 1% had occurred. This gain is due to the xenon effect but is about 1/3% greater than the gain indicated by preliminary xenon calculations. By March 31, the reactivity had returned to normal and remained so until the end of this run. This occurrence gives further evidence that approximate calculations of the xenon correction are inadequate and that reactivity changes of this nature are normal.



The reactor continued to run routinely at a power level of about 19 to 20 Mw until the end of this run. Further reduction in the fuel-channel exit-temperature spread was noted. The run was terminated after an exposure of 295 Mwd had been reached.

During the ensuing shutdown, 21 fuel elements were examined visually by means of a television camera in the fuel handling cask. They were all found to be in good condition and were reinstalled in the reactor.

About 10 days after the end of run 11 it was found that the radiation level in the main sodium gallery was somewhat higher than one would expect, although not sufficiently high to prevent maintenance work in the main sodium gallery. This observation was not surprising because it was realized that there was some fission-product contamination in the primary sodium.

A filter was installed in a fuel channel after the end of run 11, and sodium was circulated through the primary system. Further details and results of analysis of the material collected on the filter are given in section IV-B.

E. RUN 12 (May 14, 1959 to May 24, 1959)

The reactor performed normally during all of run 12. On May 15, the reactor outlet temperature of 1000°F was reached. The primary sodium flow-rate was 1040 gpm. On May 22, the reactor outlet temperature was raised to 1065°F for about 1 hr with the reactor power at 6 Mw and the primary sodium flowrate of 500 gpm. During this period steam was produced at a temperature of 1000°F. No unusual reactor conditions were observed during this run which was terminated after an exposure of 154 Mwd had been achieved.

During the 4-day shutdown which followed, the fuel element from core channel 56 was examined in the SRE hot cell and found to be within satisfactory limits with regard to rod diameters. There was no measurable change from measurements made following run 9. This element was then replaced in the reactor.



On May 26, the core gas radioactivity was found to be $1.7 \times 10^{-3} \mu\text{c}/\text{cm}^3$ activity was assumed to be xenon-133 and was considered to be normal. Xenon activity had been observed after reactor operation for many months and was attributed to small pin-hole leaks in the cladding of a few elements or to uranium contamination from the outside of new fuel elements.

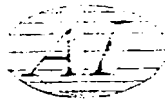
F. RUN 13 (May 27, 1959 to June 3, 1959)

This run was planned to be a repeat of run 12 with the reactor outlet temperature at 1000°F. An exposure of 150 Mwd was desired.

1. Initial Operation

The run proceeded smoothly at a reactor power of 20 Mw until 1124 on May 29 at which time a reactor scram occurred. This scram was caused by an abnormal sodium flow rate. Recovery was immediate and the reactor was returned to normal operating conditions and remained there until 0900 on May 30. At this time, several unusual phenomena started to occur. They were:

- a) The reactor inlet temperature started a slow rise from 545°F to 580°F. The rise was very slow, extending over a period of about 3 days.
- b) The log mean temperature difference across the intermediate heat exchanger started to increase which indicated an impairing of its heat transfer characteristics. A rather sharp increase in this quantity occurred on June 1.
- c) A thermocouple located in a fuel slug in the element in core channel 67 showed an increase from 860°F to 945°F. This change started at 0840 and ended at 0900 on May 30. A similar thermocouple in the fuel element in core channel 36 did not show a corresponding increase.
- d) Some of the fuel-channel exit temperatures showed a slight temperature increase of about 10°F.
- e) The moderator delta T chart shows an abrupt jump of about 30°F at 2230 on May 30. The chart shows fluctuations of about 18°F for the 4 hr immediately preceding. Prior to this it has been quite stable.



- f) The temperature indicated by a thermocouple in a probe located in corner channel 16 showed fluctuations of about 30°F. A few hours later this temperature settled down to a steady value.
- g) Although it was not noted at the time because the reactor was on automatic control, an examination of the record of shim-rod position (made after run 14) showed that a shim-rod motion corresponding to a reactivity increase of about 0.3% had occurred. This change in reactivity was gradual and extended over a period of about 6 hours. Following this the reactivity showed a steady increase of about 0.1% over the next three days of operation.

2. Tetralin Leak

By June 2, it was obvious that something had occurred to impair the heat transfer characteristics of the system. It was believed that this could not be due to oxides in the sodium because the plugging temperature had been low at the start of this run. It was decided that a tetralin leak had occurred again and was the cause of the trouble. The fairly quick recognition of the symptoms of tetralin leaking into the system was the result of the experience during run 8. The odor of tetralin was detected in the pump casing of the main primary pump. When the pump was removed after the end of this run, a leak was found in the thermocouple well in the freeze seal of the pump. (Figure II-A-8)

This run was terminated on June 3 after an exposure of only 114 Mwd. The purpose of the shutdown was to repair the main primary pump and to examine fuel. Seventeen fuel elements were visually examined by means of the television camera and found to be slightly dirty but in good condition.

3. Wash Cell Incident

On June 4, an attempt was made to wash the fuel element from core channel 56. During the washing operation a pressure excursion occurred of sufficient magnitude to sever the fuel hanger rod and lift the shield plug out of the wash cell. This event may be related to the tetralin leakage that occurred during run 13. It is possible that hydrocarbons could cause a substantial amount of sodium to be trapped in the hold-down tube on the hanger rod by blocking the sodium drain holes. This sodium could then cause the reaction. As a result of this incident, no further washing of elements was done.



The reactor cover-gas radioactivity was measured on June 13, 16, and 20. The activity was found to be about $10^{-4} \mu\text{c}/\text{cm}^3$ which is not an unexpectedly high value. More complete data are given in section IV-C.

The main primary pump was pulled on June 12. The delay of about 10 days was required to allow the radioactivity of the sodium to decay.

4. Stripping Operation

In order to remove the tetralin from the primary system, nitrogen gas was bubbled through the sodium. This stripping procedure had been used on October 12, 1958 when the secondary fill tank was purged with nitrogen in order to remove tetralin and any decomposition products.

Seventeen elements were removed from the reactor and the sodium level in the upper pool lowered to about 6 in. above the moderator cans. The nitrogen stripping process was begun on June 17 and continued until July 5 with 26 fuel elements remaining in the reactor. The sodium temperature was 350°F at the start and was raised to 425°F by the end to enhance the removal of tetralin. Nitrogen was admitted to the system through the primary sodium pump casing, passing through the heat exchanger, and then into the bottom of the reactor; 400,000 ft³ were used.

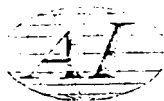
About 3 pints of tetralin and about 1500 cm³ of naphthalene crystals of unknown density were removed from the system by this process. The stripping process was terminated when no more impurities were being removed. The system then was purged for 10 hr with 4700 ft³ of helium and argon.

The primary sodium pump was reinstalled with a NaK-cooled freeze seal in place of the tetralin-cooled unit. The 17 fuel elements that had been unloaded were reinstalled in the reactor and run 14 was started.

G. RUN 14 (July 12, 1959 to July 26, 1959)

1. Temperature Spread

In view of the experience on run 8, this run was started with the expectation of encountering difficulties with the reactor fuel-channel outlet temperature. The reactor was brought to criticality at 0650 on July 12. Shim-rod positions at criticality were 46 in. out, which was about the expected position for criticality.



(The differential reactivity worth of the shim rods in this position is approximately 0.1%/in.) At 0835, as the reactor was slowly increasing power to about 0.5 Mw, it was noted that large fluctuations were present on the moderator delta T recorder. The magnitude of these fluctuations was about 10°F; whereas under normal operating conditions at 20 Mw, the fluctuation is usually less than 5°F. Also, the fuel-channel exit temperatures started to diverge, showing a spread of about 200°F. Some temperature spread is not abnormal at low reactor power. Operation continued at low powers less than 1 Mw until 1142, at which time a reactor scram occurred due to loss of auxiliary primary sodium flow. At the time of the scram, reactor outlet temperature was 485°F.

Criticality was re-established at 1215. Rod-position readings at 1300 were still 46 in., indicating no change in reactivity during the scram. Operation continued at slowly increasing power levels and temperatures. Typical reactor operating conditions during this period are shown in Table III-2.

TABLE III-2

REACTOR OPERATING CONDITIONS RUN 14
(1700 July 12, 1959)

Power (Mw)	2.7
Inlet Temperature (°F)	470
Outlet Temperature (°F)	550
Flow (gpm)	800
Fuel-Channel Exit Temperature	
Minimum	510
Maximum	770
Moderator Coolant Temperature (°F)	650

It should be realized that a possible systematic uncertainty of as much as 20% is present in the power levels given for run 14. This is caused by uncertainties in the heat balance data taken at low power levels. However, relative power levels as indicated by nuclear instruments are reliable.

Fluctuations of about 30°F were observed on moderator delta T temperature recorder with reactor power at about 1.5 Mw.



2. High Air Activity

At 1530, both reactor room (high bay area) air monitors showed a sharp increase in activity. In an attempt to reduce the activity level, the reactor pressure was lowered to less than 1 psig from its former pressure of 2 psig. A survey of the loading face shield revealed that an excessive radiation reading existed over the reactor sodium level coil thimble located in core channel 7. The initial reading was 500 mr/hr. A high bay air sample had an activity of $3 \times 10^{-7} \mu\text{c}/\text{cm}^3$ after 15 min of decay and $4.5 \times 10^{-8} \mu\text{c}/\text{cm}^3$ after 90 min of decay. At 1620, it was noted that the filter from the air sampler showed an activity level of 160,000 c/m. At 1700, a sharp increase in the stack activity to $1.5 \times 10^{-4} \mu\text{c}/\text{cm}^3$ was noted. This returned to normal by 2200.

By 1700, the radiation level over core channel 7 had reached 25 r/hr. . It was decided to shut the reactor down and replace the thimble with a standard plug. Accordingly, at 1730, reduction of reactor power was begun. At 2057, the reactor was shut down, the drive units removed, and the cask placed in operation. The sodium-level probe was removed from core channel 7, a shield plug installed in its place. A manual sodium-level probe was inserted in a spare thimble located in core channel 50. The level of the sodium was found to be 121 in. below floor level, which is normal. This device was used to check sodium level until the sodium-level indicator was reinstalled in the reactor on July 15. While the reactor was shut down, the temperature of the reactor slowly decayed to 325°F just prior to startup.

The reactor was brought to criticality at 0440, July 13. Rod positions were 49.5 in. out. The scram set-points on fuel-channel exit temperatures were set down to 800°F. Temperatures were gradually increased until at 1300 reactor operating conditions shown in Table III-3 were noted.

No significant activity was noted in the high bay area. At 1330 it was observed that the moderator delta T followed a rise in the sodium outlet temperature. The moderator temperature did not respond properly to an increase in sodium flow. It appeared that very little sodium was leaking across the grid plate for moderator coolant.

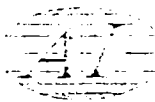


TABLE III-3
REACTOR OPERATING CONDITIONS, RUN 14
(1300 JULY 13, 1959)

Power (Mw)	2.4
Inlet Temperature (°F)	473
Outlet Temperature (°F)	542
Flow (gpm)	803
Fuel Channel Exit Temperature (°F)	
Minimum	510
Maximum	750
Moderator Coolant Temperature (°F)	605

3. Reactor Excursion

At 1728, the reactor power was at about 1.6 Mw, and a planned increase was started so as to be able to deliver heat to Southern California Edison electrical substation. After the start, the power level persisted in rising somewhat faster than expected even though control rods were being slowly inserted in an attempt to hold it back. By 1807, the power had increased to about 4.2 Mw. At this time a negative period of about 45 sec was observed and the power fell to about 2.4 Mw in about 3 min. Control rod withdrawal was started and the reactor restored to criticality at 1811. Control rod withdrawal was continued and the power slowly rose to 3.0 Mw by 1821. At this time the power started to increase more rapidly, so control rod insertion was started. In spite of this rod insertion the rate of power rise continued to increase. Three positive period transients indicating about a 50-sec period were observed at about 1824, and at 1825 a 7-1/2 sec period was indicated. At this time the reactor power was rising rapidly; so the reactor was scrammed manually by the operator. The peak power indicated on the recorder was about 24 Mw. An analysis of this sequence of events is given in section IV-D.

A setback was not initiated automatically, as it should have been at a 10-sec period. The setback is actuated mechanically by means of a cam in the period recorder. A notch in the cam trips a switch which sets back the reactor



by driving the control rods into the reactor. The setback was set to operate when the period reached 10 sec. During the excursion the period reached 7-1/2 sec without tripping the setback switch, and the power level reached about 24 Mw before the reactor was manually scrammed. Examination of the setback mechanism subsequently showed that it would operate satisfactorily only if the period decreased at a fairly slow rate. If it decreased quickly, the switch would fail to operate. The cam was modified and tested to operate at all rates of change of the reactor period.

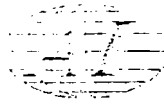
During the power excursion, the maximum temperature recorded was the fuel-channel outlet temperature of 755°F on channel 10. Moderator coolant temperature reached a maximum of 620°F as indicated by a corner channel probe thermocouple. The two metal temperatures recorded on an instrument in the control room were less than 755°F.

Recovery from the scram was made cautiously. Criticality was attained at 1955. Approximately 2-1/2 hr after the scram, reactor power reached about 2.0 Mw. Rod positions were about 52 in. out, as compared with about 49.5 in. prior to the scram. This difference was, at the time, attributed to the xenon effect following the scram; particularly in view of the fact that by 0200, July 14, the rods had returned to a position of 50.5 in. at a power level of about 4.0 Mw.

It was decided that the power excursion had not affected the reactor adversely. The spread on the fuel-channel exit temperatures and the moderator delta T had not increased following the scram. As a result, reactor power was slowly increased to a maximum of 4.0 Mw at 0700, July 14. Operation at this level continued until 1300.

At 0900, on July 14, high bay activity increased to 14,000 cpm on the air monitor. By 1100, the source of activity had been localized to channels 29 and 50 in the core loading face. Some activity was also detected at several locations around the Cerrobend seal.

Seal rings were placed on channels 29 and 50, and the holes were taped over. This action reduced the high bay airborne contamination level by a factor of 4. By 1400, high bay activity had decreased sufficiently so that the area was opened for unrestricted access.



At 1300, a scram was caused by a short circuit introduced into the demand circuit for the main primary pump. This occurred while making the electrical connections for a test in which primary flow was to be oscillated. Recovery was made rapidly. The reactor was critical at 1311 at an average rod position of 50.4 in. (The differential reactivity worth of the rods in this position is approximately 0.1%/in.) Rod positions prior to the scram, at a power level of about 3.7 Mw, were at an average of 51.1 in. At 1500, after complete recovery from the scram, rod positions were an average of 51.9 in. out. Reactor power at this time was about 3.5 Mw. Operation continued at a power level of about 3 Mw with a reactor outlet temperature of 600°F. Maximum fuel-channel exit temperature was about 735°F (core channel 10). Sodium flowrate was 900 gpm.

4. Pressure Effect on Reactivity

It was decided to pressurize and vent the reactor atmosphere once in order to reduce the radioactivity level caused by the xenon in the cover gas. At 0550, July 15, the reactor pressure was reduced from 1.8 psig to 0.6 psig, repressurized to 3.0 psig, and then reduced to 1 psig. Upon venting core pressure down, reactivity increased, causing the rod to drive in on automatic control; when core pressure was increased, reactivity decreased; hence rod was pulled automatically. The magnitude of the reactivity change indicated by rod motion was of the order of 0.01%, but the observations are not adequate to permit a reliable evaluation. On August 26, 1958, a similar qualitative pressure effect had been observed, but this occurrence was not recalled at the time. A pressure effect is not normal, and it is believed that the presence of helium gas in the sodium may account for the effect noted in 1958. Operation was continued at a power level of approximately 3 Mw and 600°F reactor outlet temperature.

5. Operation on Airblast Heat Exchanger

During the morning of July 15, a review of fuel-channel exit-temperature spread indicated that it would be pointless to continue trying to get the Edison turbine generator "on the line," since maximum power level attainable would probably be less than 4 Mw. It was decided to shut the reactor down, drain the Edison lines, fill the airblast heat exchanger, and operate at higher reactor



inlet temperatures than are possible while circulating through the steam generator. Reactor power was slowly reduced and the reactor was shut down at 1148, July 15. During the shutdown, the following activities were completed:

- a) The Edison loop was drained.
- b) The main airblast heat exchanger was filled.
- c) The reactor sodium level coil was reinstalled in core channel 7.
(New quad rings were included.)
- d) A complete helium leak check was conducted on the core loading face. As a result, new quad rings were installed on the control-rod thimble in core channel 62.

On July 16, at 0704, the reactor again achieved criticality, this time at an average rod position of 57 in. out, indicating that there had been a substantial loss in reactivity since the beginning of the run. Careful examination of the history of shim-rod positions was made which indicated that a reactivity loss of about 1.2% had occurred gradually during the four days since the start of run 14. Reactor outlet temperature on July 16 was 360°F. Intermittent operation continued at low power (less than 2 Mw) until July 20.

On July 18 at 1100, the main primary flow rate was varied over the range of 400 to 1200 gpm. No effect on reactivity was observed. At 2148 on July 18, the MG set which supplies stabilized power for the vital bus (instrument power) failed. Operation was resumed using the unstabilized Edison power. The MG set was not repaired until July 21.

During the next several days measurements of the primary sodium plugging temperature were made. The results are given in Table III-4.

On July 19 and 20, some additional tests were made in an attempt to evaluate the effect of core cover-gas pressure on reactivity. The results showed an effect, but the data do not permit a reliable evaluation of its magnitude. Varying the sodium level in the reactor may have also produced a very small effect on reactivity.

On July 19, the reactor outlet temperature was gradually raised from 360 to 540°F while the power was kept below 1 Mw. It was desired to operate

TABLE III-4

PRIMARY SODIUM PLUGGING TEMPERATURES, RUN 14

Date	Time	Sodium Temperature (°F)	Plugging Temperature (°F)
July 18	1130	400	350
July 18	1520	400	335
July 19	1000	475	390
July 19	1345	530	395
July 21	1330	575	520
July 25	0035	510	455
July 26	0700	510	350

for a while at increased temperature to see if this would improve the reactor operating conditions. This is related to the experience on run 8. It was not possible to wash fuel elements because the wash cell had not been available since June 4.

On July 20 at 0900, reactor power was increased slightly in order to begin raising loop temperature to 700°F. On July 20 at 2305, reactor cold-leg temperature reached 700°F. Reactor power level at this point was about 2.5 Mw. Sodium flow rate was 850 gpm. Maximum recorded fuel-channel exit temperature was 865°F at a reactor outlet temperature of 740°F.

On July 21 at 0210, a scram was caused by a fast period indication. It should be recalled that at this point the nuclear instrumentation was still running on "normal" Edison power. The reactor was critical at 0225 at an average rod position of 49 in. Operation continued at about 2.5 Mw.

At 0645, radioactivity in the reactor began building up, as indicated on the continuous air monitors. This buildup continued until at 1000 the two air monitors were reading 15,000 and 18,000 c/m. At 1400, the results of a high bay air sample showed that the high bay activity level was $2 \times 10^{-9} \mu\text{c}/\text{cm}^3$.



A reactor scram was initiated manually at 0945, July 21 when flow was lost in the main secondary loop. The loss-of-flow scram was caused by a low sodium level in the secondary expansion tank which resulted from a faulty level coil on the main secondary expansion tank. After the scram, fuel-channel exit temperatures dropped. When the main secondary loop was restored to service, temperature swings were noted in the reactor cold leg. At 1130, the reactor was again critical at an average rod position of 54 in. The spread in the fuel-channel exit temperatures was still present, but safety limits were not being exceeded. Prior to restarting the reactor, the vital bus was restored to service.

6. Fuel Temperatures

During the day of July 22, the fuel temperature recorder on the element in core channel 55 showed fluctuating temperatures in the 1100 to 1200°F range. This cluster was composed of various experimental fuels. The temperatures of six fuel slugs in three experimental elements were being recorded on a point recording instrument located in the high bay area. However, fuel temperatures being recorded on instruments located in the control room were very much lower. Due to lack of confidence in the reliability of the recorder on the experimental fuels, no attempt was made to operate in such a manner as to reduce the temperatures recorded by the experimental fuels instrument. After the end of this run, a calibration of this instrument was made and it was found to be in good operating condition. This instrument was being repaired during the period July 12 to July 15, so no record from it exists during the power excursion that occurred on July 13.

During the interval between 1400 on July 20 to 1300 on July 21, the instrument in the high bay area which records the temperatures in the experimental fuel elements was not completely operative. At some time during this period the maximum temperature recorded was 1350°F. An examination of the record on this experimental instrument (Figure IV-A-5), made after the end of the run, shows a maximum temperature of 1465°F recorded at 1300 on July 23.

Operation continued at power levels up to 4.5 Mw, with sodium flow rates up to 1500 gpm, and reactor outlet temperatures up to 790°F.



7. Reactor Shutdown

On July 23, it was decided to shut the reactor down, in view of the previously reported high fuel temperature for the element in channel 55 and since the fuel-channel exit-temperature spread was not improving noticeably. Shutdown was set for 1700, July 24. Until 0900, July 24, reactor outlet temperature was kept between 700 and 800°F. A few fuel-channel exit temperatures reached the 900 to 1000°F range. Most of the fuel-channel exit temperatures were below 900°F. At 0950, July 23, a reactor scram was caused by a fast period indication. It was believed that this indication was due to an electrical transient. The reactor was critical again at 1015.

Between 0000 and 0800, on July 24, while jiggling elements in an attempt to dislodge foreign material and hence lower the fuel-channel outlet temperatures, it was noted that the elements in core channels 10, 12, 35, and 76 were stuck in place. On the evening of July 22 when a similar operation had been performed, the element in core channel 10 was free.

A scram was caused by a fast period indication at 1250 on July 24.* The reactor was critical again at 1314. Accidental loss of auxiliary primary flow caused a reactor scram at 1540. The reactor was critical again at 1556.

The reactor outlet temperature was gradually reduced to 510°F, at which point the primary cold trap was put back in service at 0025 on July 25. During this last portion of the power run, rod positions were an average of 54 in. out. At 0035, the primary plugging temperature was 455°F at a sodium temperature of 510°F. Cold trapping continued, and the primary plugging temperature reached 350°F at 0700 on July 26.

On July 26, it was noted that the elements in channels 12 and 35 were no longer stuck. The element in channel 76 was somewhat freer than before, while the element in channel 10 was still stuck.

*It should be noted that the reactor has a history of spurious scrams due to apparent period transients. This is one reason that the period scram is normally bypassed during power operation above 1%. Many so-called period scrams have been traced to voltage and frequency instability in the power supplied to the log N amplifiers. As a result, a new system involving a small motor-generator set, fly-wheel stabilized, has been designed to remedy this difficulty.



On July 26 at 1120, the reactor was shut down after a total exposure of about 16 Mwd on run 14. The shutdown was made to examine each fuel element which had been running hot with the television camera and to try to clear any obstructions in channels. The first damaged fuel element was observed at 1915 on July 26.

H. EVENTS FOLLOWING THE END OF RUN 14

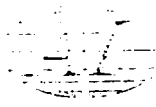
1. Fuel Examination

The first fuel element that was removed from the core was visually inspected and found to be apparently in good condition. The next element to be removed was from core channel 25. This fuel element appeared, upon inspection by means of the television camera, to have a piece of cladding missing. It was stored in storage cell 56. The third fuel element to be removed was from core channel 31. This element, upon visual examination, was found to be parted. It was removed from the reactor and placed in storage cell 35.

Fuel elements which were found by visual inspection to be intact were either reinserted into the reactor or removed to the fuel storage facility. By August 2, 6 parted fuel elements had been removed to the fuel storage facility. On August 2, a parted fuel element from core channel 12 became lodged in the fuel handling cask. Attempts to dislodge it were not successful, so it was necessary to suspend the operations of examining the fuel. This left 19 fuel elements in the reactor core. Of these, 10 had been examined visually by means of the television camera, and 9 had not yet been examined. The 10 which had been examined were apparently intact. The 9 which had not been observed all ran hot during run 14 and hence had a good probability of being damaged.

2. Fuel Handling Cask Operations

As mentioned previously, the fuel element from core channel 12 lodged in the fuel handling cask and all attempts to dislodge it were unsuccessful.



Twice before portions of broken fuel elements had stuck in this fuel handling cask and were dislodged only after considerable effort. A considerable amount of radiation exposure and contamination in the high bay area was resulting from the attempts to dislodge the jammed fuel element. When it became apparent the operation would be quite time consuming, all efforts were directed to modifying the moderator handling cask for fuel removal. The moderator handling cask had been under development for a considerable length of time, and its fabrication and assembly were nearly complete. A careful study of its construction and operation was made in order to ensure that parted fuel clusters could be handled successfully without danger in jamming. Careful consideration was given to the hazards involved in moving broken fuel elements. The completion of the assembly and testing of the new fuel handling cask took several weeks. Very thorough operational tests were performed with dummy fuel clusters in order to ensure proper operation of the device. On September 22, the removal of a corner-channel dummy element from the core was started. This was in preparation of removing the remaining fuel elements from the core. The removal of the last 19 fuel elements from the core was started on October 8. All but 2, which were found to be stuck, were removed by October 19. The present status of the fuel elements which were in the reactor during run 14 is shown in Tables III-5, III-6, and III-7.

3. Fuel Canning

The fuel that had been removed from the reactor prior to August 2 had been transferred to the storage facility in the SRE building. The remaining fuel removed from the reactor was canned prior to storage to minimize contamination of the SRE storage facility and difficulties encountered when a parted fuel cluster was to be placed in a storage cell. Moreover, this canning would have been eventually necessary in any case so that the fuel could be transferred to the Component Development Hot Cell where a more complete examination could be made. The SRE hot cell facilities have an air atmosphere and are not suitable for complete examination of unwashed or parted fuel clusters.



TABLE III-5
DAMAGED FUEL ELEMENTS

R-10	At 2200, July 27, 1959, it was found that the fuel cluster was broken in two with approximately two-thirds of the fuel cluster remaining in the fuel channel. Shield plug and broken section of fuel cluster were stored in storage cell 69.
R-12	At 1745, August 2, 1959, it was found that the fuel cluster was broken in two with approximately two-thirds of the fuel cluster remaining in the fuel channel. Shield plug and broken section of fuel cluster are contained within the fuel transfer cask awaiting transfer to a storage cell.
R-21	At 2245, October 10, 1959, an unsuccessful attempt was made to remove the fuel cluster from R-21. The hoist cable power was tripped out because of overload ≈ 800 lb. The fuel cluster was finally withdrawn from the core at 2330. Observations made in the SRE hot cell indicated that the lower third of the fuel cluster had broken off and had probably remained in core channel R-21. The portion of cluster removed has been canned and is being stored.
R-23	At 1413, October 11, 1959, the fuel element from R-23 was removed from the core. It was noted during removal operations that the element stuck momentarily after 4 ft of upward travel. The element was broken, with the lower third believed to be still in R-23. The portion of cluster removed has been canned and is being stored.
R-24	Attempts to remove the fuel cluster from R-24 had failed. This cluster, with its moderator can, was raised and blocked-up approximately 1 in. in an attempt to free the fuel cluster from the moderator can. No change was noted.
R-25	At 1915, July 26, 1959, the element was being viewed by using the portable television camera when it was noted that the cladding appeared to be split open on one of the fuel rods. The element was lowered back in the core, rotated 180°, and viewed again showing an additional ruptured fuel rod. Element was stored in storage cell 56.
R-31	At 0200, July 27, 1959, it was found that the fuel cluster was broken in two with approximately one-half of the fuel remaining in the fuel channel. Shield plug and broken section of fuel cluster were stored in storage cell 35.
R-35	At 1700, July 27, 1959, it was found that the fuel cluster was broken in two with approximately one-half of the fuel remaining in the fuel channel. Shield plug and broken section of fuel cluster were stored in storage cell 68.
R-43	At 1905, October 15, 1959, the fuel element from R-43 was removed from the core. The fuel cluster was broken in half. The portion of cluster removed has been canned and is being stored.
R-55	At 1900, July 28, 1959, the experimental fuel element was found to be broken in two with approximately one-half of the cluster remaining in the fuel channel. Broken section of fuel cluster was examined and photographed in the hot cell, then the remains of the cluster were removed from the shield plug section and placed in a container and left in the hot cell. The shield plug was placed in storage cell 73.
R-68	At 2300, August 1, 1959, it was found that the fuel cluster was broken in two with approximately two-thirds of the fuel cluster remaining in the fuel channel. Shield plug and broken section of fuel cluster were stored in storage cell 72.
R-69	At 2230, October 14, 1959, the fuel element from R-69 was withdrawn from the reactor. The cluster was broken in half. The portion of cluster removed has been canned and is being stored.
R-76	Attempts to remove the fuel cluster from R-76 have failed. In-core observations of the cluster, during removal attempts, indicate that the moderator can containing the cluster lifts as the element is raised. This cluster, with its moderator can, was raised and blocked-up approximately 1 in. in an attempt to free the fuel cluster from the moderator can. No change was noted.



TABLE III-6
FUEL ELEMENT STATUS

Core Channel	In During Stripping	Ran Hot During Run 14	Damaged	Burnup (Mwd/T)
4	yes	yes	no	581.0
9	no	yes	no	440.6
10	yes	yes	yes	645.2
11	yes	no	no	793.5
12	yes	yes	yes	747.4
19	yes	no	*	462.7
20	yes	no	no	826.1
21	yes	†	yes	852.1
22	yes	no	no	810.3
23	yes	†	yes	801.1
24	yes	†	§	303.5
25	yes	yes	yes	707.9
31	yes	yes	yes	745.0
32	yes	no	no	447.7
33	no	no	no	939.5
34	yes	no	no	1117.0
35	yes	yes	yes	541.9
36	yes	no	no	472.2
41	yes	no	no	733.9
42	yes	no	no	963.9
43	yes	†	yes	1144.4
44	yes	no	no	463.3
45	no	no	no	876.4
46	no	no	no	843.5
47	no	yes	no	271.3
53	no	no	no	516.0
54	no	no	no	759.5
55	yes	yes	yes	732.8
56	no	yes	no	593.2
57	yes	no	no	100.8
58	no	yes	no	867.7
65	no	no	no	620.7
66	no	no	no	790.3
67	no	no	no	511.7
68	no	yes	yes	870.1
69	no	yes	yes	793.5
70	no	no	no	323.7
71	no	no	no	671.1
73	no	no	no	739.5
74	yes	no	no	833.4
75	yes	no	no	812.1
76	yes	yes	§	517.8
80	yes	no	no	635.8

*Questionable
†Fluctuating
§Remains in Core



TABLE III-7

SUMMARY OF FUEL ELEMENT STATUS

Listed below are the number of elements that correspond to specific combinations of: (a) in during stripping; (b) ran hot during run 14; and (c) damaged

Number of Elements	In During Stripping	Ran Hot During Run 14	Damaged
6	yes	yes	yes
1	yes	yes	no
13	yes	no	no
11	no	no	no
2	no	yes	yes
4	no	yes	no
1	yes	no	*
3	yes	†	yes
1	yes	†	§
1	yes	yes	§

* Questionable

† Fluctuating

§ Remains in Core

A considerable amount of study was required to prepare the SRE hot cell for the fuel cluster canning operation. Special equipment was designed and fabricated to provide an inert atmosphere around the element in order to minimize the risk of a fire in the hot cell during the canning operation. The new equipment included a special tube with a transparent section for a viewing window and sleeve which could be raised when it was desired to disconnect the hanger rod from the fuel element. The container for canning a fuel element is placed in this tube and the assembly is then filled with argon gas. The fuel element is then lowered from the fuel handling cask into this tube while the inert atmosphere is maintained. After canning the fuel element, it is transferred to storage. A complete trial canning run was made on September 29, using a corner-channel dummy.



4. The Sodium System

Circulation has been continuously maintained in all four sodium systems since the end of run 14. Temperatures have been held at about 400°F by means of piping heaters. Cold trapping has been continuous on the primary sodium system.

On September 23, the surface of the sodium was viewed through a window which had been installed in the top shield of the reactor. The surface of the sodium appeared to be clean and reflective.

5. Tests and Observations

A considerable number of tests and examinations has been made upon materials removed from the reactor. Fuel and cladding have been examined in the hot cell along with foreign material which has been found adhering to some of the fuel elements. Samples of the primary and secondary sodium have been analyzed, radiation levels measured, and the cover-gas radioactivity evaluated. Details of the results of these observations are presented in section IV.

6. Recovery Equipment

Apparatus needed for the removal of the broken fuel element pieces from the reactor core has been procured. Viewing windows and lights have been installed in the reactor. A borescope which will be used to examine the process tubes and the moderator cans was obtained. Several types of "fishing" tools have been designed and tested in a mockup.

7. Improved Fuel Washing Procedures

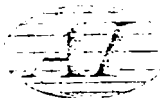
A detailed study of the fuel wash cycle had been under way since the incident following run 13. Tests are being performed to study the pressure surges in a wash cell while a fuel element is being washed. A redesign of the washing procedures and equipment is in progress so that fuel elements can be washed without damage.

8. Preparation of Charts and Data

Charts and tables have been prepared which are useful in describing the reactor history and operating conditions. Several of these are presented



later in this report. Only those data believed to be pertinent to the fuel damage or needed to describe reactor operating conditions have been included. Charts are presented which show reactor power, temperatures, reactivity, etc., during runs 13 and 14. An analysis has been made of various phenomena that could influence reactivity. Reactor kinetics studies were made on the power excursion that occurred at 1825 on July 13. All available information on fuel and moderator temperatures was carefully examined. Records of radioactivity levels were studied. Information was obtained from the examination of fuel and other reactor components. Plans were formulated for the gathering of additional information and data. The details and results of these activities are given in section IV.



IV. DATA AND EVALUATION

A. FUEL TECHNOLOGY

1. Uranium Metallurgy

A condensed review of pertinent metallurgical aspects of uranium, uranium-rich alloys, and thorium will provide a clearer picture of the SRE fuel element damage. SRE Core I contained 35 standard 7-rod elements of unalloyed uranium, one 19-rod UO_2 element, 2 Th-7.6 wt % U elements, and 5 experimental elements containing uranium alloys, uranium, and Th-5.4 wt % U alloy. The uranium alloys included U-2 wt % Zr, U-1.5 wt % Mo, U-1.2 wt % Mo and contained the same percent enrichment as the standard fuel, 2.8 wt % U^{235} . Table IV-A-I indicates the physical property data of interest on both U and Th.

TABLE IV-A-I
PERTINENT PROPERTIES OF URANIUM AND THORIUM

	Melting Point (°F)	Crystal Structure	Phase Changes	Density (g/cm ³)	Thermal Cond. (cal/cm-sec-°C)
U	2060	α , orthorhombic	α 75 to 1220°F	19.0 to 18.3	0.063
		β , tetragonal	β 1220 to 1420°F	18.3 to 18.1	0.086
		γ , cubic	γ > 1420°F	18.1 to 18.0	0.095
Th	3090	<2550°F fcc >2550°F bcc	minor one at 2550°F	11.9 (20°C)	at 20°C, 0.090 at 1200°F, 0.11

The physical properties of uranium are directly affected by the method of fabrication and the impurities present (particularly carbon). The unalloyed uranium was fabricated by rolling in the high alpha phase followed by beta heat treatment to randomize the grain orientation. The SRE fuel was exceptionally pure material; C content was between 50 and 250 ppm. The average density at room temperature was 19.0 g/cm³. Uranium has adequate strength properties in the alpha phase but decreases in ductility when both alpha and beta phases are present. The cubic gamma phase is relatively soft. The low alloy additions to uranium will markedly increase the strength in the alpha phase and produce a



sluggish alpha-beta phase transformation. However, the effects on melting point, phase change temperatures, density, and thermal conductivity will be relatively minor. In the U-2 wt % Zr alloy, there is a change in phase from a simple system to a complex system at a slightly higher temperature than unalloyed uranium. The effects of irradiation on these properties are not well known under SRE temperature conditions, but are believed to be minor. The principal effect observed to date on the properties of unalloyed uranium is the increase in strength and hardness at the lower alpha phase temperatures.³

Since thorium has a cubic structure, it is a relatively simple metal and has normal metallic properties. It has lower strength than uranium at low temperatures but this reverses at higher temperatures. Capsule irradiations have indicated excellent stability at 1% burnup at 1200°F. Relatively little is known of the effects of radiation on the properties of Th-U alloy at SRE conditions.

The radiation distortion in all metal fuels is a major problem. It is of two types: (a) anisotropic growth with no density change; and (b) swelling, accompanied by a density decrease. Uranium, due to its anisotropy, has been shown to grow extensively at low alpha phase temperatures. The usual temperature associated with growth is less than 840°F and swelling generally occurs above 840°F. This transition between the two types of deformation does not occur at a definite temperature and is further complicated by additional factors, such as thermal cycling and burnup rate. Due to the high surface temperature of SRE fuels, swelling appears to be the main problem. The SRE fuel has been destructively examined at various exposure intervals, and some marked dimensional changes have been observed (see Figure IV-A-1).

2. Fuel-Clad Compatibility

Both uranium and thorium form low melting alloys with all major constituents in the stainless-steel clad. Table IV-A-2 shows the eutectic melting points of uranium and thorium alloys with major chemical elements in 304 stainless steel.

4

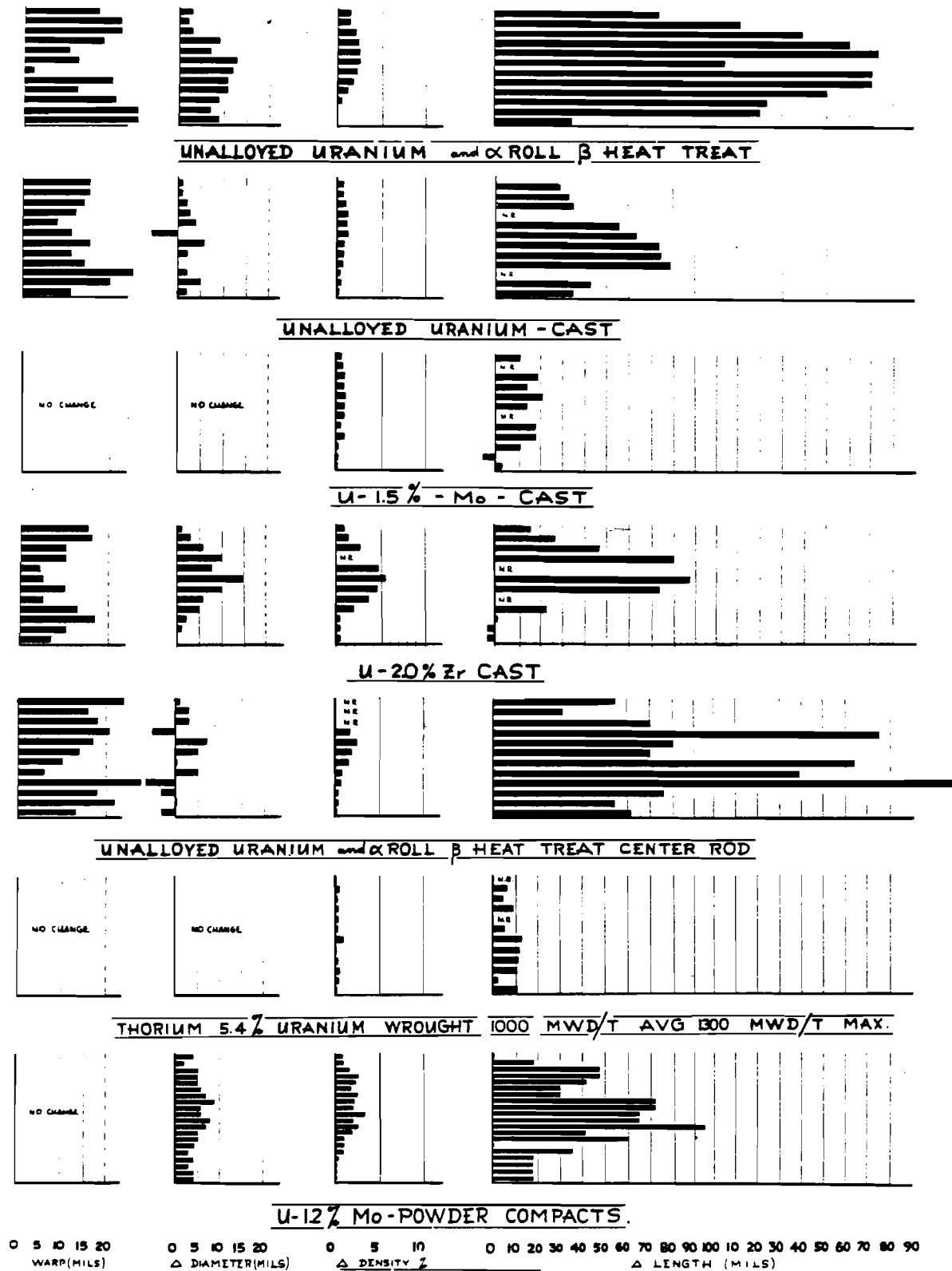


Figure IV-A-1 Radiation Effects on SRE Fuel
(burnup 850 Mwd/T maximum)



TABLE IV-A-2

EUTECTIC COMPOSITIONS OF URANIUM AND THORIUM

U base		Th base	
Composition	Melting Point (°F)	Composition	Melting Point (°F)
U-5 wt % Cr	1578	Th-25 wt % Cr	2265
U-12 wt % Ni	1365	Th-7 wt % Ni	1830
		Th-30 wt % Ni	1875
U-12 wt % Fe	1340	Th-17 wt % Fe	1580

At the present time there are only a few out-of-reactor data on the rate of formation of the most significant eutectic, uranium-iron. During the solid-solid reaction between uranium and iron, all alloy compositions from pure iron to pure uranium will be found. The effect of sodium or radiation on this reaction is not well known. The solubility of both uranium and iron in sodium is low at the eutectic temperature. British results⁴ show that a 0.020-in. stainless-steel can is penetrated in one minute at 1560 to 1740°F. More recent tests at Atomics International⁵ show that uranium reacts with stainless steel within seconds at 2010°F, within minutes at 1790°F, and within a relatively few hours at 1560°F (nonreproducible results to date). Tests are continuing in the 1400 to 1560°F range for more precise reaction rates.

Important factors which affect the reaction rate are the surface oxide layer on the uranium and the degree of contact between the two materials. All fuel slugs in SRE have been centerless ground to 250-rms surface finish. Furthermore, all fuel slugs were electropolished before assembly and thus contained at most a relatively thin oxide film. The exact oxygen content of the NaK bond is not known but was believed to be low. It has been observed by numerous experimenters that the uranium will getter oxygen from the NaK. It is also known that NaK wets uranium oxide more easily than it does uranium metal. Removal of irradiated slugs from destructive examinations after

run 8 has shown that all slugs were relatively clean. Thus, it is reasonable to assume that a thin oxide film was present on the uranium and was not considered undesirable.

The slugs are loose in their jackets (nominal 10-mil annulus) and consequently probably contact the tube at all times at the side or ends. The fuel and clad make additional contact either through fuel diameter increases or fuel warp. Due to the radiation-induced surface wrinkling of the U, the contact between the SRE uranium fuel slugs and the stainless-steel clad would be point-to-point contact. The unalloyed uranium and the U-2 wt % Zr alloy slugs had been observed to grow in diameter sufficiently to stretch the clad slightly in the former case and to at least contact the clad in the latter case. The surface wrinkling of the unalloyed uranium examined at the 850-Mwd/T exposure level was sufficiently severe to estimate only point-to-point contact by this mechanism. The degree of diameter increase, and thus intimacy of contact, is directly proportional to burnup. The measured diameter increases were of sufficient magnitude to contact the clad and occurred at an exposure of 850 to 950 Mwd/T. The fuel slug which had this diameter increase was located near the midplane of the reactor, or position of maximum exposure. The fuel slugs also exhibited sufficient warp at much lower exposures (100 Mwd/T) to cause only point contact between fuel and clad at all slug positions in the 6-ft rod length (see Figure IV-A-1). The warp measurements indicated a saturation of this effect at low exposures and in no case was it sufficient to cause stretching of the clad.

3. Fuel Operating Limits

Design conditions for SRE fuel operation are based on two primary factors: (a) temperature; and (b) burnup. These are not independent variables and are influenced by numerous additional factors which are only now becoming known. It is important to note that the fuel elements in the SRE are operating under untried conditions. There is little data from other reactors that provide sufficient information for even reasonable extrapolation. A few capsules irradiated by AI at MTR and initial data from other sites indicated swelling was a major problem. Knowing this, the operational limits of the fuel were approached with caution. Both destructive and nondestructive examinations were



made at intervals during the reactor operating history to permit sound extrapolations for true core life. These radiation stability data are further supported by measured fuel temperatures at various positions in the core. All of the experimental elements and six standard elements were temperature monitored (see Figure IV-A-2). Each of these elements contained two thermocouples. All of the thermocouples on four of the standard elements were inoperative by the start of run 14.

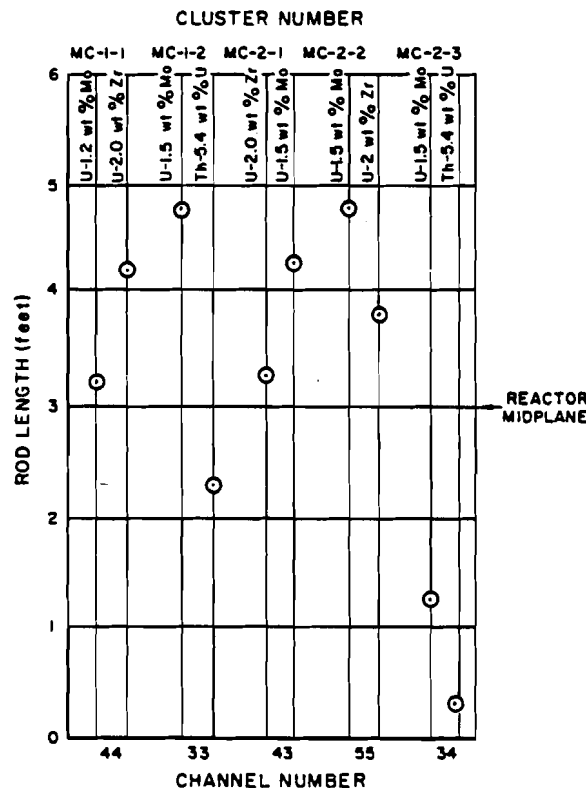


Figure IV-A-2. Thermocouple Distribution in SRE Fuels

The initial design limits were 2500-Mwd/T burnup at 1200°F. This temperature corresponds to the alpha-to-beta phase transformation in uranium. It was conservatively selected due to lack of data and from out-of-reactor results of thermal-cycling tests in this temperature range. The burnup limit was purely an estimate. Hot channel factors were included in the 1200°F limit. Fortunately, under normal operation, the hot channel factors appeared conservative. The operating peak fuel temperature at full power was calculated to be in the range of 1065°F. The peak temperature initially occurs slightly

below the middle of the element, or 36 to 42 in. from the top. Calculations indicate that the position of the peak temperature may shift upward from 12 to 18 in. depending on the position of the control and safety elements. The relation of the center and surface temperatures are shown in Figure IV-A-3.

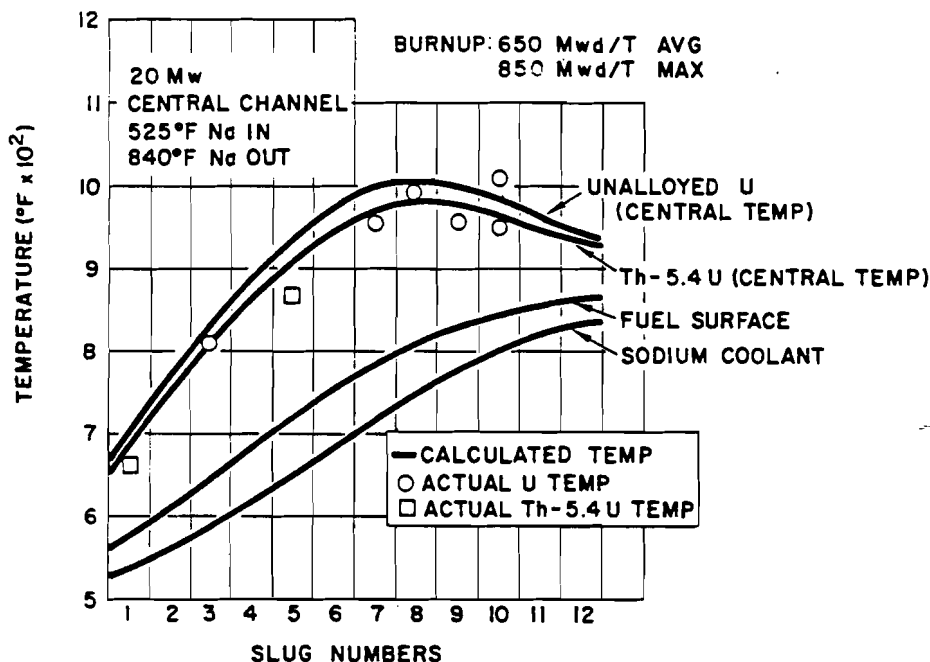


Figure IV-A-3. Temperature Distribution in SRE Fuel

4. Fuel Element History

The primary fuel material in the SRE was unalloyed uranium. In addition, experimental fuel assemblies previously described were included in the core and occupied principally the central core area to achieve more rapid burnup. The positions occupied and the exposure accumulated through run 14 are described in Figure IV-A-4 and Table IV-A-3. There are additional data in Table IV-A-3 which show the fuel thermocouple positions and the number of inspections and washings.

The radiation-damage data on all of the fuel material types at the 850-Mwd/T exposure level at the end of run 8 are summarized in Figure IV-A-1. This Figure represents one destructive examination of a mixed cluster. There were other hot-cell fuel examinations, both destructive and nondestructive, before and after the 850-Mwd/T exposure. A complete list of these examinations

TABLE IV-A-3

HISTORY OF FUEL ELEMENTS IN SRE DURING RUN 14

Core Position	Fuel Element Number	Type of Fuel	Orifice Size	Total Burnup MwD/T	Damaged	Highest Channel Temp. During Run 14	Highest Fuel Temp. at Time (18:00-7/23) of Highest System Sodium Temp.				In Run Number						In June-July Stripping	Number Inspections	Number Handlings	Number Washings	Remarks
							T/C Depth (in.)	Temp. (°F)	T/C Depth (in.)	Temp. (°F)	8	9	10	11	12	13					
4	SU-1-5	std	0.233	576.9	no	970					x	x	x	x	x	x	x	13	12	6	
9	SU-1-6	std	0.370	435.1	no	750					x	x	x	x	x	x	x	10	17	0	
10	SU-1-47	std	0.304	640.4	yes	915					R47	no	no	no	x	x	x	10	25	13	SU-1-7 in runs 8, 9, 10, 11
11	SU-1-8	std	0.348	788.4	no	823					x	x	x	x	x	x	x	9	21	11	
12	SU-1-9	std	0.294	742.6	yes	844					x	x	x	x	x	x	x	14	26	16	
19	SU-7-1	UO ₂	0.890	449.7	no	750					no	no	x	x	x	x	x	9	17	9	SU-1-10 in runs 8, 9
20	SU-11-1	std ²	0.348	820.9	no	770					x	x	x	x	x	x	x	7	11	2	
21	SU-1-12	std	0.400	847.3	yes	845					x	x	x	x	x	x	x	7	15	2	
22	SU-1-13	std	0.415	804.8	no	735					x	x	x	x	x	x	x	7	16	8	
23	SU-1-14	std	0.400	796.2	yes	881					no	x	x	x	x	x	x	5	16	4	SU-1-40 in run 8
24	SU-1-15	std	0.319	298.5	e	880					R24	no	no	no	x	x	x	8	20	7	SU-1-16 in runs 8, 9, 10, 11
25	SU-1-40	std	0.250	703.1	†	828					x	x	x	x	x	x	x	9	17	5	
31	SU-1-17	std	0.348	739.5	yes	894					no	x	x	x	x	x	x	3	3	0	SU-3-1 in run 8
32	SU-22-1	ThU	0.504	437.4	no	740	15	735	45	730	x	x	x	x	x	x	x	11	14	2	
33	SU-2-1	mxz	0.435	932.4	no	750	57	780	69	705	x	x	x	x	x	x	x	8	12	1	
34	SU-2-2	mxz	0.435	1108.7	no	750					R19	R19	no	no	x	x	x	11	21	6	SU-1-38 in runs 8, 9, 10, 11
35	SU-1-10	std	0.415	536.4	yes	854					x	x	x	x	x	x	x	11	18	3	in control room
36	SU-1-27	std	0.356	466.4	no	752	15	725 [‡]	27	740	x	x	x	x	x	x	x	11	20	9	
41	SU-1-18	std	0.370	728.4	no	750					x	x	x	x	x	x	x	14	23	5	
42	SU-1-19	std	0.445	997.1	no	750					x	x	x	x	x	x	x	5	10	0	
43	SU-2-3	mxz	0.480	1135.8	yes	852	21	840	33	1130	x	x	x	x	x	x	x	6	6	0	SU-2-4 in run 8
44	SU-22-2	ThU	0.628	452.8	no	3407					no	x	x	x	x	x	x	15	30	12	
45	SU-1-20	std	0.480	870.8	no	750					x	x	x	x	x	x	x	9	18	8	
46	SU-1-21	std	0.400	838.2	no	750					no	x	x	x	x	x	x	5	11	6	SU-1-47 in run 8
47	SU-1-22	std	0.294	266.5	no	774					x	x	x	x	x	x	x	10	18	8	
53	SU-1-23	std	0.356	510.2	no	745					x	x	x	x	x	x	x	13	21	4	
54	SU-1-24	std	0.415	753.2	no	738					x	x	x	x	x	x	x	4	9	0	
55	SU-2-5	mxz	0.413	726.1	yes	860	15	1290	27	1035	x	x	x	x	x	x	x	10	22	15	SU-1-3 in runs 8, 9, 10, 11, 12, 13
56	SU-1-44	std	0.400	587.4	no	745					R70	no	no	no	no	no	x	5	8	0	SU-1-25 in runs 8, 9, 10, 11
57	SU-12-1	mxz	0.415	95.2	no	750					no	no	no	no	x	x	x	9	13	6	
58	SU-1-28	std	0.387	861.4	no	745					x	x	x	x	x	x	x	8	13	7	
65	SU-1-29	std	0.262	616.4	no	750					x	x	x	x	x	x	x	9	15	6	
66	SU-1-30	std	0.348	784.9	no	750					x	x	x	x	x	x	x	9	14	2	in control room
67	SU-1-26	std	0.433	505.5	no	750	3	700 [‡]	21	715	x	x	x	x	x	x	x	9	16	6	
68	SU-1-31	std	0.415	864.4	yes	890					x	x	x	x	x	x	x	8	17	6	
69	SU-1-32	std	0.400	874.0	yes	835					no	x	x	x	x	x	x	12	20	3	SU-1-44 in run 8
70	SU-1-2	std	0.356	318.3	no	750					x	x	x	x	x	x	x	9	22	8	
71	SU-1-33	std	0.242	667.0	no	835					x	x	x	x	x	x	x	10	23	12	
73	SU-1-34	std	0.294	734.7	no	735					x	x	x	x	x	x	x	7	16	11	
74	SU-1-35	std	0.356	828.0	no	750					x	x	x	x	x	x	x	5	12	8	
75	SU-1-36	std	0.348	807.0	no	750					x	x	x	x	x	x	x	2	13	10	SU-1-43 in run 8
76	SU-1-4	std	0.307	512.9	e	812					no	x	x	x	x	x	x	11	17	7	
80	SU-1-37	std	0.291	631.0	no	760					x	x	x	x	x	x	x				

*Still in core.

†Only cladding damage.

‡Fuel element control temperatures.





MAIN PRIMARY SODIUM INLET AND
OUTLET PIPES ON THIS SIDE

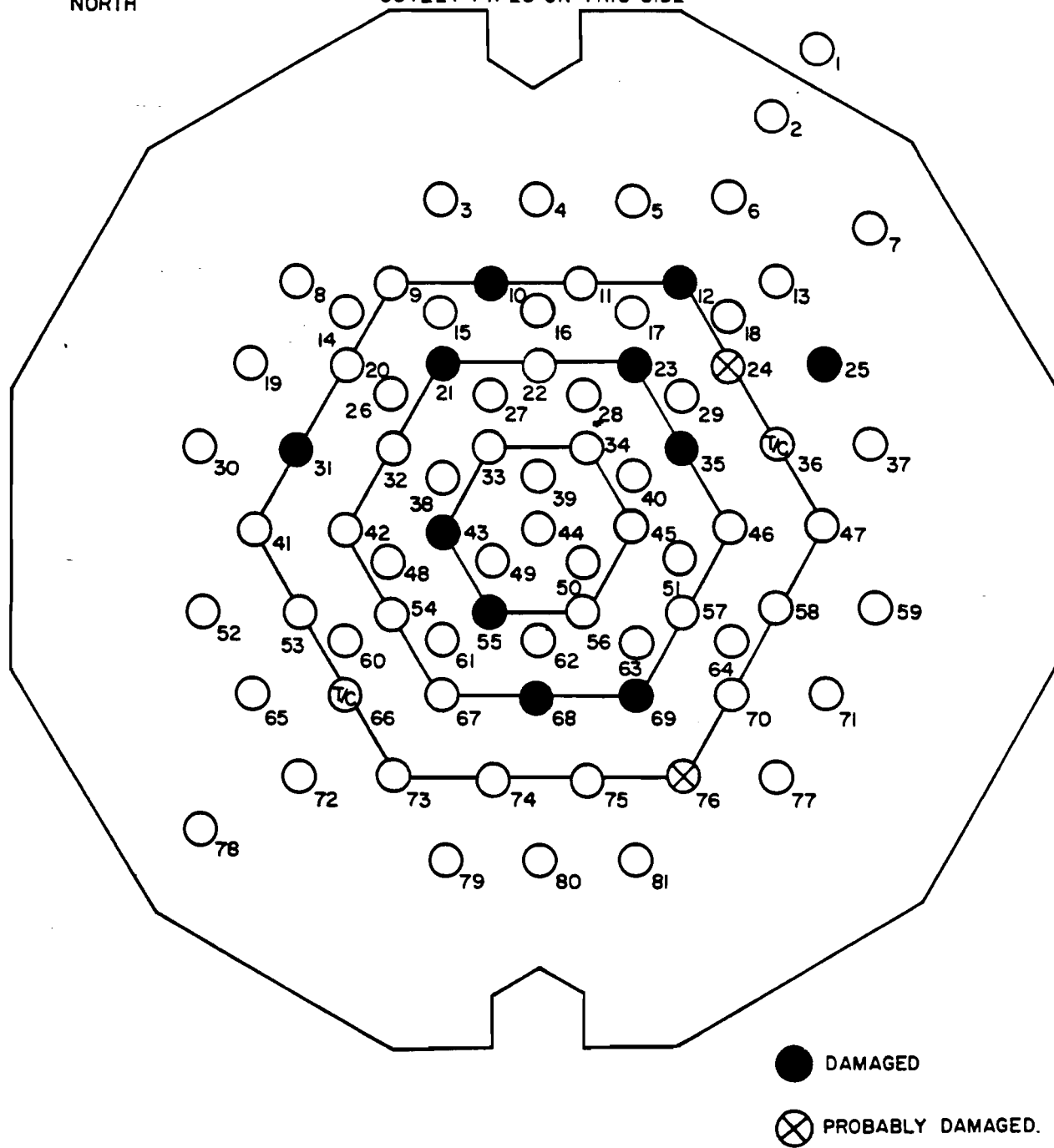


Figure IV-A-4. Location of Damaged Elements in the Core



is shown in Table IV-A-4. It includes 5 destructive, 20 nondestructive, 24 visual, and 16 miscellaneous examinations. The 850-Mwd/T major destructive examination is referenced in Table IV-A-4 as SU-2-4. After the 850-Mwd/T examination, there were two principal nondestructive examinations at 950 Mwd/T and after the short-exposure 1000°F steam run. Neither of these examinations indicated an increase in clad diameter.

The radiation damage varied with each type of material, as shown in Figure IV-A-1. The unalloyed uranium (main standard fuel) had a wrinkled surface, grew in length by 0.210 in., increased in average diameter by 0.013 in., decreased in density by 3%, and warped up to 0.028 in. The U-2 wt % Zr alloy was equally poor, but not in exactly the same characteristics. The other alloys of U-Mo and Th-U were relatively stable. Only the unalloyed uranium had a wrinkled surface.

5. Fuel Element Central Temperatures

Many of the fuel elements in the SRE were instrumented with thermocouples located in the center of the fuel material at various positions in the core. Both standard elements and experimental elements contained this instrumentation. The radial and horizontal locations of the thermocouples in the core are shown in Figures IV-A-2 and IV-A-4. There are two standard elements with central fuel thermocouples that record data in the reactor control room. The remaining thermocouple measurements are recorded on instrumentation outside of the control room.

The normal peak temperature for either standard or experimental fuels at full 20-Mw power was in the range of 1050 to 1075°F. Although the design temperature was 1200°F, the lower temperature is the result of the conservative hot channel factor calculation.

During run 14, a peak temperature of 1465°F was recorded for the element in channel 55 at about 1300 on July 23rd. The complete plot of this temperature history is shown in Figure IV-A-5. As noted in this figure, there was a period of approximately 36 hr during which the fuel temperature in this channel exceeded the normal temperature. This particular thermocouple was located 27 in. from the top of the 6-ft fuel length (above the reactor midplane).

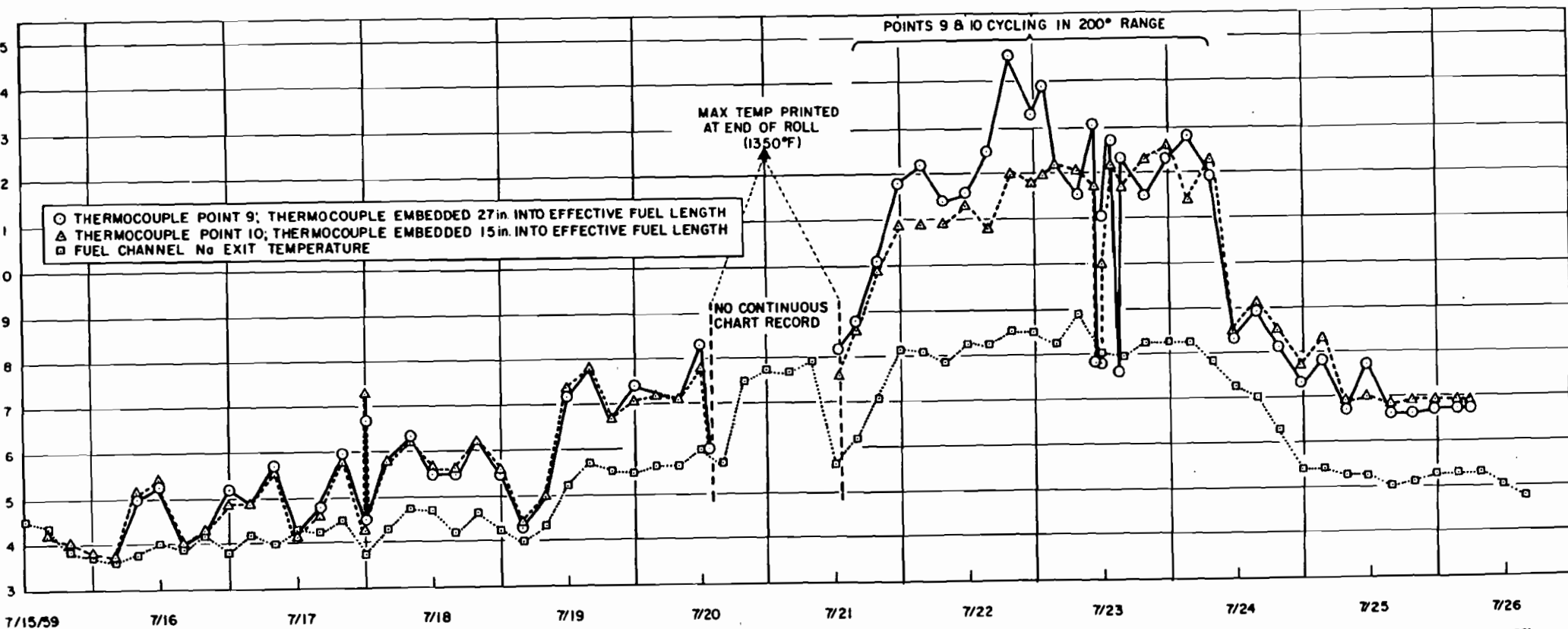


Figure IV-A-5. Temperature History of Element in Channel 55

TABLE IV-A-4*

HOT CELL EXAMINATIONS OF SRE FUEL

Date	Plug and/or Fuel Number	Type of Exam ^a	Remarks
5/14/58	71520-028 SU-1-1	D	Removed rod 81P (remainder in SC 43 as of 1/24/59)
6/20/58	71520-025 SU-1-2	D	Removed rod 371P (remainder in SC 25 as of 8/1/59)
8/7/58	715134-002 SU-1-3	ND & OC	Destructive in wash (WC "B")
8/7/58	71605-003 SU-1-42	ND & OC (new 0.300 in.)	See remarks for 9/8/58
8/7/58	71564-013 SU-1-43	ND & OC	Believed to have been placed in SC 96
9/3/58	71564-001 SU-2-4	ND	Mixed cluster containing rods 204, 581 etc. (location unknown)
9/3/58	715134-002 SU-1-3	ND	Placed in R-56 (orifice (orifice size 0.400 in.))
9/8/58	71605-003 SU-1-42	OC	Placed in SC 49 (listed in file, appears ruptured)
9/22/58	71564-047 SU-1-4	D	Removed rod 169P (storage cell "B")
10/3/58	715134-002 SU-1-3	ND	Placed in R-56
10/6/58	71564-001 SU-2-4	ND	See note on 9/3/58
10/6/58	715111-008 SU-3-1	ND	Placed in R-32 (SC-11 on 12/10/58)
10/9/58	71564-002 SU-1-39	ND & OC (new 0.356 in.)	Placed in SC-32
10/29/58	71520-035	ND	Destructive in wash (WC "C"; 5 rods canned in SC 29) 2 rods in WC "C"
11/5/58	71564-010 SU-1-26	V	Element approved and placed in R-67
11/5/58	71564-012 SU-1-27	V	Element approved and placed in R-36
11/5/58	71520-041 SU-1-33	V	Element approved and placed in R-71
11/6/58	71520-049	V	Record incomplete
11/6/58	71520-029 SU-1-30	V & OC	Element approved and placed in R-66 (OC on 10/10/58 new 0.346 in.; no log)
11/6/58	71520-032 SU-1-45	V	Element set aside due to deposit on wire wrap and rod SC-37
11/6/58	71520-028 SU-1-1	V	Element approved but records hazy as to location (incomplete washing showed some NaO deposit)
11/6/58	71520-026 SU-1-44	V	Element approved and placed in R-70 (black speckled)
11/6/58	71564-051	V	Record incomplete (dark grey spot on lower section)
11/6/58	71564-037 SU-1-36	V	Element approved and placed in R-75
11/7/58	71520-046 SU-1-7	V	Element approved and placed in R-10
11/7/58	71564-013 SU-1-43	V	Element approved and placed in R-76
11/7/58	71520-038 SU-1-9	V	Element approved and placed in R-12 (poor wash job)
11/7/58	71520-052 SU-1-5	V	Element approved and placed in R-4
11/7/58	71520-053 SU-1-16	V	Element approved and placed in R-25
11/7/58	71520-008 SU-1-17	V	Element approved and placed in R-31
11/7/58	715135-005 SU-1-34	V	Element approved and placed in R-73
11/7/58	71520-005 SU-2-2	V	Element approved and placed in R-34
11/8/58	715134-034 SU-1-41	V	Element approved and placed in R-45
11/8/58	71520-033 SU-1-23	OC (new 0.356 in.)	Element approved and placed in R-53
11/8/58	71520-040 SU-1-20	V	Element approved and placed in R-45 (very dark in color)
12/10/58	71605-003 SU-1-42	OC	Record incomplete
12/15/58	715145-019 SU-1-24	OC	Element approved and placed in R-54 (bottom 18 in. very black)
12/15/58	71605-003 SU-1-42	V	Sample taken from orifice plate and rod
12/15/58	71564-051	V	Record incomplete
1/10/59	715134-002 SU-1-3	ND	Believed in R-56
1/24/59	71520-025 SU-1-2	OC & rod change (new 0.400 in.)	1/31/59 OC 2 (new 0.356 in.; placed in R-70)
1/24/59	71520-028 SU-1-1	OC	Record incomplete
1/26/59	71564-047 SU-1-4	OC & rod change (new 0.307 in.)	Placed in R-76 (1/31/59)
1/27/59	71520-043 SU-1-22	OC (new 0.415 in.)	Placed in R-47 (1/31/59)
1/30/59	715134-002 SU-1-3	ND	V taken prior to washing then ND (placed in R-56)
2/9/59	71564-001 SU-2-4	V	Rod 204 removed in preparation for destruction (thermo- couple perhaps broken prior to cell entry)
2/9/59	S SU-22-2	ND	Element approved and placed in R-44
2/16/59	71564-001 SU-2-4	D	Total cluster
3/2/59	715134-002 SU-1-3	ND	Orifice plate crusty and gummy (cluster also crusty; placed in R-56)
4/6/59	715134-002 SU-1-3	ND	Element approved and placed in R-56
4/7/59	71520-040 SU-1-20	ND	Element approved and placed in R-45
4/8/59	71520-027 SU-1-38	ND	Destruction in wash (5 rods in SC 77; 2 rods in WC "A")
5/13/59	715134-002 SU-1-3	V (may have been more)	Removed rod 57 and put on 209
5/25/59	715134-002 SU-1-3	ND	Placed in R-56 (destructive in WC "B" 6/4/59)
5/25/59	71520-040 SU-1-20	ND	Element approved and placed in R-45
5/26/59	715134-002 SU-1-3	D	Rod 57 removed in preparation for destruction
7/9/59	71520-026 SU-1-44	OC (new 0.400 in.)	Element approved and placed in R-56 (7/10/59)
TOTALS			
	a) Destructive		5
	b) Nondestructive		20
	c) Visuals		24
	d) Orifice change		14
	e) Rod changes		2

* Legend: D = destructive; ND = nondestructive; OC = orifice change; R = reactor channel; SC = storage cell;
V = visual; WC = wash cell



The damaged section of most of the fuel rods, including this element, was roughly 12 in. below the reactor midplane. Thus, the maximum temperature that occurred was probably considerably in excess of the 1465°F observed. The exact temperature may never be precisely known. However, observations of microstructure and eutectic compositions of various fuel components may provide additional data on which to base a more exact peak temperature.

All fuel monitoring thermocouple data have been examined. There were several standard fuel thermocouples that became inactive during previous reactor operation. During runs 13 and 14, there were six fuel elements in the reactor that were providing fuel-temperature data. Four elements were located in the central area of the core and two were located in the second and third rings of fuel. Thermocouples on the latter two were in standard elements recording in the reactor control room. The other four were experimental elements. The location and maximum temperatures recorded during power runs 13 and 14 are shown in Table IV-A-5.

During run 13, there are inconsistencies in temperatures at various levels. The maximum temperature 1125°F at the 27-in. level occurred between two lower temperatures, 975°F at the 21-in. level and 1025°F at the 33-in. level. Although the 1125°F reading appears high, the 975°F temperature appears low. It is difficult to ascertain the true significance since there are minor variations in fuel element hardware, such as orifice plate size, thermal conductivity of alloys, and thermocouple standardization, that could affect the measurements. It would appear, however, that channel 55 ran slightly hot during run 13.

Experimental clusters in channels 33 and 34, which were not damaged, ran at much lower temperatures during run 14 than the adjacent elements which were damaged.

Since both elements in channels 43 and 55 were damaged, and the peak temperatures were significantly different, it can be surmised that the damage occurred either at different times or to different degrees. Since the experimental fuel recorder was being repaired during the calendar period July 12 to July 15, the exact time sequence during this period is not known.

TABLE IV-A-5
SRE FUEL TEMPERATURES

Channel Number	Element Number	Thermocouple Depth (in.)	Fuel Material	Run 13		Run 14	
				Maximum Temp (°F)	Time & Date	Maximum Temp (°F)	Time & Date
33	SU-2-1	15	U-1.5 wt % Mo	1050	1200, 5/30; 1600, 6/1	760	0001, 7/23
33	SU-2-1	45	Th-5.4 wt % U	950	1200, 5/30; 0001, 6/2 to 0800, 6/2	750	
34	SU-2-2	57	U-1.5 wt % Mo	850	0001, 6/2 to 0800, 6/2	800	0001, 7/23
34	SU-2-2	69	Th-5.4 wt % U	725		750	
43	SU-2-3	21	U-2.0 wt % Zr	975	1600, 6/1	900	0600, 7/24
43	SU-2-3	33	Th-5.4 wt % U	1025		1100	0001, 7/24
55	SU-2-5	27	U-1.5 wt % Mo	1125	0400, 5/29	1465	2000, 7/22
55	SU-2-5	15	U-2.0 wt % Zr	1100	1600, 5/29	1400	Between 1300, 7/20 and 1300, 7/21
36	SU-1-27	27	U	1000		780	
36	SU-1-27	15	U	-	-	-	-
67	SU-1-26	21	U	925	-	720	-
67	SU-1-26	3 (C)	U	-	-	-	-



The two standard fuel elements monitored in the reactor control room did not indicate any high temperatures during any period; neither of these elements was damaged.

6. Effects of Contamination During Run 14

The examinations of fuel elements to date have been principally visual. No broken elements have been examined in detail. During the removal of two broken elements, a few pieces of fuel slugs and cladding separated from the element and were retrieved for examination. Additional small pieces of clad, wire wrap, and carbonaceous appearing material were removed for analysis. The types of analyses performed to date include (a) visual, (b) dimensional, (c) microscopic and metallographic, and (d) chemical.

a. Fuel Element Visual Examinations

The three visual techniques used to examine all fuel elements have been television, hot cell, and periscope. For television examination, the camera is located inside the fuel cask at the bottom. The resolution on the screen does not allow minute details to be examined. The technique does provide an excellent opportunity to observe gross defects. Broken elements were first discovered after run 14 with this method. The second technique is an SRE hot cell procedure with modifications for containment of inert nitrogen gas to minimize fire hazards. The hot cell observations were made in conjunction with the canning of the fuel elements. All of the last 17 elements removed from the core were canned.

The time spent on detailed visual examination in the hot cell has been small. All of the damaged elements appear quite similar; therefore, a fairly careful visual examination was made only on the first element. These positions of fracture are determined to be between 1/3 and 2/3 of the length, measured from the top of the element. It is not planned to examine each damaged element unless the visual inspections indicate more than one type or mechanism of damage. A typical damaged element is shown in Figures IV-A-6, IV-A-7, and IV-A-8. The composition of the fuel in that element is shown in Figure IV-A-9. At least one damaged element will be transported to the Component Development Hot Cell (CDHC) for more detailed study.

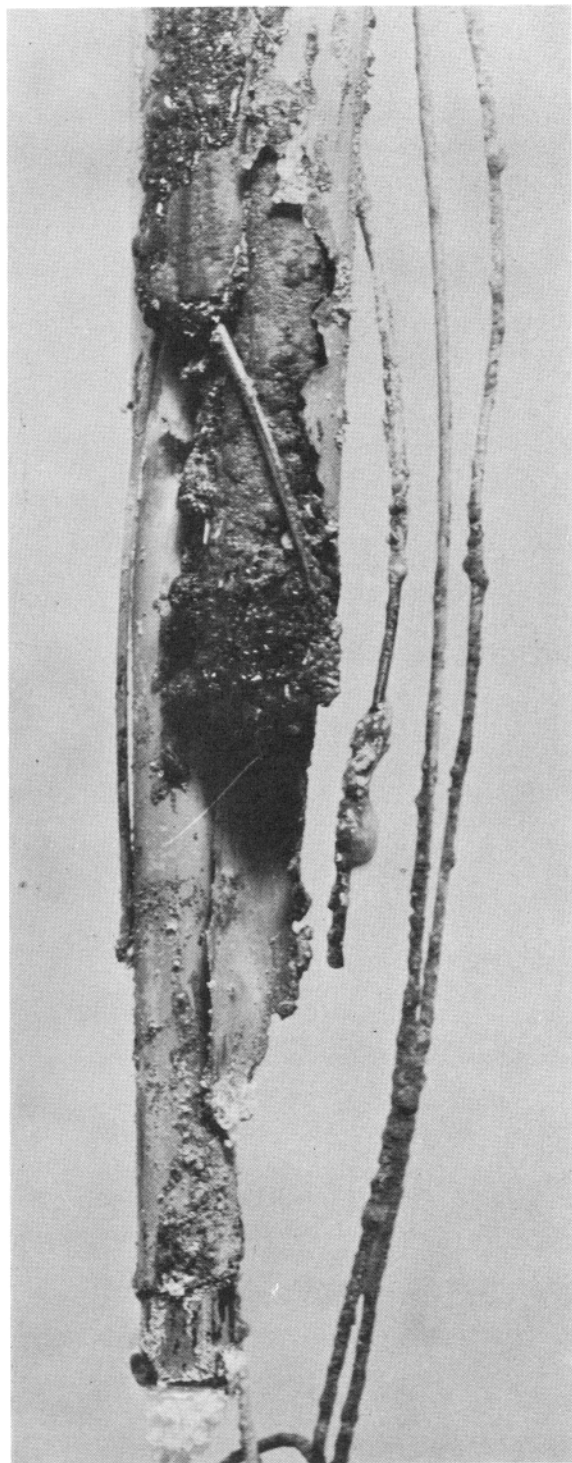


Figure IV-A-6. Bottom of Damaged Element in Channel 55



Figure IV-A-7. Midsection of Damaged Element in Channel 55

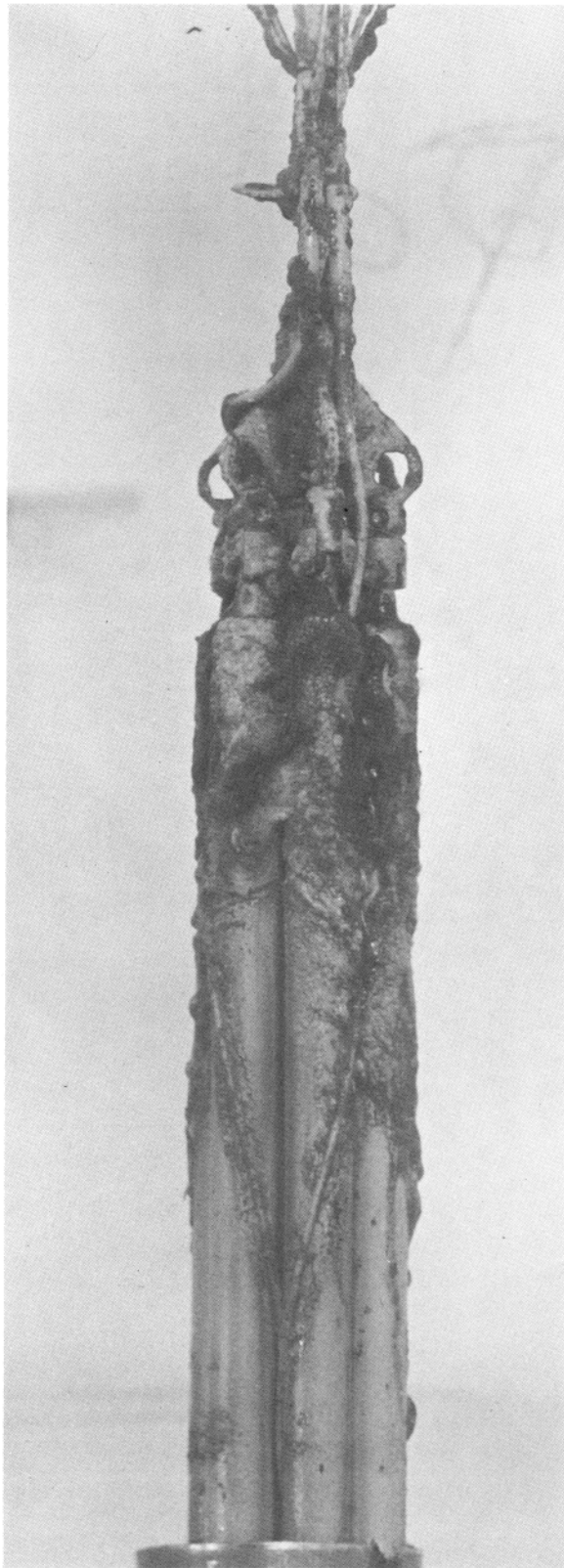


Figure IV-A-8. Top of Damaged
Element in Channel 55

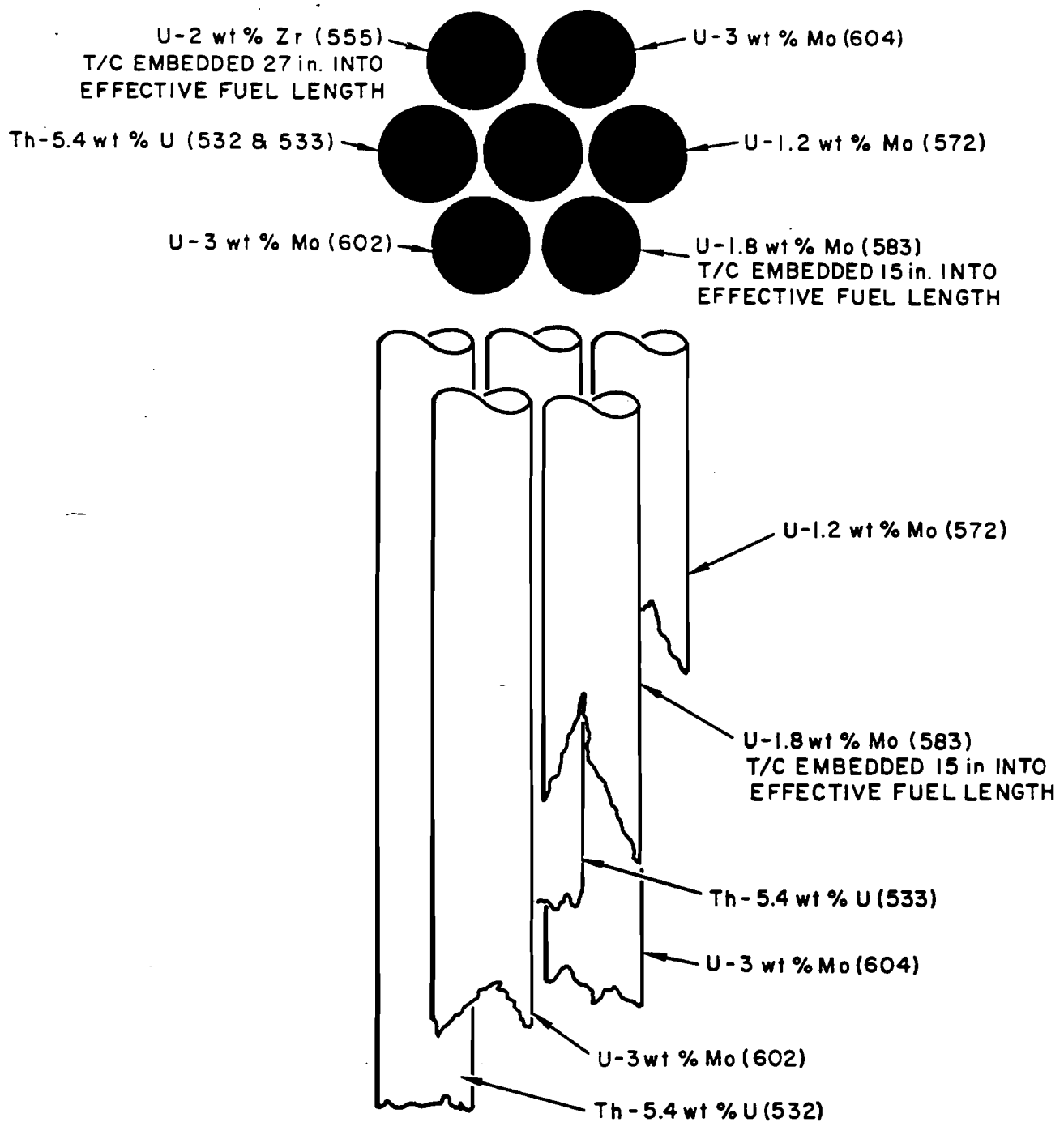


Figure IV-A-9. Identification of Fuel Rods from Element in Channel 55



A third visual method was recently introduced. It consisted of a periscope mounted inside the reactor vessel above the sodium level with illumination provided in other access holes. A clear observation of each withdrawn element can be made. This successful method was used sometimes with, sometimes without, the television camera examination.

b. Cladding Analyses

Pieces of clad, wire wrap, and fuel slugs have been examined in greater detail at the CDHC using microscopy, magnifying glasses, and stereo-photos. Small sections of clad were available from damaged elements from channels 55 and 12. These pieces fell off during fuel-element-removal operations. Photographs of the cladding from the element in channel 55 are shown in Figures IV-A-10 and IV-A-11. Typical sections of the damaged clad were observed. The inside of the clad contained a thick, rough, adherent layer of material. Chemical analysis indicated 71 wt % U and 5 wt % Fe. This section of clad had a very jagged edge and contained some holes.



Figure IV-A-10. Small Piece of Cladding I from Element in Channel 55

Other small pieces of clad were chemically analyzed in the as-received and pickled conditions. The as-received material contained 90 wt % U on the inside surface and 10 wt % U on the outside surface. This same section after pickling in HNO_3 indicated no uranium on the outside and 1 wt % U on the inside. None of these clad specimens were magnetic and thus are not believed to have nitrided.

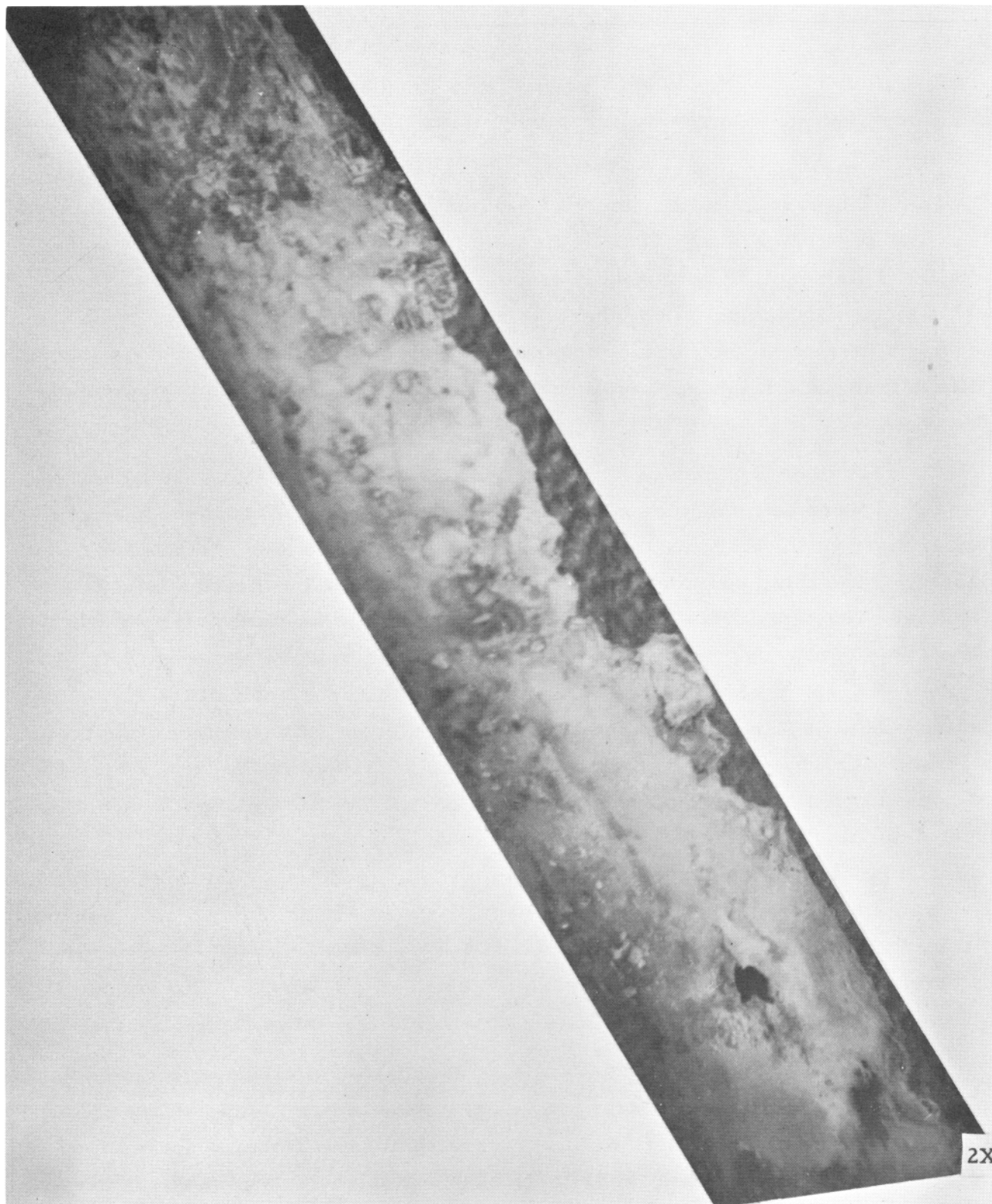


Figure IV-A-11. Small Piece of Cladding II from Element in Channel 55



A second specimen was pickled and dissolved for chemical analysis. Duplicate results showed good agreement in composition; 70 to 75 wt % U and 25 to 30 wt % Fe. The clad was brittle in some areas and ductile in others; thus, indicating local rather than general reactions.

Other specimens of cladding were analyzed for carbon content and showed an increase from the standard 0.08 wt % carbon content of 304 stainless steel to 0.36 wt % carbon. Thus, in this section carburization may have occurred. This result is not unlikely since high temperatures were known to exist in this area. A conclusion of general carburization or nitriding must await a thorough analysis at known positions and known temperatures. Out-of-pile tests indicate that sodium system carburization or nitriding is not an anticipated condition.

The three pieces of fuel rod recovered from the damaged element in channel 12 were held together with pieces of clad. The first piece is a single slug encased in the cladding. The second consists of two slugs encased in cladding. The third contained three slugs held together intermittently with cladding. Through careful previous identification, the original positions of these slugs in the fuel rods were located. The locations are shown in Figure IV-A-12. Note that these slugs are from the upper half of the element and from external appearance show extensive reaction. These pieces are from the element in channel 12 which became severely jammed in the transfer cask. Attempts to free the element resulted in the parting of these pieces from the main element. Examination of the ends and edges of the clad indicated: (1) fracture or brittle failure, rather than melting, and (2) a corrosion reaction in streams lengthwise on the clad, perhaps U-Fe eutectic. A stereophotograph of the edge fracture is shown in Figure IV-A-13. The corroded section showing the streaming effect is shown in Figures IV-A-14 and IV-A-15. Summary of analyses of materials from damaged fuel elements are shown in Table IV-A-6.

Metallographic examination of all of the clad specimens is incomplete. Only one specimen has been examined. Etching of the specimen has been difficult. It is hoped to correlate this microstructure with that observed in out-of-reactor tests. These latter tests have shown various microstructures depending on the temperature of reaction. Thus, this examination technique may also provide additional data on temperatures reached in the damaged fuel area.

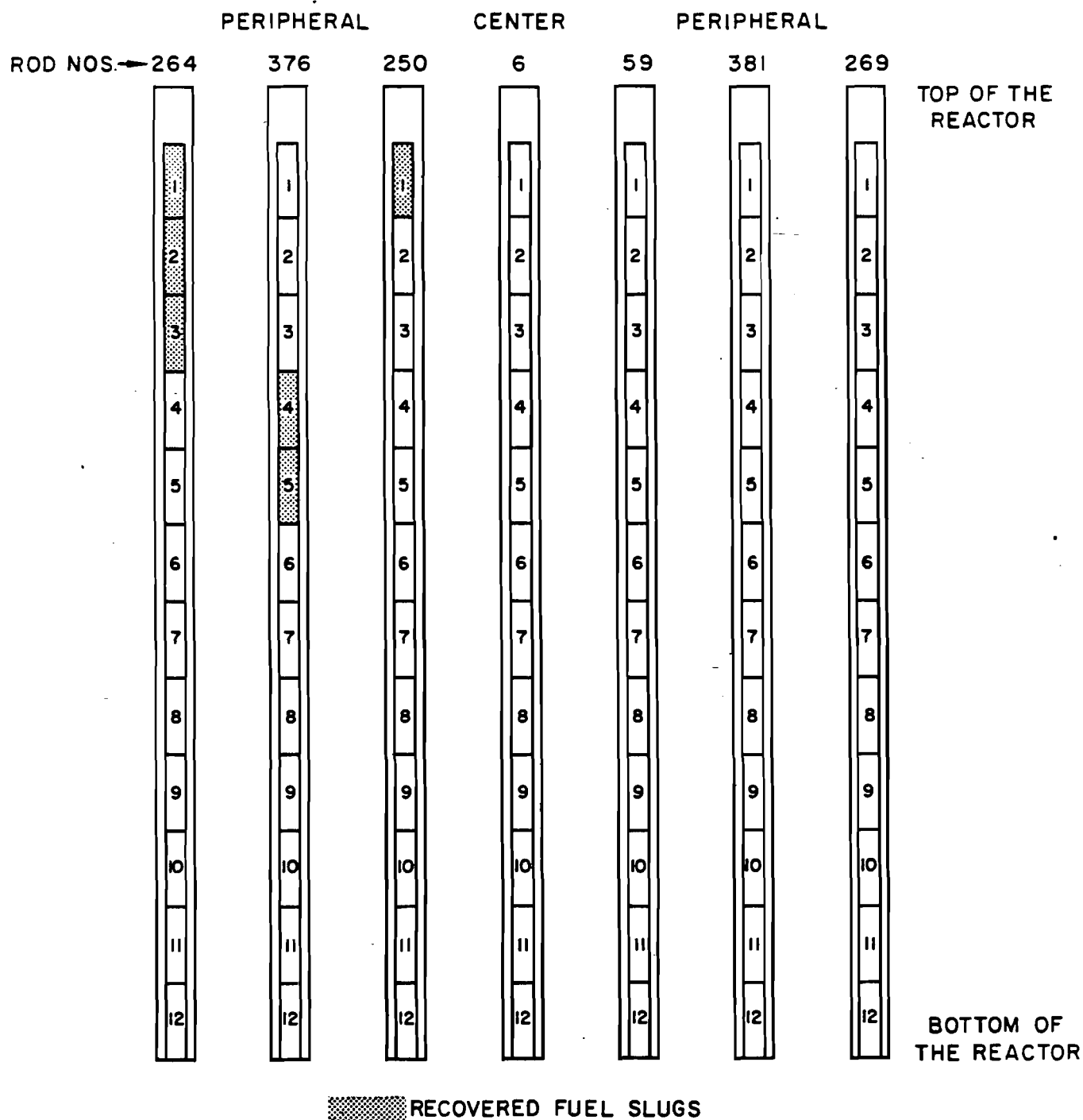
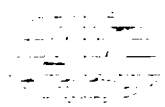


Figure IV-A-12. Location of Recovered Slugs in Channel 12.

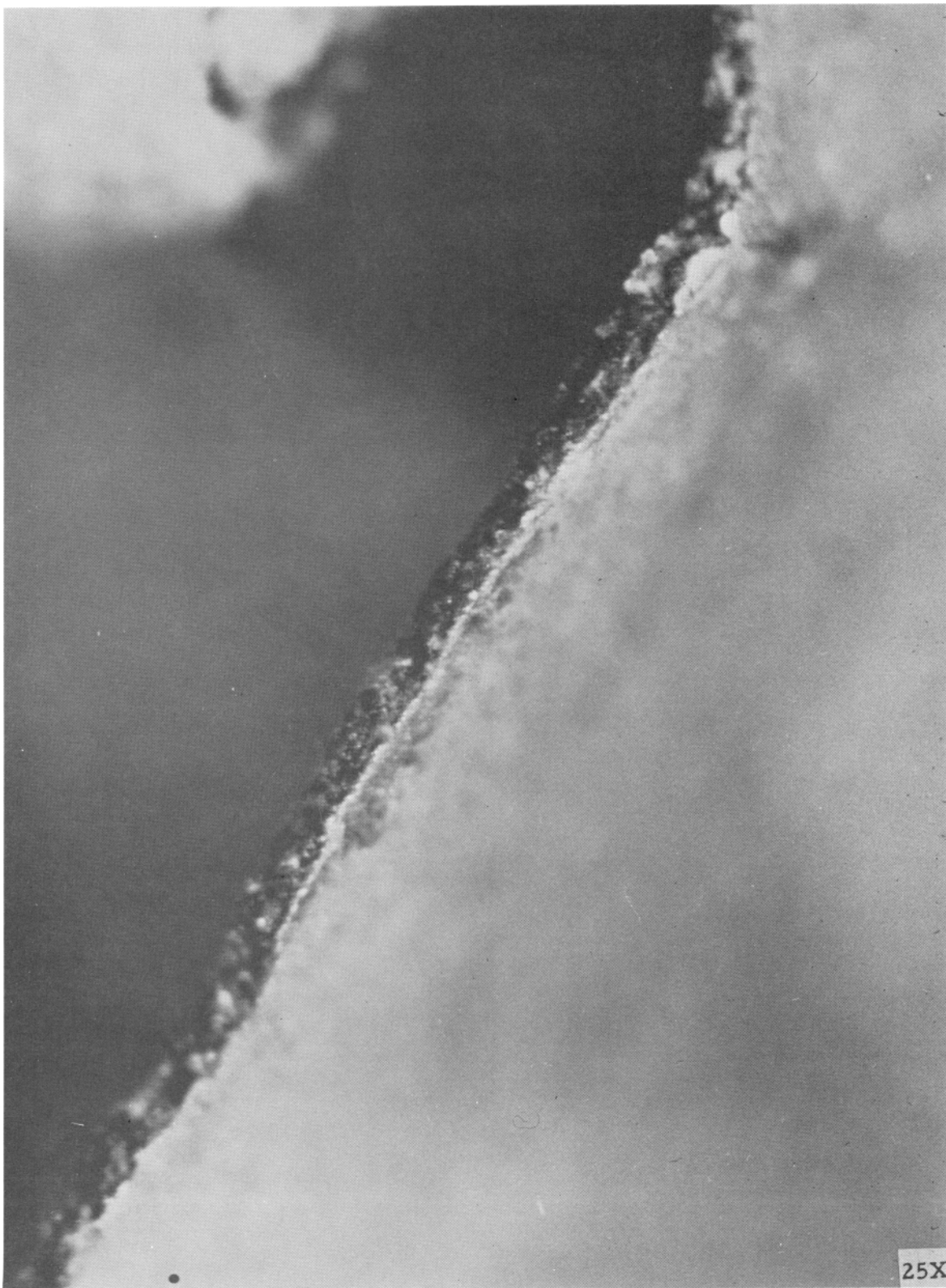


Figure IV-A-13. Edge of Cladding Rupture



Figure IV-A-14. Streaming Reaction I on Cladding
from Element in Channel 12

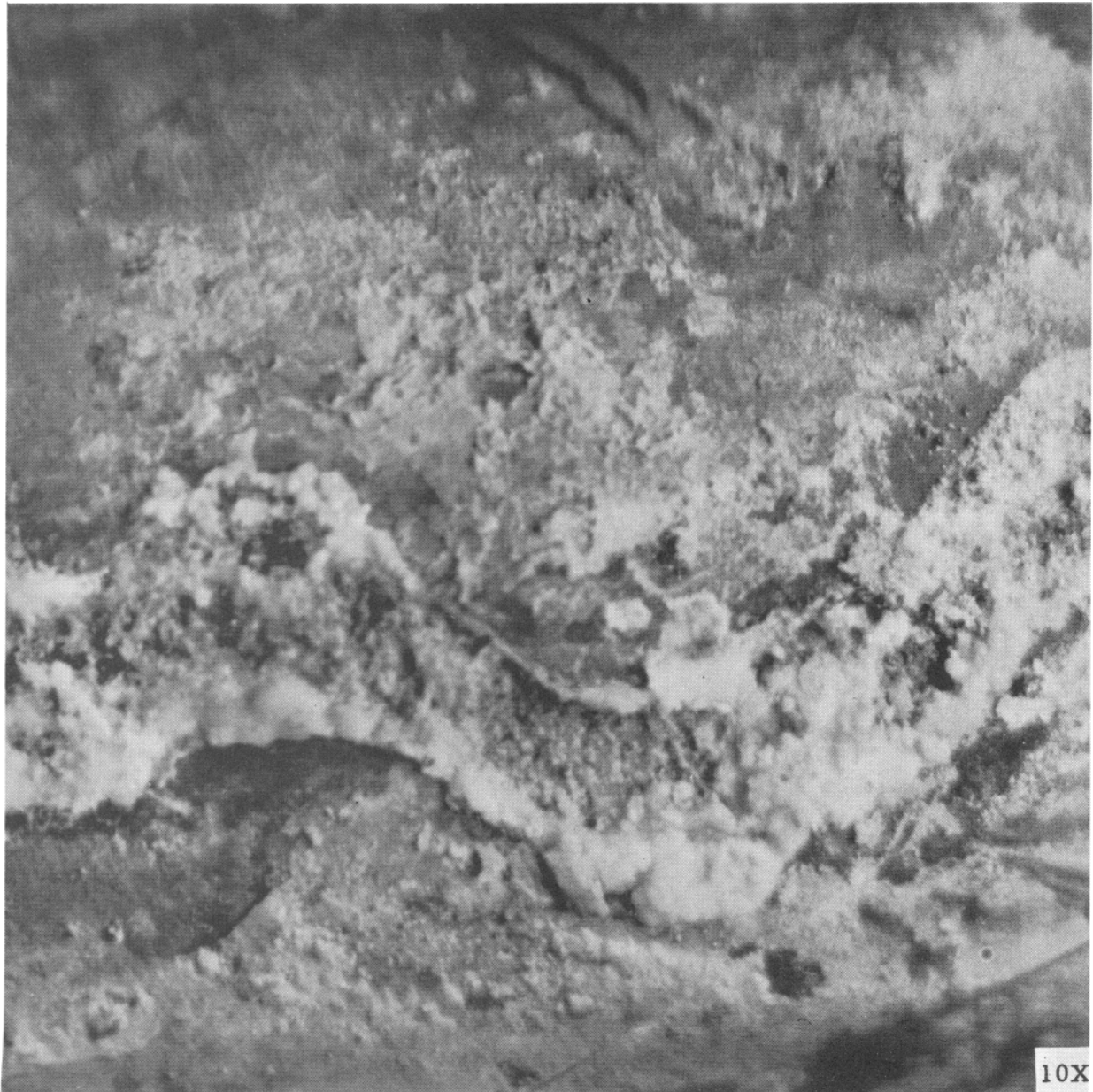


Figure IV-A-15. Streaming Reaction II on Cladding from Element in Channel 12

TABLE IV-A-6

ANALYSES OF MATERIALS FROM ELEMENT IN CHANNEL 55

Item Analyzed	Sample Condition	Analytical Method	Results	Remarks
1. <u>Element 55 CDHC</u> Cladding piece	As received	X-ray fluor.	90% U	Inside surface
	As received	X-ray fluor.	10% U	Outside surface
Cladding piece	Washed in conc. HNO_3	X-ray fluor.	1% U	Inside surface
		X-ray fluor.	nil U	Outside surface; also had a dull metallic luster
Cladding piece	Washed and soaked in conc. HNO_3	Wet chem.	71.5% U 26.4% Fe	Total solution
	Washed and soaked in conc. HNO_3	Wet chem.	73% U 23.6% Fe	Total solution
Cladding piece	Washed and soaked in conc. HNO_3	Vacuum fusion	5030 ppm O_2 70 ppm H_2 120 ppm N_2	Duplicate samples for results
Cladding piece	Washed and soaked in conc. HNO_3	Conductometric and combustion	0.36% C	Total destructive test
Material taken from the element on inside of clad as received	In solution with conc. HNO_3	Wet chem.	70.6% U	Total sample run
2. <u>Element 55 SRE</u> Na residue from the top of fuel element	Dissolved in HCl	Wet chem.	17% Na 3% Fe 6% C	These values were calculated from weights given in report.
Na residue from the top of fuel element	Dissolved in HNO_3	Combustion and X-ray fluor.	14.5% C	Includes CO_2 pickup
Wire wrap sample	Washed with conc. HNO_3	X-ray fluor.	nil U trace Mo	Solution analysis separate (metal only)
Wire wrap sample	Washed with conc. HNO_3	Wet chem.	82% U 8.8% Fe	Solution only
Wire wrap sample	HNO_3 cleaned metal sample	Combustion	0.11% C	

* The first sample is from a piece of fuel element 55 that fell from fuel handling cask.



c. Wire Wrap Chemical Analysis

The 0.090-in. -diam 304 stainless-steel wire wrap on the seven-rod fuel element is used to separate fuel rods and provide uniform cooling of the central rod and inside surfaces of the peripheral rods. The wire wrap is welded at the top and bottom only. As shown in Figures IV-A-6, IV-A-7, and IV-A-8, the wire wrap is broken and considerably distorted. Samples of the wire wrap from the first damaged element in channel 55 were removed and chemically analyzed. Results are shown in Table IV-A-6. One sample showed no uranium and a trace of molybdenum. Another showed strong evidence of the presence of approximately eutectic composition material, 82 wt % U + 9 wt % Fe. A carbon analysis showed a slight but not significant increase in carbon content, 0.11 wt % C. These analyses are from relatively few samples and will be verified as additional specimens are taken.

d. Dimensions of Fuel Specimens

The three pieces of fuel rods briefly described above (Section IV-A-6-b) were measured in CDHC. Results are summarized in Table IV-A-7 and represent fuel-plus-clad measurements except as noted. The original outside diameter on all fuel rods was 0.790 in. \pm 0.002 in. In many sections of these samples this dimension increased by a large percentage. The maximum increase noted was to 0.952 in. Generally the increases were to about 0.850 in. This increase may be due to: (1) any eutectic formed occupying a larger volume than the constituents, (2) swelling of the uranium fuel slug as the entire slug temperature increased, (3) the formation of other compounds (external or internal) with the foreign materials by reactions between the fuel, Na, Na oxide, and tetralin decomposition products. The damaged pieces are no longer round.

During the dimensional analysis, individual fuel-slug identifications were made by determination of the numbers stamped on the end. A typical slug end from the damaged area is shown in Figure IV-A-16. The ends are severely cracked.

e. Analyses of Foreign Material from Fuel Element

Samples of the material that clung to the upper fuel element hardware were removed from the element in channel 55 during hot-cell examination. The

TABLE IV-A-7

DIMENSIONS OF FUEL SLUGS FROM ELEMENT IN CHANNEL 12

	End (in.)	Middle (in.)	End (in.)
Specimen From Rod 250 Containing One Slug in Clad	0.784	0.787	0.801
	0.781	0.824	0.810
	0.788	0.814	0.823
Specimen From Rod 376 Containing Two Slugs in Clad	0.878	0.868	0.883
	0.857	0.833	0.878
	0.886 (near split in clad)	0.854	0.830 (near split)
Specimen From Rod 264 Containing Two Slugs in Clad	0.751 (slug only)	0.829	0.836
	0.757 (slug only)	0.827	0.907
	0.751 (slug only)	0.855	0.952
Specimen From Rod 264 Containing One Slug in Clad	0.770	0.769	0.790
	0.792	0.791	0.772
	0.773	0.768	0.793

material changed in character during the two hours in the hot cell due to reaction of the sodium with the moisture in the air. It had a black tar-like appearance. Some samples of this material had a gummy consistency and some were brittle at the time chemical analyses were made. Chemical analyses showed the material contained 6% carbon as free particles, 17% sodium, and 3% iron. The remainder probably consisted of oxide, hydroxide, carbonate, and water because the sample was handled in air. Table IV-A-6 is a tabulation of these analytical results.

f. Analytical Calculation of Cladding Temperatures

Graphite temperatures measured during the latter portion of run 14 in the vicinity of channels 21 and 23 are shown in Table IV-A-8. The temperature differential across the graphite is quite large compared to temperature differentials of 16°F or less obtained during power run 4. Using these data, the assumption that the channel was plugged, and that the helium gap in the



Figure IV-A-16. End of Fuel Slug from Element in Channel 12

TABLE IV-A-8

MODERATOR TEMPERATURE MEASUREMENTS

Date 1959	Hour	Channel 23			Channel 21				Reactor Power (Mw)	Reactor Sodium Temperature		Main Primary Flow (gpm)
		5 ft Down Center (°F)	5 ft Down Outside (°F)	Exit (°F)	2 ft Down Center (°F)	5 ft Down Inside (°F)	5 ft Down Outside (°F)	Exit (°F)		Inlet (°F)	Outlet (°F)	
7/20	2105	803	765	743	782	783	765	726	1.56	650	693	860
7/21	0500	871	862	780	812	846	795	750	2.14	658	694	1500
	1500	658	624	627	635	649	624	612	1.47	537	525	925
	2120	842	791	780	791	812	778	765	1.50	670	710	925
7/22	0530	896	863	820	879	896	846	778	2.24	685	745	925
7/24	0505	905(max)	905(max)	-	905(max)	905(max)	905(max)	-	3.68	685	745	1510
	2300	649	589	-	591	615	576	-	1.77	462	508	900
7/25	0530	598	567	-	563	576	546	-	1.31	473	507	900
	2300	593	554	-	554	571	541	-	1.16	475	505	900
7/26	0645	598	559	-	559	580	550	-	0.96	480	505	900
8/18	1400	376	372	-	372	372	375	-	-	379	-	1200



moderator can was 0.007 in., the extrapolated temperature profiles shown in Figure IV-A-17 were obtained for channel 23. The indicated temperature uncertainty in Figure IV-A-17 is due to uncertainty in the values of thermal conductivity. As may be seen for the assumed conditions, a power level of 2 Mw is sufficient to raise the cladding temperature above that required for the formation of the eutectic or other low melting alloys. A power level of 3.6 Mw could elevate the temperature past the boiling point of sodium. If a larger helium gap is assumed, the temperatures are much higher.

7. Mechanisms of Cladding Failure

The fuel element cladding failed when the stainless steel alloyed with the uranium fuel. Insufficient coolant flow in the fuel channel permitted the temperature of the fuel-clad interface to increase to a level where solid-solid diffusion of iron and uranium could occur at a significant rate. At all locations where temperatures were above the melting point of the iron-uranium eutectic (1340°F), this diffusion resulted in the formation of an alloy with some liquid phase present. This liquid phase would not necessarily have the composition of the eutectic. The liquid would first form at the inner surface of the cladding where the temperature was high and the uranium concentration in the steel at the maximum. When the alloy formation had proceeded to a point where the fuel cladding remaining could no longer sustain its load, failure occurred.

The belief that the fuel cladding failure occurred by this mechanism is supported by chemical analyses of pieces of cladding and spacer wire. It is unlikely that either carburization or nitriding contributed in a major way to the cladding failure. None of the cladding specimens examined was found to be magnetic; thus the specimens are not believed to have nitrified extensively. Some carburization occurred in the region of failure as must be expected with the sodium saturated with carbon and with temperatures sufficiently high to produce accelerated solid diffusion of uranium into the cladding. Perhaps the best argument against the likelihood of failure by carburization or nitriding is the integrity of the 19-rod oxide cluster which was in channel 19. This element was observed, by means of the television camera, to be severely plugged upon removal from the reactor, yet suffered no parting of the fuel cladding.

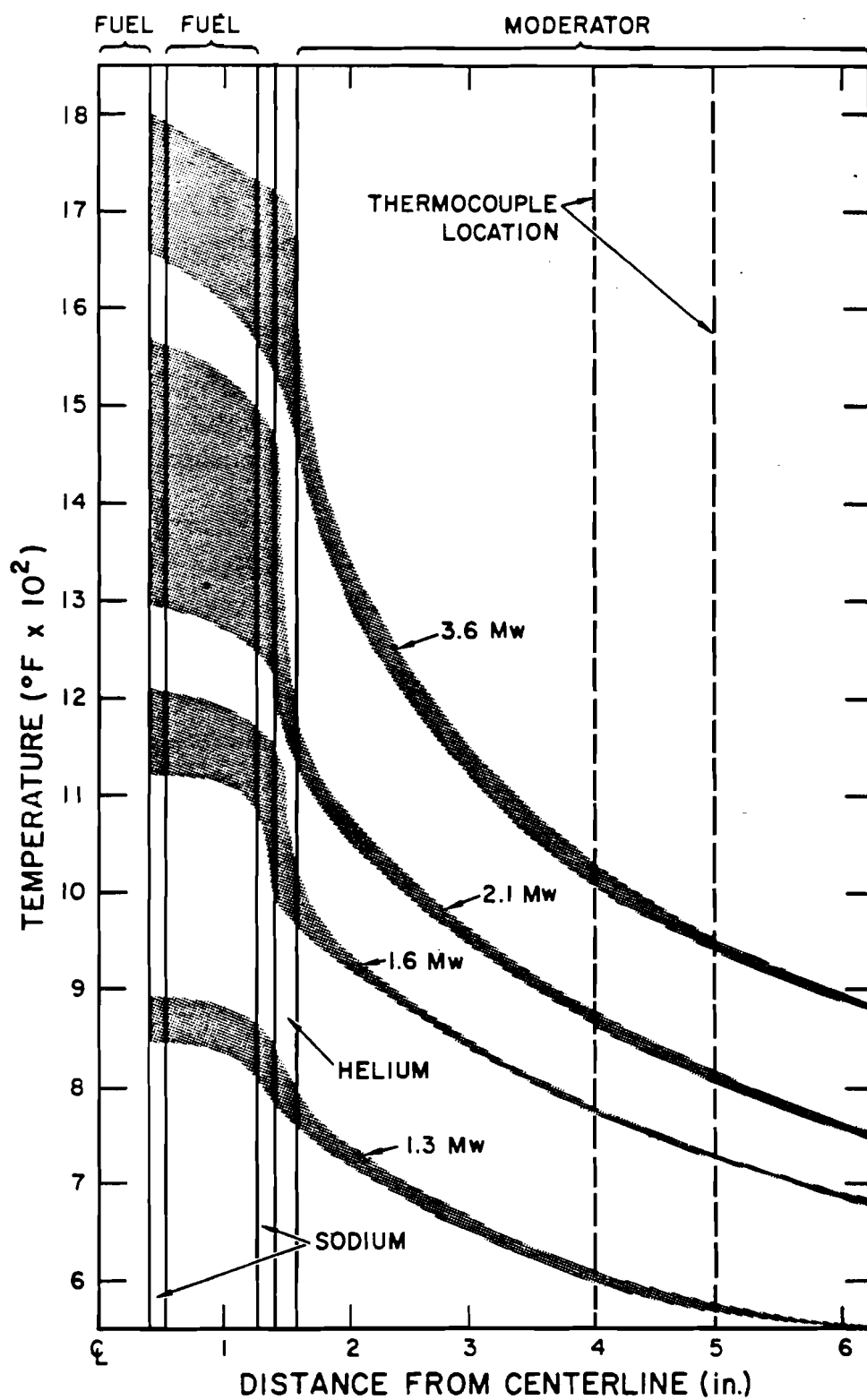
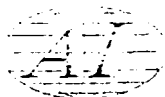


Figure IV-A-17. Temperature Profiles in Moderator and Fuel



It seems quite likely that the first cladding failure occurred during the afternoon of the first day (July 12) of run 14. This conclusion is drawn from the observation that the radioactivity in the high-bay area (over the reactor loading face) increased markedly at this time and was almost certainly due to leakage of reactor cover gas into the area. It was believed at the time that a seal had failed on the sodium level probe. It now seems more likely that the leak had existed for some time and was suddenly noticeable because of the large increase in the radioactivity of the cover gas. The activity in the radioactive gas decay tanks also showed a sharp increase with the first samples taken after the start of run 14 on July 15 (see Figure IV-C-1). The activity in these tanks decayed continuously after July 15, indicating that most of the cladding failures had occurred by this time.

The temperature history of the element in channel 55 (Figure IV-A-5) shows that the temperature of the uranium was increasing after July 15, reaching a peak of 1465°F on July 23. This element parted at a point roughly 20 in. below the thermocouple. The parting probably occurred prior to July 15 however, and the increasing temperatures at the thermocouple were due to the formation of an additional plug in the region of the thermocouple.

Examination of the radiation history of the reactor cover gas shows that no large amount of gaseous activity had been released to the system prior to run 14. This supports the conclusion that no gross fuel cladding failures (other than the possibility of pinhole leaks) occurred until run 14.



B. REACTOR COOLANT CONTAMINATION

1. Potential Contaminants

a. Tetralin

Tetralin has been used in the SRE to provide cooling for the reactor structure and system components, i.e., freeze seals and bearing housings of the four centrifugal pumps in the heat transfer circuits, freeze seals for the main and auxiliary system valves and moderator-reflector inlet valve, mass transfer assembly, diffusion cold traps, and the biological shield. Tetralin is a derivative of naphthalene made by hydrogenating one ring completely, leaving the other unchanged. It is a clear colorless liquid with high solvent power and low toxicity. The commercial material has a boiling point in the range of 405 to 420°F; it has a specific gravity slightly less than 1; it decomposes in the temperature range of 800 to 850°F.

The location of the coolant lines in some of the components listed is such that a failure in the line could result in tetralin being admitted to the sodium system. Prior to the operation of the SRE, experiments were performed to answer questions on the effect of liquid sodium on the decomposition of tetralin, reaction of decomposition products of tetralin with sodium, and the effects of the decomposition products of tetralin on system components. It was concluded from these experiments that the reported thermal decomposition temperature of 800 to 850°F was the temperature at which rapid decomposition occurred. These experiments also indicated that, in the presence of sodium, the decomposition temperature is reduced to about 675°F. The decomposition rate of tetralin is so greatly increased in the presence of sodium, that if tetralin were to leak into the SRE sodium during operation at design temperatures, it would quickly decompose to hydrogen, free carbon, and a mixture of low molecular weight aliphatic hydrocarbons. In the temperature range 470 to 675°F, the rate of decomposition is rather slow and, in this temperature range, hydrogen and naphthalene are the major decomposition products. At temperatures below 475°F, little decomposition results.

Hydrogen and carbon are the two elements of concern, which result from high temperature decomposition of tetralin. Much of the hydrogen will be absorbed by the sodium, and the remainder will collect in the cover gas.



The zirconium in the moderator cans will absorb hydrogen from the sodium, and, as the hydrogen content of the sodium is depleted, the hydrogen in the cover gas will be absorbed by the sodium. Ultimately, a large fraction of the hydrogen will be absorbed into the zirconium, and the remainder will be in dilute solution in the sodium. This assumes that hydrogen is not lost from the cover gas through venting or purging to the decay tanks.

The carbon resulting from the decomposition of tetralin will dissolve in the sodium up to the limit of its solubility at reactor operating temperature, and the excess will probably exist in the form of small particles. The dissolved carbon will ultimately cause carburization of the stainless steel heat-transfer-system components to an extent that is a function of both time and temperature.

Experiments have been performed at Atomics International on the time and temperature dependence on carburization of SS in carbon saturated sodium. Some of the results of these experiments for carburization of Type 304 SS to a depth of 2% of the wall thickness in a number of SRE components are shown in Table IV-B-1.

TABLE IV-B-1
EXPOSURE TIME FOR CARBURIZATION *
OF STAINLESS STEEL †

Section Thickness (in.)	Exposure Time (hours)					
	1000°F	1100°F	1200°F	1300°F	1400°F	1500°F
0.010 (fuel-rod cladding)	49	7	2	1	0.03	0.004
0.058 (heat-exchanger tubing)	1,750	244	50	12.2	1.2	0.17
0.250 (piping)	31,700	4580	1100	230	22.5	3.2

* To 2% of wall thickness

† Type 304



Volume carburization to a depth of 2% is a very safe limit for all components of the SRE system. For heavy sections of the SRE system such as tank walls and piping at sodium temperatures less than 1100°F, the time required for carburization to a depth of 2% is many thousand hours. The strains in these components are sufficiently low to result in no impairment in the physical properties of the system.

In the fuel jacket, where strains are known and are very low, carburization to much higher concentration can be safely tolerated. Some carburization may have occurred in the high temperature runs, but there is yet no evidence that carburization contributed to the fuel cladding failure.

Carburization of the stainless steel will result in depletion of the carbon content in the sodium. If there is excess carbon in the system (that is, undissolved carbon in the form of particles) more carbon will then dissolve in the sodium, where it will be available for further carburization of the stainless steel.

The initial carbon content of the sodium, as it was charged into the SRE system prior to reactor startup, was less than 20 ppm. Analyses for carbon that were made prior to run 8 indicated that the carbon content was less than 50 ppm. By visual observation that solid carbon particles were present in the system sodium in December 1958, April 1959, and June 1959, it can be assumed that the system has been saturated with carbon ever since run 8.

b. Oxygen

The reaction of oxygen with sodium will produce sodium oxide, Na_2O , which is soluble in sodium to an extent determined by the temperature. This dependency on temperature is the basis for the design of the oxide removal system used in the SRE. A bypass stream of sodium from the system is cooled enough to produce precipitation of sodium oxide which is removed from the system and retained in the cold trap.



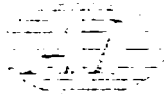
The solubility dependency on temperature that is exhibited by sodium oxide results also in the possibility of unwanted deposition of solid sodium oxide in other parts of the system where low temperatures exist. Undissolved sodium oxide can plug flow passages, reduce flow to critical equipment, and interfere generally with system operation. For this reason it is good practice to limit the oxygen content to a value less than saturation at the lowest system temperature, preferably to less than 10 to 20 ppm.

Another effect of the oxygen content of the sodium is that it has been shown to be one of the most important factors affecting corrosion in sodium systems. At oxygen contents above 100 ppm, the corrosion rate for many materials is markedly accelerated. This problem is of little concern to the SRE, because the oxide concentration is maintained substantially below 100 ppm during power operation.

Oxygen can enter the system by means of in-leakage of air through seals or during fuel handling operations, by introduction as an impurity in the initial sodium charge, and in the helium introduced in the system as the cover gas; or by admission of air to the system when, during repair operations, portions of the system are open. Following reactor shutdowns, the SRE sodium system is operated at low temperature, circulating the sodium through the cold trap, until such time as the oxygen content is down to a safe level for high temperature operation. The oxygen concentration is determined by means of a plugging indicator which is a device that also depends upon the temperature effect on oxide solubility for its operation. A bypass stream of sodium is slowly cooled in a heat exchanger which is located just prior to a flow restriction. When the saturation temperature is reached, sodium oxide precipitates, plugs the flow restriction, and causes a sharp change in the flowrate meter on the plugging indicator. Using a solubility curve, this temperature, which is referred to as the plugging temperature, can be directly related to the oxygen content.

2. Indications of Contamination During Runs 8 and 13

Each fuel element in the SRE is orificed to allow an approximately equal temperature rise in each channel through the core. A wide variation in the fuel-channel exit temperatures indicates an abnormal distribution of coolant among



the fuel channels. This situation may be due to improper orifice selection or to restriction in flow passages in the fuel channels. The variation among exit temperatures increases with power level. At full design power of 20 Mw, fuel-channel exit-temperature spread of about 100°F is considered acceptable. At low power of 1 to 2 Mw, the maximum spread of about 20°F is normal. Table IV-B-2 shows some selected values of fuel-channel exit-temperature spread during runs 8, 12, 13, and 14. The fuel-channel exit-temperature spreads for run 12 are typical of a good run.

Run 8 started on November 29, 1958, but operation was restricted to low power because a very wide spread of fuel-channel outlet temperatures existed. The maximum difference in outlet temperature between the coldest channel and the hottest channel was about 385°F at a power level of 3.6 Mw. In addition to the high fuel-channel exit-temperature spread, it was noted that the plugging temperature was also high. It was believed at the time that high oxide concentration was the cause of the abnormally large temperature spread. The delay in bringing the reactor to power was to permit cold trapping to be done to reduce the oxide concentration. The oxide was presumed to have been introduced during the interval between runs 7 and 8, when the primary sodium was pumped back and forth between the core tank and the primary fill tank while repairs were being made to the primary sodium system. This was done in order that the sodium could be heated in the primary fill tank and returned to the core to maintain the core tank and the moderator can assembly at suitable temperature. It was known that the primary fill tank had a substantial amount of sodium oxide deposited in it. The sodium in the fill tank dissolved the sodium oxide (the maximum concentration being determined by the fill-tank maximum temperature), and then on return to the cooler core tank, which was at a lower temperature, this sodium oxide was precipitated.

Because of the excessive temperature spread, one fuel element was removed from the reactor from channel 9 for examination and a sample of sodium remaining on the element obtained for analysis. Black specks were observed to be present in the sodium sample. A second element, from channel 10, was examined and appeared to be black at the bottom. Washing of these elements removed the foreign material, which resulted in a decreased temperature spread. A total of 15 elements was washed and the reactor was

TABLE IV-B-2

FUEL-CHANNEL EXIT-TEMPERATURE SPREAD

Run Number	Date	Time	Reactor Power (Mw)	Maximum Spread of Fuel- Channel Exit Temperatures (°F)
8	12-7 -58	0900	0.8	55
	1-9 -59	0900	16.6	180
	1-24-59	1700	19.0	165
12	5-15-59	0300	1.3	20
	5-17-59	1300	20.3	95
13	5-30-59	0500	20.6	100
	5-31-59	1100	19.5	125
	6-1 -59	0500	19.6	135
	6-2 -59	0700	19.2	140
14	7-13-59	1300	2.0	230*
	7-14-59	0300	2.0	180†

*Before power excursion. Some thermocouples indicating variations of 50° over short time intervals.

†After power excursion.



restarted. The run was interrupted again for further fuel element washing when high exit temperatures occurred. Operation was resumed, but increased coolant flow rates were required to minimize the temperature spread.

During run 8, on January 7, 1959, a sample of core cover gas was bubbled through cyclohexane, and an analysis was made for tetralin or its derivatives. Naphthalene was identified by spectrophotometer. Because no gas flow measurements were made, interpretation of the results was only qualitative, but it was definitely established that tetralin was present in the system. Previous to this time it had not been realized that tetralin had entered the primary sodium system. (A leak of tetralin in the main primary pump case occurred in June, 1958, but it was thought that none of this tetralin had entered the primary sodium.)

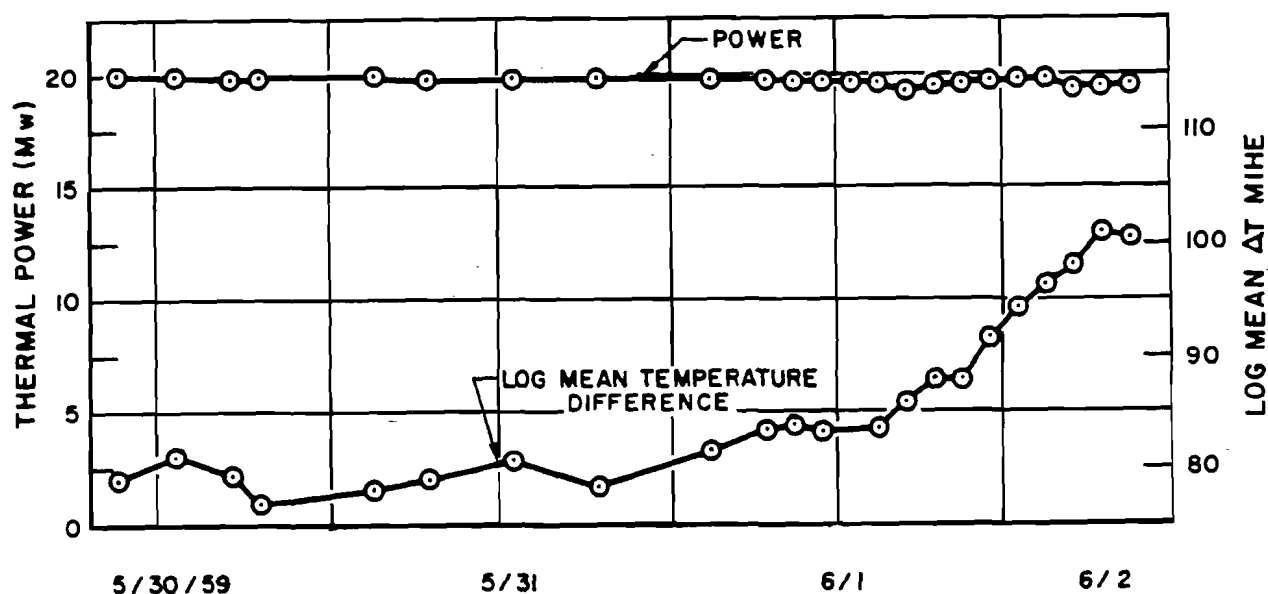
Following run 8, preparations were made to obtain samples of the foreign material in the core. A filter was installed in an empty fuel channel after run 11 and sodium was circulated through the primary system. The filter consisted of three screens in series, 20-, 60-, and 100-mesh. One large particle of the dimensions $1/4 \times 3/8 \times 1/32$ in. was obtained; however, most of the material lodged on the 60-mesh screen. The material was removed from the screens and analyzed. Solids that were insoluble in methyl alcohol were identified as carbon or carbon compounds by the combustion method. The large particle was examined visually and appeared to consist of pieces of carbon and a white material agglomerated into the large piece. The white material was assumed to be sodium and sodium oxide. Upon analysis, the sample of black material that was removed from the fuel element from channel 9 (during run 8) showed approximately 9 wt % of amorphous carbon in addition to sodium and sodium oxide. The sample was characterized as being hard and brittle.

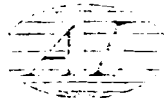
Referring again to Table IV-B-2, during run 13, it can be observed that a satisfactory fuel-channel exit-temperature spread was obtained during the early part of the run; that is, a spread of 100°F was the maximum at 20.6 Mw up until May 30. Starting the following day, at approximately the same power level, the temperature spread began to increase. At the same time the reactor inlet temperature gradually rose from 545°F to 580°F and the run was terminated on June 2.



A plot of the log mean temperature difference across the main intermediate heat exchanger, Figure IV-B-1, for the last part of run 13 shows that the temperature difference increased from 76 to 101°F, indicating that the heat exchanger was being fouled by some unknown material or that the flow area in the heat exchanger was being restricted.

All of these factors were recognized as symptoms of tetralin leaking into the system because of the similarity to the previous experience with the tetralin leak prior to run 8.





downcomer, and carried naphthalene out through the vent line. Naphthalene was identified by the characteristic odor.

At the conclusion of the nitrogen stripping, 4700 ft³ (STP) of helium was used to purge the reactor system.

An investigation of possible nitriding effects on stainless steel as a result of bubbling nitrogen through carbon-bearing sodium was started at the time of the stripping operation. So far as is known, the solubility of nitrogen in sodium is so small that it cannot be measured. Therefore, only negligible quantities of nitrogen could be retained in the sodium by this particular mechanism. However, nitrogen could be retained in the sodium by either of two other mechanisms: (a) reaction with calcium impurity to form calcium nitride; and (b) formation of calcium or sodium cyanide (or cyanate) in carbon-bearing sodium. The calcium nitride or the sodium cyanide then could be carried throughout the primary cooling circuit by liquid sodium and could come into contact with various metal surfaces of stainless steel and zirconium. Nitriding could occur at a rate depending upon temperature and to a depth depending on time.

Preliminary conclusions of the tests are that nitriding will occur below the liquid level of either calcium-bearing or carbon-bearing sodium. Type 304 stainless steel exposed to carbon-bearing sodium with nitrogen cover gas at 1200°F will nitride rather than carburize. (Although this particular test has not been performed at 1000°F, it is believed that the same results will occur but at a lower rate.)

At 1000°F, it is estimated that the 0.010-in. -thick stainless steel fuel cladding will be nitrified to a depth of 2% in only 230 hours. Nitriding to a depth of 2% may be somewhat conservative, and if the data are extrapolated to a depth of 10% the time required is increased by a factor of 25 to about 5800 hours. This represents about 240 days of operation with sodium at 1000°F.

There is some evidence that nitriding of zirconium occurs in sodium systems under the same conditions that cause nitriding of 304 stainless steel. There is ample data in the literature on nitriding of zirconium in gaseous nitrogen at temperatures above 700°F. Specific diffusion rate data are not readily available below 1550°F, but there is an indication that the penetration



rate is more rapid for zirconium than for 304 stainless steel at temperatures of interest. The literature indicates that room temperature mechanical properties of zirconium are affected appreciably by nitriding, but above 700°F there is little effect on these properties.

Temperature conditions and nitrogen-stripping procedures were repeated on a small scale in preliminary tests performed at Atomics International on sodium containing carbon. The system was purged with helium to remove any remaining nitrogen cover gas. After reheating to 1200°F, it was found that nitriding then occurred to the same extent as when a nitrogen cover-gas was present. This indicates that significant quantities of nitrogen were tied up by calcium impurity and/or carbon during the bubbling operation and this source provided a means of nitriding during subsequent reheating to the higher temperatures.

These tests indicate that similar sources for nitriding may still remain in the sodium in the SRE primary system. Because this sodium has not been above 1000°F (except in overheated fuel channels) since the nitrogen-stripping operation, it is likely that no nitriding has resulted from this operation.

4. Indications of Contamination During Run 14

a. Temperature Effects

The fuel-channel exit-temperature spread was the most significant indication that either oxide or tetralin contamination was still present in the primary sodium during the early part of run 14. Note in Table IV-B-2 a value of temperature spread of 230°F at 2.4-Mw power on the first day of operation. Some fuel-channel exit temperatures were varying as much as 50° over 5-min intervals as indicated on the recorder. The fuel-channel exit temperature spread had been as high as 260°F during the time prior to the reactor excursion which occurred on July 13. After the excursion, the maximum temperature spread was reduced somewhat for a period of time to 180°F at 2.0-Mw power.

Studies were made of the fuel channel exit temperatures which occurred during portions of power run 14. All damaged elements appear to have exhibited symptoms of temperature fluctuation. This fluctuation was apparent at the very outset of power run 14, but did not appear prevalent during run 13.

Those elements which ran hot during run 14 but did not fail, did not show this symptom. The one channel (R-25) which exhibited damage to the cladding but remained intact, exhibited the fluctuation characteristic only sporadically.

During operations at reduced powers with a low temperature drop across the core, calculations are not normally made of the log mean temperature difference across the main intermediate heat exchanger. It was therefore not known whether the fouling of the heat exchanger as indicated in run 13 had been cleared up or whether the situation was still in existence.

The consistently high plugging temperatures and the fact that no improvement could be realized in spite of nearly isothermal operation (low core delta T) up to 700°F also indicated that the system was functioning abnormally. Previous experience had shown that excess sodium oxide could be removed by cold trapping after running with high system temperatures, over a period of a few days.

The moderator delta T fluctuations and abnormal response to system changes presented further evidence of difficulty. The observation that the moderator temperature did not respond properly to an increase in sodium flow, indicated that insufficient sodium was leaking across the grid plate for moderator cooling. This could have been the result of fouling or plugging of the relatively small flow passages around the moderator can pedestal which is at the lowest system temperature.

b. Tetralin Leakage

Some idea can be obtained of the amount of carbon and hydrogen released to the sodium by in-leakage of tetralin to the primary system prior to run 14. The best estimate of the time at which the leak started is about May 30, as indicated by loss of heat transfer coefficient in the primary heat exchanger and related phenomena (see Chronology of Events, Section III). The effects of the leakage became important in changing the LMTD of the primary heat exchanger by June 1 (see Figure IV-B-1). The reactor was shut down on June 3, but pump operation continued until June 12.

The tetralin leaked into sodium at about 1000°F from May 30 to June 3. At this temperature the tetralin would immediately vaporize and



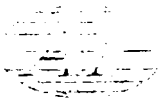
quickly decompose, probably all the way to hydrogen and carbon. For the following 9 days the tetralin leaked into the sodium at about 350°F; at this temperature it would stay in the liquid form.

If it is assumed that the leak rate was constant (discussed below), approximately two-thirds of the tetralin was admitted to the system in liquid form. If the tetralin floated to the surface of the upper sodium pool (density difference about 0.07 gm/cm³ at 4000°F), the nitrogen stripping operation (conducted between June 17 and July 5) should have removed essentially all of the liquid tetralin. About 3 pints of liquid tetralin were recovered in this operation, together with about 1 lb of naphthalene crystals. This would indicate a total tetralin leakage into the primary system of the order of 1 gallon. This estimate neglects the possibility of formation of an emulsion which might prevent removal of part of the tetralin.

Tetralin leaked through a small (about 1/32-in. -diam) hole worn through the wall of the freeze-seal gland of the main primary sodium pump. The pump shaft was hard surfaced in the area of the freeze seal. The plating loosened during pump operation, and a fragment of the hard material wore through the wall of the freeze-seal gland as the shaft rotated. It is impossible to estimate the amount of tetralin leakage from the size of the hole in the freeze seal gland, since it opened into a region of frozen sodium.

Another way of estimating the tetralin leakage is to examine the makeup rate in the tetralin system. Unfortunately, the normal makeup rate is approximately 2.5 gallons per day, so that a loss of a few additional gallons during the period from May 31 to June 12 would not be noticed. However, the fact that there were no unusual additions of tetralin to the system during this period indicates that the leakage into the primary system must have been considerably less than a barrel (55 gallons).

While the evidence is not conclusive, it seems likely that the total tetralin leakage during and following run 13 was 1 to 10 gallons, corresponding to about 8 to 80 lb. Since tetralin is 90.9% carbon and 9.1% hydrogen, this corresponds to a range of about 7 to 70 lb of carbon and about 0.7 to 7 lb of hydrogen. These figures represent all of the carbon and hydrogen available



from the tetralin based upon the estimated in-leakage of 1 to 10 gallons and assuming complete dissociation of tetralin to the elements.

5. Hydrogen Effects

It is conceivable that most of the estimated quantity of 0.7 to 7 lb of hydrogen (120 to 1200 ft³ at STP) could have reacted initially with the sodium to form sodium hydride. Any remainder of the hydrogen could have collected in the helium cover-gas above the sodium in the upper plenum. If all of this hydrogen reacted to form sodium hydride and were uniformly mixed with the 50,000 lb of sodium, the concentration of sodium hydride would be about 0.03 to 0.3 wt %. The solubility of sodium hydride in sodium decreases from several wt % at 1000°F to about 0.01 wt % at 510°F. Tetralin first entered the system into 1000°F sodium with the reactor operating at full power, and all of the sodium hydride would have been in solution in the upper plenum. Subsequently, in the colder portions of the cooling system and also when the reactor was cooled down, some sodium hydride would have precipitated or be carried in suspension in the circulating sodium.

6. Carbon Effects

If all of the 7 to 70 lb of carbon were uniformly distributed in the 50,000 lb of sodium, the carbon concentration would be increased by about 0.01 to 0.1 wt %. Under the most favorable conditions (for carbon solubility) of temperature and oxide content, one could expect at best a solubility of 0.02 wt % of carbon in sodium.⁸ The primary system was known to be saturated with carbon since the tetralin leak prior to run 8. The carbon added during run 13 presumably only added to the amount of solid carbon particles in the system.

Excess carbon could be floating on top of the sodium in the upper plenum as finely divided particles. Depending on the size and density of the agglomerated particles, they may disperse throughout the sodium or sink to the bottom of the core tank. Carbon could also deposit out as a film on pipe walls and tank walls. When the primary pump was removed recently, it was noted that a black film was on the pump casing and a thick film of carbonaceous material was deposited on the pump impeller. Regardless of the form and location of the carbon, as long as it can contact the sodium, this carbon serves as a source for carburization of materials in the primary cooling system.



7. Oxygen Effects

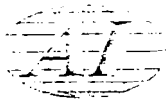
In addition to any pickup of trace amounts of air during normal operation and fuel handling, oxygen could have been introduced into the sodium during the nitrogen-stripping operation which followed run 13. An analysis of a sample of this nitrogen gas was performed on August 12 and revealed an oxygen impurity content of 0.06 wt %. Assuming this analysis as typical, it has been calculated that 240 ft³ (21.4 lb) of oxygen at STP was introduced along with the nitrogen. If this oxygen all went into solution in the sodium, it is estimated that it would increase the oxygen concentration by 428 ppm, which corresponds to a saturation temperature of 760°F. It is probable that only a fraction of this oxygen actually went into solution, due to nonideal contact between the gas bubbles and sodium.

The oxides present in the sodium probably were involved in formation of the plugs in fuel channels. It also should be noted that there are interdependent relationships between the solubility of oxides and other materials in sodium. For example, the solubility of carbon in sodium at a given temperature increases with increasing oxygen content.⁸ As another example, the apparent solubility of oxygen is increased⁹ with the addition of NaH.

An extremely important effect of the oxide content may be the reaction: fission products + sodium oxide → fission-product oxide + sodium. This reaction indicates that sodium oxide might react with or complex the fission products to form an oxide agglomerate. This fission-product oxide could collect in the cold trap, and may account for the very high activity level which has been observed in the cold trap.

8. Mechanisms of Restriction of Coolant Passages

The partial blockage of coolant flow in the fuel channels is clearly indicated by the spread in sodium temperatures at the outlet of the fuel channels. The actual mechanism of restriction of coolant flow is not clearly understood. It is known that the sodium system contained carbon particles, sodium oxide, perhaps sodium hydride, and decomposition products of tetralin. The manner in which these materials were deposited on heat transfer surfaces, both in the core and in the intermediate heat exchanger, seems to revolve about the admission of tetralin into the system.



Two types of deposits have been noted on the fuel elements. One type is in the nature of a plug which fills some or all of the passages between fuel rods and between the outer rods and the fuel channel. This type of deposit was clearly observed after run 14 on the 19-rod oxide cluster. It was located at the top of the cluster and was several inches long. Its outer surface was cylindrical, of roughly the diameter of the fuel channel, and appeared to be quite solid when viewed through the television equipment on the fuel handling cask. This element was returned to the core and removed at a later date. When removed the second time it was observed that much of the deposit had fallen or been washed from the element during passage through the upper sodium pool.

The element from channel 55 had a plug near the top which must be presumed to be similar to that on the oxide cluster. It must not be inferred, however, that such deposits formed preferentially at the tops of the elements. It is quite likely that such deposits formed near the point of cladding failure on each of the broken elements.

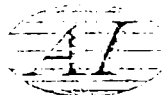
The second type of deposit which has been observed is in the nature of a surface fouling. This type was not observed until the last of the whole elements was removed from the core nearly three months after the end of run 14. The lower section of each of the seven rods appeared to be coated with a dark material which, while covering the surface, did not block the coolant passages between rods. The deposition of one mil of an organic film on a fuel rod would increase the fuel-clad interface temperature by about 100°F with the reactor operating at 4 Mw. Such surface fouling would not be detected by the outlet channel thermocouple. It is possible that during run 14 these areas were occupied by more complete plugs (the outlet channel sodium temperatures indicated serious flow restriction) which had partially disintegrated as sodium flow was maintained after the termination of run 14. Since all of the broken elements ran hot during run 14, it would appear that blockage rather than fouling produced the fuel cladding failure.

The time of formation of the deposits is of interest. The deposits started to form about May 30, as indicated by an increasing spread in outlet channel temperatures. At this time and until shutdown on June 3, the sodium



temperatures were high and decomposition of the tetralin was quite rapid. The deposition may have accelerated after the termination of run 13, when liquid tetralin and perhaps heavy hydrocarbons were present in the primary system.

Prior to the nitrogen-stripping operation, 17 of the 43 fuel elements were removed from the core. It is probable that during stripping most of the nitrogen passed through empty fuel channels with only minor bubbling through occupied channels. With no sodium circulation during this period, it is unlikely that deposits were accumulating. The stripping operation probably added a considerable amount of oxide to the system. Examination of Table III-6, Fuel Element Status, reveals that 11 of the 13 damaged elements (including the two which stuck in the process channels) were in the core during the stripping operation, which might indicate that the plugs formed during this period. It is possible that during removal of the 17 elements from the reactor prior to the stripping operation, passage through the upper sodium pool dislodged a large part of any plug which had previously formed. The most likely period for the formation of deposits is therefore the interval between termination of run 13 and the removal of the main primary pump (June 3 to June 12). The precise nature of the deposits as they existed at the beginning of run 14 will probably never be known. The best specimen, taken from the element from channel 55 after the termination of the run, was heavily contaminated by reaction of the contained sodium with air and moisture in the SRE hot cell. The SRE was not equipped with apparatus necessary to obtain an uncontaminated specimen.



C. RADIOLOGICAL CONSIDERATIONS

1. Primary Sodium Activity

a. Activity Levels of Irradiated Sodium

Although Na^{24} decays with a 15-hour half-life, early experimental work performed particularly at KAPL indicated the presence in virgin sodium of significant quantities of impurities. The overall effect of these impurities is to effectively limit the decay of sodium activity to between 10^{-5} and 10^{-6} of its original activity. This fact was taken into account in establishing the specifications for the SRE sodium. The saturation activities resultant from assuming the maximum acceptable concentration of each element permitted by the SRE sodium specification is about $20 \mu\text{c}/\text{cm}^3$ (neglecting both the Na^{22} activity and, of course, that from Na^{24}). Most of the constituent activities have half-lives longer than that of Na^{24} . To this should be added a contribution from activation of any corrosion products and any fission products which may be present. It is evident, therefore, that even without fission-product contamination, the "long-lived" activity in the sodium would not be negligible.

b. Analytical Methods

Sampling of primary coolant in the SRE is accomplished in two different locations, either at the Materials Evaluation Facility or in the reactor pool. Gamma-ray scans are usually run on a portion of the sodium sample utilizing a 256-channel analyzer. On various occasions, gamma-ray spectrometry was performed after chemical separation of the major components indicated by the gross scan.

The specific activity obtained after chemical separation is usually a factor of about 10 (or slightly less) less than from the gross scan. The very limited size of the sodium sample from which the chemical separations start, the fact that the final counting statistics are low due to the relatively low sample activity present at the start of chemical separation, and the errors inherent in using subtraction techniques in analyzing the gross gamma scans, would possibly produce variations of the order noted. Another possible explanation is that the sodium samples may contain fine carbon particulates which are known from other experimental work to concentrate the activity. These particulates



would be present during the gross scans but would be removed by the chemical separations techniques.

No data to support the validity of either explanation is available at this time. Similarly, no verifiable explanation can be offered as to why samples taken on the same day, but in different locations, yielded markedly different specific activities for the same isotope. This information is presented in order to prevent misinterpretation of the activity trends exhibited in the specific activity measurements.

c. Analyses

The results of the analyses of sodium samples are shown in Table IV-C-1. The decay of sample 8 taken after run 14 is shown in Table IV-C-2.

Gamma-ray spectrometry performed on this sample using a 256-channel analyzer has yielded the specific activities shown in Table IV-C-3. All data have been corrected back to shutdown time on July 26. Several other isotopes, Co^{60} and Mn^{54} , were minor contributors to the activity, as were Na^{22} and Na^{24} . Any information relative to the extent of the original release of activity which can be deduced from this data is limited by a number of factors:

- 1) Since the reactor was last shut down on July 26, the shorter lived fission-product activity would have decayed to insignificant proportions before the sodium sample was removed.
- 2) Some of the fission products could be present beyond their limit of solubility.
- 3) More dense particles may have settled out in the core tank or at low points in the system.
- 4) The more volatile products may have escaped prior to the time the sample was taken.
- 5) Some fission products may have deposited on the interior surfaces of the cooling system.
- 6) Some fission products were possibly accumulating in the cold trap or the hot trap prior to the time the sample was taken.



TABLE IV-C-1
RADIOISOTOPIC CONTENT OF PRIMARY SODIUM SAMPLES

Sample Number	Location	Date of Removal	Date of Scram	Specific Activity* ($\mu\text{c/gm of Na}$)													
				²⁴ Na	²² Na	¹³¹ I	³⁵ Sr	⁵¹ Cr	¹⁰³ Ru	¹⁰⁶ Ru	¹³⁷ Cs	⁴⁵ Zr-Nb	¹⁴¹ Ce	¹⁴⁰ Ba-La	¹¹³ Sn	²⁰³ Hg	¹³⁴ Cs
2 [†]	MEF [†] Reactor surface	10/2/58	9/25/58	0.19(6)	0.62(-2)	0.51(-2)	0.28(-3)	0.40(-1)	0.59(-3)	0.22(-2)	0.50(-3)	-	-	-	-	-	
3 [‡]		2/6/59	1/29/59	-	0.93(-2)	0.18(-1)	-	-	-	0.36(-3)	-	0.26(-2)	0.19(-1)	0.55(-2)	0.48(-3)	-	-
3 [‡]	Pool	2/6/59	1/29/59	-	0.12(-1)	0.16(-1)	-	-	0.80(-3)	-	0.65(-3)	0.52(-1)	0.54(-3)	0.24(-3)	-	-	
4	MEF	2/6/59	1/29/59	-	-	8.9	-	-	-	-	0.52	-	-	5.5	1.8	-	
5 [‡]	Reactor surface	4/12/59	4/6/59	-	0.57(-2)	-	-	-	-	-	0.38(-2)	0.26(-2)	-	-	<0.37(-2)	-	
6**		4/12/59	4/6/59	-	0.46(-2)	-	-	-	-	-	-	0.22(-2)	0.21(-2)	-	-	<0.33(-2)	-
7	Pool	4/12/59	4/6/59	-	-	0.40(-1)	-	-	-	-	0.15(-1)	0.29(-2)	0.43(-1)	-	-	-	
7	MEF	4/14/59	4/6/59	-	-	-	-	-	-	-	-	-	-	-	-	-	
8	Pool	8/2/59	7/26/59	-	-	0.74	-	-	0.95	-	1.26	14.7	5.96	1.65	-	0.2(-1)	

* Values in parenthesis indicate power of 10 by which the value should be multiplied.

† Materials Evaluation Facility.

‡ Identified by gamma spectrometry following chemical separation for Zr, Ru, Cr, La, and I.

** Identified by gamma spectrometry following chemical separation for Ce and I.



TABLE IV-C-2
DECAY OF SODIUM SAMPLE 8

Date	Activity ($\mu\text{c/gm}$)
August 11, 1959	19.8
August 21, 1959	16.3
August 25, 1959	16.1
September 3, 1959	13.6
October 12, 1959	7.3

TABLE IV-C-3
ISOTOPIC CONTENT OF SODIUM SAMPLE 8
(Analyzed August 11, 1959)

Isotope	Specific Activity ($\mu\text{c/gm}$)
Ce ¹⁴¹	5.96
I ¹³¹	0.74*
Ru ¹⁰³	0.95*
Cs ¹³⁷	1.26*
Zr ⁹⁵ - Nb ⁹⁵	13.9
Cs ¹³⁴	0.02*
Ba ¹⁴⁰ - La ¹⁴⁰	3.30
Total	26.1

*Activity determined after chemical separation and corrected to date of reactor shutdown July 26, 1959.

However, in spite of the above limitations, an attempt was made to estimate the fraction of fission products released to the coolant by using the data in Table IV-C-3. The results are presented in Table IV-C-4.

From Table IV-C-4, a release fraction of the order of 10^{-4} is indicated. The iodine release fraction falls close to the other isotopes, which indicates that, even though the iodine is very volatile, it did not escape to the cover gas because it undoubtedly combined with the sodium as rapidly as it was evolved. No iodine was ever detected in reactor cover gas samples.

TABLE IV-C-4
CALCULATED RELEASE FRACTION OF FISSION PRODUCTS
(Identified in Sodium Sample 8)

Isotope	Amount Formed	Amount* Released	Release Fraction
Zr ⁹⁵ + Nb ⁹⁵	6.87×10^5 (sum)	3.06×10^2 (sum)	4.45×10^{-4}
Ce ¹⁴¹	1.80×10^5	1.31×10^2	7.28×10^{-4}
Ba ¹⁴⁰ - La ¹⁴⁰	8.25×10^4 (each)	3.63×10^1 (each)	4.26×10^{-4}
Cs ¹³⁷	6.55×10^3	2.77×10^1	4.23×10^{-3}
Ru ¹⁰³	1.05×10^5	2.09×10^1	1.99×10^{-4}
I ¹³¹	2.94×10^4	1.63×10^1	5.50×10^{-4}
Cs ¹³⁴	10^2 †	4×10^{-1}	4×10^{-3}

*Based upon concentrations indicated by sodium sample.

† From neutron capture.

d. Fission Products in NaK Bond

The question arises as to whether the fission-product activity observed in the sodium can be accounted for on the basis of the fission-product activity in the NaK bond alone or, in addition, a mechanism of overheating of the slugs must be postulated to account for the fission products. At this time sufficient measurements to provide adequate data to answer this question satisfactorily have not been made. However, some insight into this problem may be gained by examining the available information.



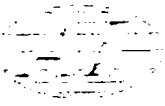
Experiments have previously been performed in which the amount of fission products released to the NaK bond of the fuel element were measured during normal operation of the SRE. The data obtained for the fission product activity present in the NaK bond of a single fuel rod made up of unalloyed uranium slugs which had been irradiated for 850 Mwd/T are presented in Table IV-C-5.

The middle column in the above table gives the number of atoms present in the bond, calculated back to "out-time" (i.e., to the time at which the fuel rod was removed from the reactor). The last column lists the fraction of the total amount of fission products produced which were released to the bond. Considering only the recoil mechanism as a means for fission products to enter the bond, a theoretical release fraction of 3.5×10^{-4} was obtained. The exact correspondence with the measured release fraction for Cs^{137} is probably fortuitous. For all other isotopes the release fraction is smaller, indicating that the number of atoms diffusing out of the fuel slugs is small or that this effect is entirely masked by settling of the fission products or deposition on the surface of the slugs or cladding.

TABLE IV-C-5
FISSION PRODUCT ACTIVITY IN NaK

Isotope	Atoms Present in Bond at Out-Time	Release Fraction at Out-Time
Ce^{141}	1.5×10^{-4}	6.9×10^{-7}
I^{131}	4.0×10^{15}	1.3×10^{-4}
Cs^{137}	3.5×10^{17}	3.5×10^{-4}
Zr^{95}	6.4×10^{14}	1.4×10^{-6}
Sr^{90}	3.1×10^{14}	3.1×10^{-7}

Since it might be expected that the same fraction of total atoms formed would be released to the NaK bond regardless of the total accumulated exposure (burnup), unless the fuel was exposed to conditions such that the mechanism by which atoms were lost to the bond was changed, a comparison was made between the experimental release fraction and that calculated based on the data



from sodium sample 8. To affect such a comparison the data must be adjusted to account for the ratio of the number of rods broken to the total number of rods in the core and differences in release fractions for the experimental rods containing various alloyed slugs which were also present in the core. The adjusted values compared favorably for the iodine and cesium, thus suggesting the possibility that most of the fission-product activity released to the sodium in the SRE primary system came from the bond.

Some of the isotopes apparently have too low a release fraction to the bond to account for the amount found in the sodium. Closer scrutiny may possibly explain some of the differences noted, e.g., on the basis of observations made during pyrochemical processing of fuel, the Zr-Nb isotopes should not be released to any great extent compared to some of the other elements. There is always the possibility that the Zr-Nb activity which was measured was due to activation of corrosion products from the zirconium moderator cans or from corrosion of the activated zirconium cans. Formation and decomposition of zirconium hydride is one mechanism by which this could occur.

e. Uranium and Plutonium

Another aspect of concern is the amount of fissionable material (uranium and plutonium) which was introduced into the sodium coolant. The extent of release of these materials is of importance since, in future operations, if the present sodium charge is used, they may continue to circulate in the coolant stream and thus produce additional quantities of fission products. The uranium and plutonium can get into the coolant by a variety of mechanisms:

- 1) By solubility in sodium of either the elemental material or its compounds. (The solubility of the latter would certainly be enhanced in the presence of cyanide salts.)
- 2) During formation of the iron-uranium alloy, intermetallic compounds of iron or nickel may have formed with the fissionable materials, and these may have a finite solubility in the sodium.
- 3) Overheating of some of the fuel slugs may have resulted in additional amounts of plutonium diffusing out of the slug.



- 4) Spallation of friable fissile material (due to effects such as irradiation or oxide formation) or by eutectic formation.

An analysis was performed some time ago on the NaK bond of an unalloyed SRE fuel rod which had been irradiated during normal operation to an exposure of 650 Mwd/T. No U^{238} or U^{235} was detected in the bond, but about 10^{-6} gm of plutonium was detected. Since it was estimated that 1 gm of Pu had been formed in the fuel, this results in a release fraction of 10^{-6} . Comparing this release fraction with that of about 10^{-4} for the fission products, it may be seen that the Pu release fraction is 1/100 as great. This is to be expected since much higher energies are released to the fission products as a result of fission.

f. Weight of Fission Products

One last piece of information is perhaps of interest, namely the total weight of fission products which may have been released to the sodium. Considering a total accumulated burnup for the entire core of 2250 Mwd, assuming that 1 Mw corresponds to fission of 1 gm of material per day, and using the calculated average release fraction of about 4×10^{-4} , it is calculated that a total of 0.9 gm of fission products were released to the sodium. This corresponds to a concentration in sodium of only 0.04 ppm.

g. Conclusions

Several conclusions can be drawn from the information which has been presented in this section:

- 1) Very meager experimental data is available concerning the extent of radioactivity in the primary sodium coolant.
- 2) The significance of radiometric analyses performed on the sodium samples is only good to within a factor of 10.
- 3) In spite of items 1) and 2) above, it is evident that fission products, as well as activated impurities in the sodium, and possibly activated corrosion products (i.e., Cr^{51}), were present in the sodium prior to run 14.

- 4) At some time between the start of run 11 and the termination of run 14, substantial quantities of fission products (possibly 2 to 3 orders of magnitude greater than previously detected) were introduced into the coolant stream.
- 5) The quantities of activity measured in sodium sample 8 indicate that most of the fission products released to the sodium as a result of the fuel damage apparently came from the NaK bond and not directly from the fuel.

2. Radioactivity from Primary System Components

a. Main Primary Gallery

Prior to run 8, there had been numerous occasions during which access to the main primary gallery was accomplished. The majority of these occasions occurred following runs 2, 3, and 4. Up until this time, i.e., to the end of run 4 (on May 28, 1958), the total accumulated reactor exposure was only 217.0 Mwd. During these occasions of access, general radiation levels were hardly measurable. (Access is normally not attempted until at least 2 weeks after shutdown to permit the Na^{24} to decay.)

No additional access was attempted until after run 7 (at which time the total accumulated reactor exposure was 1120.8 Mwd), when general modifications were to be made to the heat transfer system. During this occasion, specifically, in October 1958, the maximum radiation levels in the general area of the moderator coolant pump were reported to be about 50 Mr/hr (October 14). Below shield blocks 1 and 2, the radiation level was about 21 mr/hr (on October 11).



Access was not achieved again until April 1959, following the completion of run 11 which brought the total accumulated reactor exposure to 2141.1 Mwd. Radiation levels measured on April 18 varied from 50 to 420 mr/hr. It should be noted that, at this time, the primary system had been drained to the fill tank. Additional measurements made 5 days later (a total of 17 days after shutdown) indicated no significant decay. This could not be due to Na^{22} activity since the sodium samples taken during this period indicated an Na^{22} content of only about $0.005 \mu\text{c/gm}$.

Following the termination of run 14, which had brought the total accumulated reactor exposure to 2425.8 Mwd, radiation measurements were made in the gamma facility. These were accomplished, without removal of the large shield blocks, by simply inserting a Jordan detector in the gamma facility. The data recorded thus far are shown in Table IV-C-6.

TABLE IV-C-6
RADIATION LEVELS IN GAMMA FACILITY

Date	Dose Rate (r/hr)	
	Measured	Calculated
August 12, 1959	2.9	-
August 13	2.8	-
August 17	2.5	1.4
August 25	1.9	1.2
August 31	1.2	1.1
September 14	1.1	1.0
October 5	0.7	0.7

The calculated results were obtained considering only those isotopes known to exist in the channel 34 sodium sample removed on August 2 and analyzed on August 11 (see Table IV-C-3). No information of this type is available prior to this time so that comparison with earlier data is not possible.

It is apparent that the increasing background in the galleries, as the total accumulated reactor exposure has continued to increase, indicates a definite accumulation of radioactive material on the pipe surfaces. This is exemplified by the radiation measurements taken during the April 1959 access period, at which time the sodium in the gallery had been drained to the primary fill tank.

b. Main Primary Gallery Atmosphere

The activity in the main primary gallery atmosphere, prior to run 14 was $\sim 1 \times 10^{-5} \mu\text{c/cc}$. On August 11, 1959, following termination of run 14, a value of about $2 \times 10^{-5} \mu\text{c/cc}$ was measured. As a result, it does not appear that airborne contamination in the gallery atmosphere has increased due to the fuel damage.

c. Primary Cold Trap Radioactivity

Radiation measurements taken at the cold trap, located in the primary sodium service vault which is adjacent to the fill-tank vault, serve only in a qualitative way to indicate the extent of foreign radioactivity removed from the sodium coolant.

Radiation measurements of the cold-trap activity are not routinely taken; rather they are obtained only when it is anticipated that the information gained will be of significance to the reactor operation. It should also be noted that the cold trap is usually operated when the reactor is shut down or at low power and, then, only when the oxygen content in the coolant exceeds 10 ppm. Some representative values of the dose rate from the cold trap are included in Table IV-C-7. It must be added that the radiation detector cannot always be repositioned accurately and that, as a result, because of shadowing effects, the dose rate can change by as much as a factor of two.

From a review of data taken prior to run 8 and after run 11, as well as after run 14, it is apparent that the radiation levels increased by almost a factor of 100 from April 1959 to August 1959. Because the cold-trap dose rates



TABLE IV-C-7

RADIATION LEVELS FROM THE COLD TRAP

Date	Dose Rate (r/hr)	Date	Dose Rate (r/hr)
September 26, 1958	0.3	August 13, 1959	81 [†]
September 27, 1958	0.55 [*]	August 17, 1959	72 [†]
September 28, 1958	0.1	August 18, 1959	68
September 29, 1958	0.05	August 25, 1959	80
October 4, 1958	0.001	August 31, 1959	70
November 13, 1958	0.3	September 2, 1959	73
November 17, 1958	1.5	September 9, 1959	65
November 18, 1958	1.0	September 11, 1959	63
November 21, 1958	0.06	September 14, 1959	65
April 5, 1959	1.0	September 16, 1959	69
August 8, 1959	63 [†]	October 5, 1959	50
August 12, 1959	63 [†]		

*Increased to 1.5 later in day.

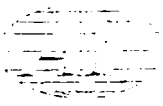
†Extrapolated by inverse square correction.

are so much higher than values measured in the gamma facility, it can be concluded that the cold trap is removing fission products from the sodium stream.

Cold trapping was started during run 14. However, radiation measurements could not start until August 8 (due to the radiation hazard from the high radiation levels of Na^{24}), at which time the dose rate, extrapolated to near the surface, was about 70 r/hr. It is possible that initial cold-trap dose rates, had they been measured, would have yielded significantly higher values.

3. Reactor Cover Gas Activity

The helium cover gas over the sodium pool is in direct communication with the primary sodium fill-tank atmosphere which vents directly to the gaseous storage tanks. Reactor cover gas reaches the storage tanks principally on three occasions:

- 
- a) When the reactor is brought up to temperature, the sodium level in the pool rises, thus forcing the helium cover gas to the storage tanks.
 - b) Whenever the operating pressure is reduced.
 - c) Whenever the reactor cover gas is purged.

Also, during normal reactor power operation, it is important to note that there is a small amount of leakage past the pressure relief valve which separates the filltank atmosphere from the storage tanks. As a result of this leakage, radiation measurements of the cover gas activity have only limited meaning, even when information is available concerning the operating history of the reactor, including power level, length of operating, and amount of cover gas bled off to the storage tanks. General trends of the activity level in the cover gas, however, can be of some use.

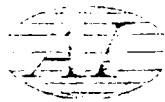
The cover gas is sampled at a location downstream from the core (rather than at the reactor loading face) using an evacuated ($\sim 2000\text{-cm}^3$) chamber. Some of the results of radiation measurements are listed in Table IV-C-8. Where possible, appropriate comments have been added concerning the extent of purging or pressure relieving which had taken place. This table presents one of the most vivid indications of the amount of activity released as a result of the fuel damage. From the table it is apparent that general activity levels in the cover gas are in the range of 10^{-3} to $3 \times 10^{-4} \mu\text{c/cm}^3$. Immediately following normal power operation, the cover-gas activity will be somewhat higher, e.g., the $0.06 \mu\text{c/cm}^3$ value recorded on February 26, 1959 which was taken shortly after shutdown from run 9.

The measurements made after the start of run 14 clearly indicate that an extremely high radioactivity concentration had been introduced into the cover gas. It is important to note here that if any fuel elements had ruptured during run 12 or 13, one would expect to note a significantly higher cover gas activity than was measured in June 1959. This could lead to the conclusion that fuel elements did not start to rupture until run 14 had started. However, some small cladding failures could well have occurred and gone unnoticed due to the background activity which normally is present in the cover gas.



TABLE IV-C-8
ACTIVITY HISTORY OF THE REACTOR COVER GAS

Date	Specific Activity ($\mu\text{c}/\text{cm}^3$)	
December 11, 1958	1.9×10^{-3}	
December 14, 1958	3.0×10^{-4}	
December 15, 1958	1.0×10^{-3}	
February 14, 1959	1.7×10^{-3}	
February 26, 1959	0.06	(taken shortly after end of run)
May 26, 1959	1.7×10^{-3}	
June 13, 1959	2.4×10^{-4}	
June 16, 1959	1.8×10^{-5}	
June 20, 1959	3.8×10^{-5}	(during N_2 stripping operation)
July 18, 1959	-	(sample chamber read 30 mr/hr at surface pressure)
July 29, 1959	-	(reactor cover gas bled down to negative)
August 1, 1959	5.5	
August 12, 1959	0.87	
August 19, 1959	-	(cover gas purged on August 19 and 20)
August 20, 1959		
August 25, 1959	0.05	
August 28, 1959	0.082	(this sample showed no decay in 48 hr)
August 30, 1959	0.082	
September 1, 1959	0.085	
September 16, 1959	0.07	(cover-gas purging operation started)
September 22, 1959	0.01	
September 24, 1959	0.01	
September 29, 1959	4.0×10^{-3}	



The decay of a cover gas sample taken on August 12, 1959 was followed for several days yielding the results shown in Table IV-C-9.

TABLE IV-C-9

DECAY OF REACTOR COVER GAS SAMPLE

Date	Activity ($\mu\text{c}/\text{cm}^3$)
August 14, 1959	0.87
August 28, 1959	0.15
September 3, 1959	0.08
September 14, 1959	0.025

A gamma scan of this sample on September 14, using the 256-channel analyzer, indicated $0.010 \mu\text{c}/\text{cm}^3$ of Xe^{133} and $0.016 \mu\text{c}/\text{cm}^3$ of Kr^{85} . Based on this data, the specific activity at shutdown on July 26 considering only the Kr^{85} and Xe^{133} isotopes would have been about $7.4 \mu\text{c}/\text{cm}^3$, almost all of which would be due to 5.3 day Xe^{133} . The contribution from other (short lived) Xe and Kr isotopes, would certainly result in a value well in excess of several hundred $\mu\text{c}/\text{cm}^3$. That such an extremely high concentration did in fact exist is borne out by the off-scale readings of decay tank activity (see Figure IV-C-1).

4. Activity in Gaseous Storage Tanks

The gaseous storage tanks are an integral part of the gaseous radioactive waste handling system, receiving activity from the sodium fill tank (communicating directly with the reactor cover gas), the wash cells, and the fuel handling cask.

There are four storage tanks, each of which have a capacity at 100 psig of 2700 ft^3 at STP. When the activity in the tanks is determined to have reached a sufficiently low value, the gas may be bled from the storage tanks through a flow-rate meter and discharged out the building vent line. Activity is released only when calculations indicate that levels at the discharge point (stack) will be less than $1 \times 10^{-7} \mu\text{c}/\text{cm}^3$. If the activity can be attributed solely to xenon, a value of $1 \times 10^{-5} \mu\text{c}/\text{cm}^3$ is permitted.



Radiation measurements of the activity level in the storage tanks are accomplished by the same sampling chamber utilized in sampling the reactor cover gas. A summary of data on the activity concentration in the storage tanks is shown in Figure IV-C-1 and in Table IV-C-10.

As was the case with the reactor cover-gas activity, the activity concentration in the gaseous storage tanks provides a great deal of insight into both the magnitude of the radioactivity release and the time of the release. From Figure IV-C-1, it can be seen that, in general, the storage-tank activity levels do not exceed $1 \times 10^{-3} \mu\text{c}/\text{cm}^3$. Slight increases detected in early and mid-December can be attributed to fuel washing operations. The increase to $7 \times 10^{-3} \mu\text{c}/\text{cm}^3$ on December 19, 1958 is due to the re-startup and power operation of run 8. The increase in activity following run 11 is, again, attributable to fuel handling operations. The increases in mid and late May are most probably attributable to the operation of the reactor at full power and not to fuel damage. This may be inferred since the activity level did not rise significantly above values usually encountered during or after previous power runs. Also, following run 13, a total of 17 of the fuel elements was removed from the reactor; visual examination with the TV camera indicated that all were in good condition.

The first storage tank sample taken on July 15, 1959, after the start of run 14, indicated an extremely high activity; so high in fact that the counter had not been calibrated in that range. The sample chamber itself read several mr/hr at the surface, which can be compared with the value of 30 mr/hr from the reactor cover-gas sample taken on July 18, 1959. From the fact that the activity in the storage tanks decayed continually following July 15, it can be concluded that most of the fuel damage must have occurred just after the start of run 14 (within the first 3 days).

5. Radioactivity in High Bay Area

a. Airborne Activity

High airborne activity concentrations in the high bay area, although not a frequent occurrence, have been detected occasionally throughout the history of the SRE. These instances can be associated with different types of events; e.g., on December 12, 1958, following fuel handling operations, several drops of sodium were noted on the indexing ring over the hot cell. These drops, which

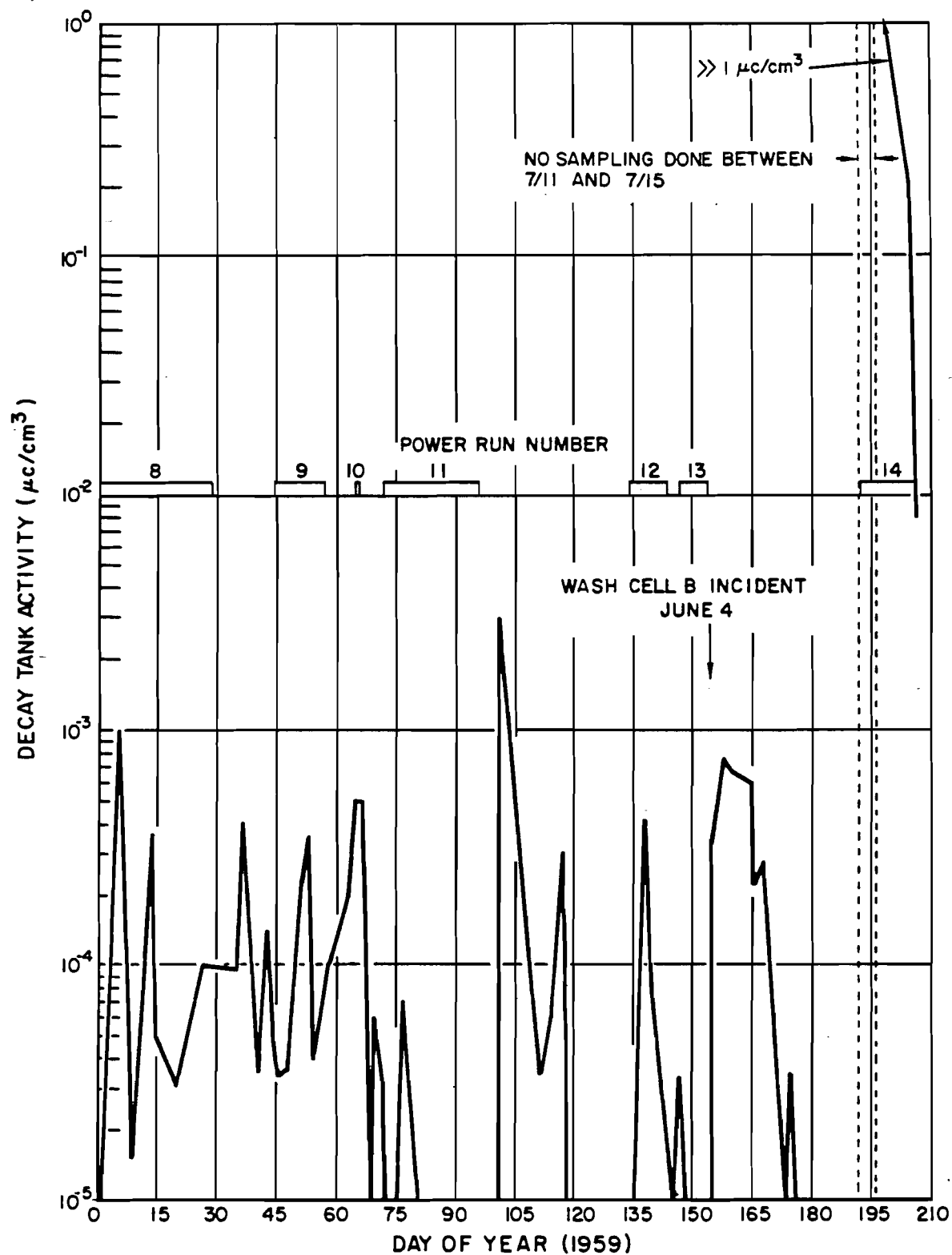


Figure IV-C-1. Radioactive Gas Decay Tank Activities
(Lines between points do not represent decay.)



TABLE IV-C-10

RADIOACTIVE CONCENTRATIONS IN GAS DECAY TANKS

Date	Activity ($\mu\text{c}/\text{cm}^3$)
November 18, 1958	$< 10^{-7}$
November 19, 1958	$< 10^{-7}$
November 23, 1958	$< 10^{-7}$
November 24, 1958	$< 10^{-7}$
November 25, 1958	5×10^{-7}
November 26, 1958	$< 10^{-7}$
November 27, 1958	$< 10^{-7}$
December 2, 1958	4.6×10^{-7}
December 3, 1958	4.6×10^{-7}
December 9, 1958	6×10^{-6} (washed fuel from R-9)
December 10, 1958	5×10^{-6}
December 11, 1958	8×10^{-6}
December 12, 1958	1.2×10^{-4} (washed fuel from R-10)
December 13, 1958	2.4×10^{-4}
December 14, 1958	3.0×10^{-5}
December 15, 1958	4.4×10^{-6}
December 16, 1958	2×10^{-5}
December 17, 1958	2×10^{-6}
December 18, 1958	6×10^{-6}
December 19, 1958	7×10^{-3} (first measurement after restart of run 8)
December 20, 1958	7×10^{-5}
December 21, 1958	1.5×10^{-5}
December 22, 1958	1.4×10^{-5}
December 23, 1958	4×10^{-6}
December 24, 1958	4×10^{-5}
December 26, 1958	8×10^{-5}
December 27, 1958	2×10^{-5}
December 28, 1958	8×10^{-6}
December 29, 1958	2×10^{-6}
December 30, 1958	2.7×10^{-6}
July 25, 1959	0.08
July 27, 1959	0.04
July 28 - Aug. 22	bleeding at 4 cfh
August 22, 1959	0.07
Aug. 22 - Sept. 16	bleeding at 4 cfh
September 16, 1959	0.065



read $2 \text{ r/hr} \beta - \gamma$ and $0.1 \text{ r/hr} \gamma$, caused the high bay area monitors to indicate an increased airborne activity concentration. Several days later, on December 19, 1958, a leaky thimble containing the number 4 safety rod caused an increase in the airborne activity in the high bay area. Following run 8, additional relatively infrequent instances of above normal airborne activity levels in the high bay area occurred.

Prior to about July 1959 there was little history of gaseous activity leaking from the top shield area, but after that time activity has been detected at the loading face shield on numerous occasions. From an examination of the cover-gas activity data, this can perhaps be attributed to the fact that there has always been gas leakage in this area, but the cover-gas activity concentrations were sufficiently low prior to that time that no significant levels were detected at the loading face. The onset of higher cover-gas activity levels would be sufficient to raise the activity concentration in the gas leakage to more significant proportions. This became quite evident during run 14, when numerous increases were noted on the high-bay airborne-activity monitors.

The activity levels during run 14 are shown on Figure IV-C-2. This data was recorded by a model AM-2 continuous air monitor. This unit is a fixed filter, integrating-type recording air monitor, and primarily measures the beta activity of the particulates building up on the filter through which the air passes. A G-M detector output records the average counting rate in counts per minute. Since quantitative interpretation of the counting rate in terms of airborne activity concentration causing the buildup is dependent upon the beta energy and the decay rate of the activity, the continuous air monitors are often used in only a qualitative fashion, i. e., to indicate an increase in the airborne radioactivity concentration. The actual concentrations shown on Figure IV-C-2 are measured by a different technique.

In interpreting the graph, three items should be noted:

- 1) When the counting rate exceeds 20,000 cpm, the instrument is inoperative until the filter is changed. During the time preceding filter change, the airborne activity concentration could decrease, as was probably the case between 1630 on July 12, 1959 and 0250 on July 13, 1959.

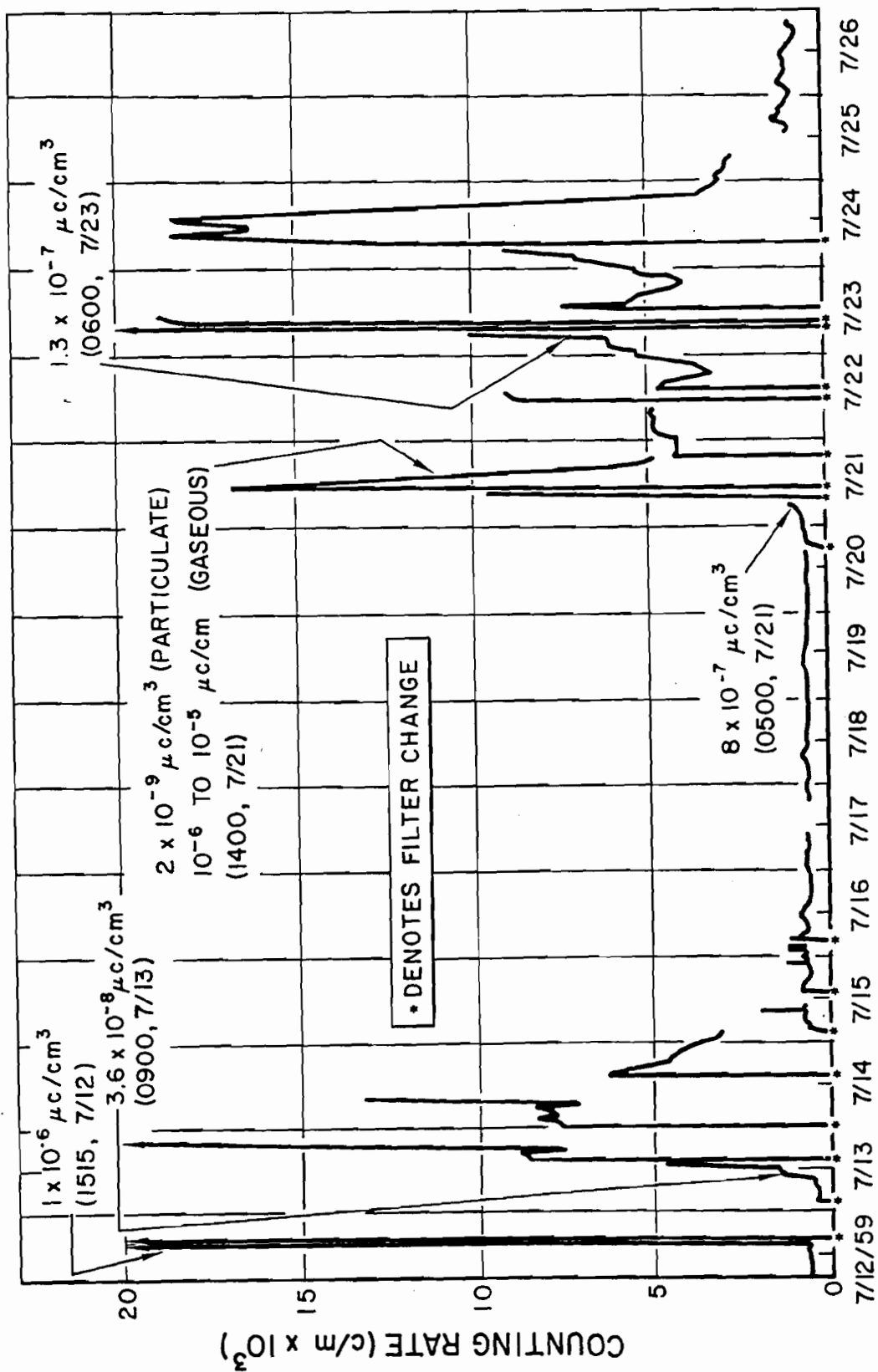


Figure IV-C-2. High Bay Area Airborne Activity
(Concentrations shown made with spot sampler.)

- 2) The spikes at 0842 on July 16, 1959 could have been caused either by instrument malfunction or by an increase in the external gamma radiation background.
- 3) The rate of decrease in counting rate is governed by both the rate of decrease in airborne activity concentration and by the radioactive decay rate, which cannot be less than the negative slope of the graph.

In addition, proper interpretation must be made of those indications of increased activity which occurred simultaneously with the occurrence of high radiation levels in the high bay area; e. g., the increase starting at 1515 on July 12, 1959 was the reason for the radiation survey in the high bay area which moments later led to the discovery of a high radiation field over core channel 7.

The exact cause of the high activity levels which occurred on July 21-24 has not been established. From examination of the gaseous decay-tank activity data, it is apparent that at least some of the fuel damage occurred prior to July 15. If most of the gaseous activity can be attributed to Xe and Kr isotopes, then it would appear that the level of cover-gas activity would have been below the point where leakage through the top shield would have been detected. However, if new leaks developed in the O-rings on the loading-face-shield plugs, or if additional fuel damage occurred during this time, high levels of the type noted would have occurred. If it were fuel damage, it does not appear that the extent of damage was as severe as that which occurred earlier (prior to July 15 during run 14).

b. Radiation Levels

During the operational history of the SRE, there have been several instances in which high radiation levels were detected in the high bay area. In all cases, these have occurred as a direct result of fuel handling operations.

There were three instances of note which occurred prior to June 1959, resulting in high radiation levels in the high bay area. In each case apparently sound fuel elements were put in the wash cells and, upon removal, were found to have been damaged; some rather severely. Subsequent handling of these elements resulted in the occurrence of rather high radiation levels.



Following run 8, but prior to run 14, the only instance in which high radiation levels resulted was the wash cell incident, which occurred on June 4, 1959. This incident, which resulted in a pressure surge in wash cell "B" during an apparently routine fuel washing operation, lifted the shield plug out of the wash cell. The resultant radiation levels in the high bay area reached values as high as 10 r/hr near the wash cell.

During run 14, the only instance of high radiation levels occurred on July 12 when both high bay area monitors showed an increase in activity. Subsequent radiation surveys indicated a dose rate of 500 mr/hr on the reactor loading face shield over the sodium level indicating thimble in core channel 7. Slightly over an hour later, at 1700, the radiation level reached 25 r/hr. The reactor was shut down and the thimble replaced with a standard shield plug. This action eliminated the source of radioactivity, as evidenced by radiation surveys performed on the following day when the reactor was brought back to power operation. The leakage was found to be due to faulty O-rings.

Following the termination of run 14, the fuel handling cask was used to inspect the fuel elements in the reactor. The inspection was to be accomplished by viewing the elements individually with the TV set, as they were drawn up into the cask. During the course of this operation, it was found that several of the fuel elements were severely damaged. During inspection and handling of these damaged elements in the fuel handling cask, additional fuel slugs became dislodged and dropped to the bottom of the cask. Operations directed towards removal of these slugs resulted in occasional radiation levels as high as 1000 r/hr at 1 ft from the slugs. However, the maximum total exposure received by operations personnel during these cask operations did not exceed 1 rem in a single week.

c. Reactor Building Contamination

Prior to run 8, normal reactor building contamination levels were less than 50 disintegrations per minute (dpm) per 100 cm², except over the loading-face-shield area where general levels were about 100 dpm/100 cm². In general, levels in excess of these values are caused by operations involving use of the fuel handling cask. On such occasions, contamination levels in the loading-face-shield area have been noted to increase to 5000 dpm/100 cm² and to

1000 dpm/100 cm² in other parts of the high bay area. (In order to minimize the spread of contamination during operations involving the fuel handling cask, plastic sheets are placed along the path of cask motion.) Contamination levels in other parts of the building (e.g., the office area) are essentially at background level. (The office area contamination level is normally limited to <30 dpm/100 cm²).

Following run 8 and prior to run 14, the contamination level did not depart appreciably from this pattern. However, the wash cell "B" incident of June 4 created extremely high contamination levels within the entire building. The maximum contamination level detected as a result of this incident was about 700,000 dpm/100 cm² (taken approximately 24 hr after the incident); this was found on the fuel handling cask which was located about 25 ft from wash cell "B". Contamination levels in the mezzanine office area reached about 70 dpm/100 cm². Within several days, the general high bay area had been decontaminated and restored to normal contamination levels, except for the area immediately around the wash cells. The entire high bay floor area was then covered with plastic sheeting. Following this, fuel handling operations were reinstituted.

The next instance of above normal contamination in the reactor building, with the exception of that resulting from routine fuel handling operations, occurred after the termination of run 14 during attempts to free a fuel slug which had jammed the fuel handling cask after it had removed a damaged fuel element from the core. During subsequent operations attempting to free the cask, extremely high-level contamination developed. Very fine pieces of stainless steel, fuel, and sodium oxide became distributed over the reactor loading face, causing radiation fields in excess of 25 r/hr. Contamination levels in other parts of the high bay area reached 11,000 dpm/100 cm². No significant increase in contamination level was found in other parts of the building. About one week after the cask operations started, contamination levels became somewhat more widespread, extending to "colder" areas on the first floor, with the levels reaching about 1000 dpm/100 cm². By about September 8, however, contamination levels on most of the high bay floor area had been reduced to <100 dpm/100 cm² and new plastic sheeting was installed. Some localized areas on the walls and instrument panels in the high bay area were still contaminated to levels in excess



of 1000 dpm/100 cm². Decontamination efforts have reduced the remainder of the area to normal contamination levels.

6. Stack Effluent Activity

Radioactivity routed to the stack from the gaseous storage tanks passes through absolute filters and is then diluted with 25,000 cfm of outside air. Exhaust from the high bay area is not vented to the stack but rather to a separate outlet located on top of the high bay area. The high bay exhaust is passed through CWS filters only when potentially hazardous operations are in progress within the reactor building, e. g., during reactor operation or fuel handling. The original design of the gaseous waste handling system incorporated radiation-level-actuated by-pass valves in the line leading from each source of gaseous activity to the storage tanks. In this way, automatically and depending on the activity level, the gas would be vented either to the stack or to the storage tanks. This system was later modified, because of malfunction, and a manually operated bypass was placed in the reactor control room.

Prior to run 14, there had been no indication that activity concentrations in the stack effluent had exceeded allowable values. On several occasions, the stack monitor had indicated the presence of high activity levels, but the cause could always be traced to either instrument malfunction or the fact that the instrument was responding to direct radiation (usually resultant from radiation beams existing at the same time in the high bay area).

Two instances in which the stack monitor readings indicated activity concentrations in excess of allowable values were noted during run 14. The first of these occurred on July 12 at 1700, at which time the stack activity rose sharply to a value of $1.5 \times 10^{-4} \mu\text{c}/\text{cm}^3$. This instance of apparent high activity levels occurred simultaneously with the high radiation levels which were detected above core channel number 7 and, as a result, the stack monitor was responding to this direct radiation. The activity level returned to normal by 2200 on the same day. The second instance occurred on July 15 at 0600; this time the stack activity rose sharply to $7 \times 10^{-5} \mu\text{c}/\text{cm}^3$. The activity level continued intermittently high until about 1100 on July 15. No explanation can be offered for this second occurrence unless it is assumed that the storage tank bypass switch had inadvertently been placed in the bypass position. If this were

in fact the case, the activity concentrations in the cover gas were certainly sufficient magnitude to cause the high stack effluent activities noted.

Although allowable values for the stack effluent are based on not exceeding a value of $1 \times 10^{-7} \mu\text{c}/\text{cm}^3$ (and $1 \times 10^{-5} \mu\text{c}/\text{cm}^3$ if Xe can be identified as the offender) at any time, allowable stack effluent concentrations are averaged over a one-year period. Therefore, the consequences of this latter release were not serious in any way and the release did not disturb the ability of the SRE to continue to vent radioactivity to the atmosphere.

7. Environmental Contamination

A continuous program of routine monitoring of soil, vegetation, water and airborne activity in the Santa Susana area has been underway since 1954. For the last several years, the environmental monitoring program has included monthly sampling of 14 different locations for soil and vegetation and 4 locations for water. A single continuous air monitor is also operated. The sampling locations are shown on Figure IV-C-3.

All soil, vegetation, and water samples are analyzed for α and β - γ activity. The analysis is performed by conventional techniques.

The results of the analyses performed on all soil and vegetation samples (from the 14 sampling locations) since January 1958 are summarized in Figure IV-C-4. Similar data for each of the four water sampling stations are listed in Table IV-C-11. It should be noted that, in the case of the water samples, no activity was detectable on numerous occasions. This is due, primarily, to two factors; namely that the activity levels were below the lower limit of sensitivity of the instrumentation and that, on some occasions, the background activity in the counting room area was somewhat higher than normal.

Analysis of the results obtained from the soil and vegetation samples have clearly indicated increased activity levels resultant from nuclear explosions and rainfall. For example, the relatively large increase noted in both the α and β - γ activity associated with soil and vegetation samples in March and April of 1958 is attributable to a combination of (a) the 3 to 6 detonations of megaton size reportedly set off in eastern Russia in March of 1958 and (b) the rather heavy rainfall that occurred during the last half of March (a total of 4.3 in.

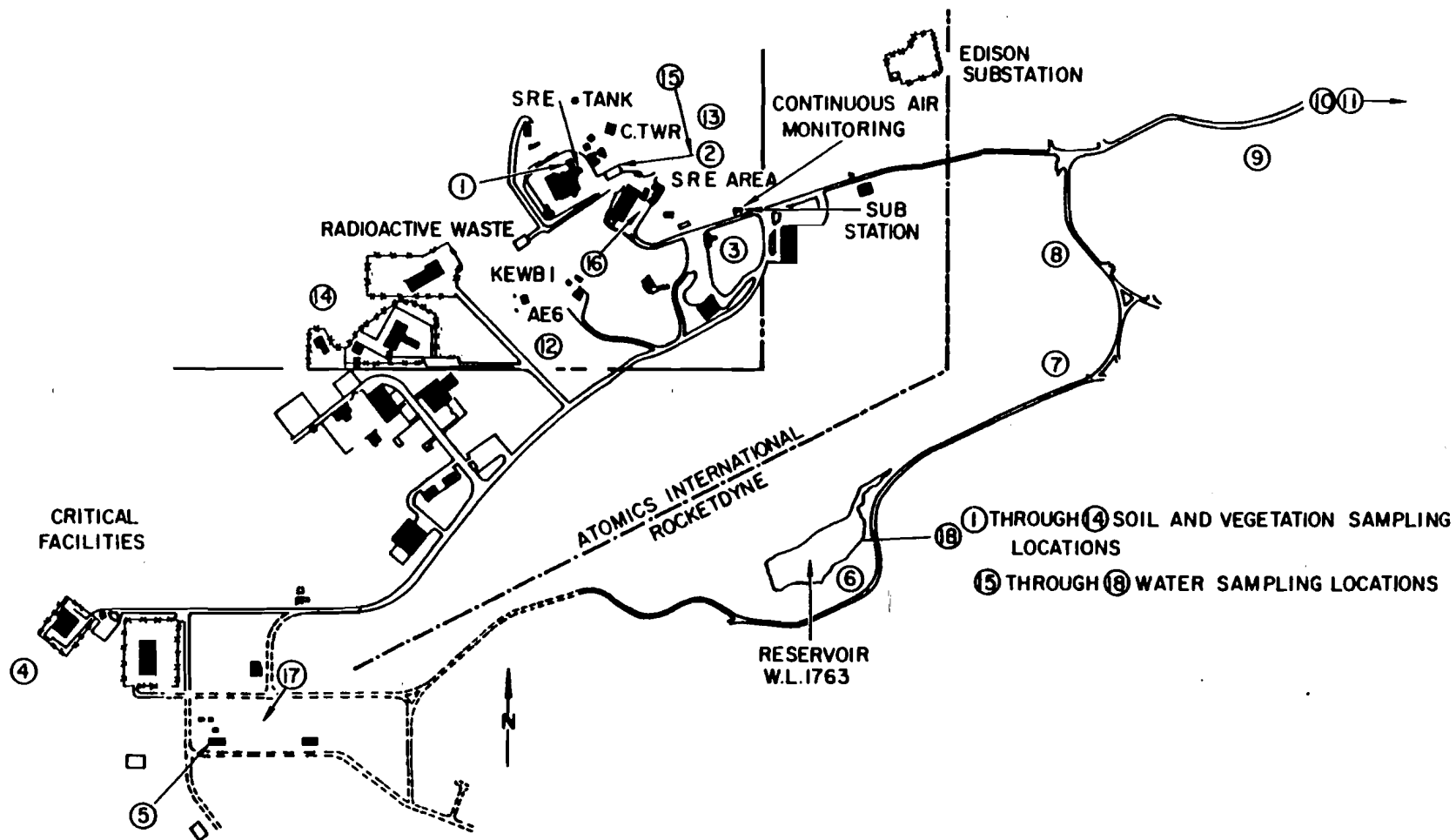


Figure IV-C-3. Environmental Monitoring Stations

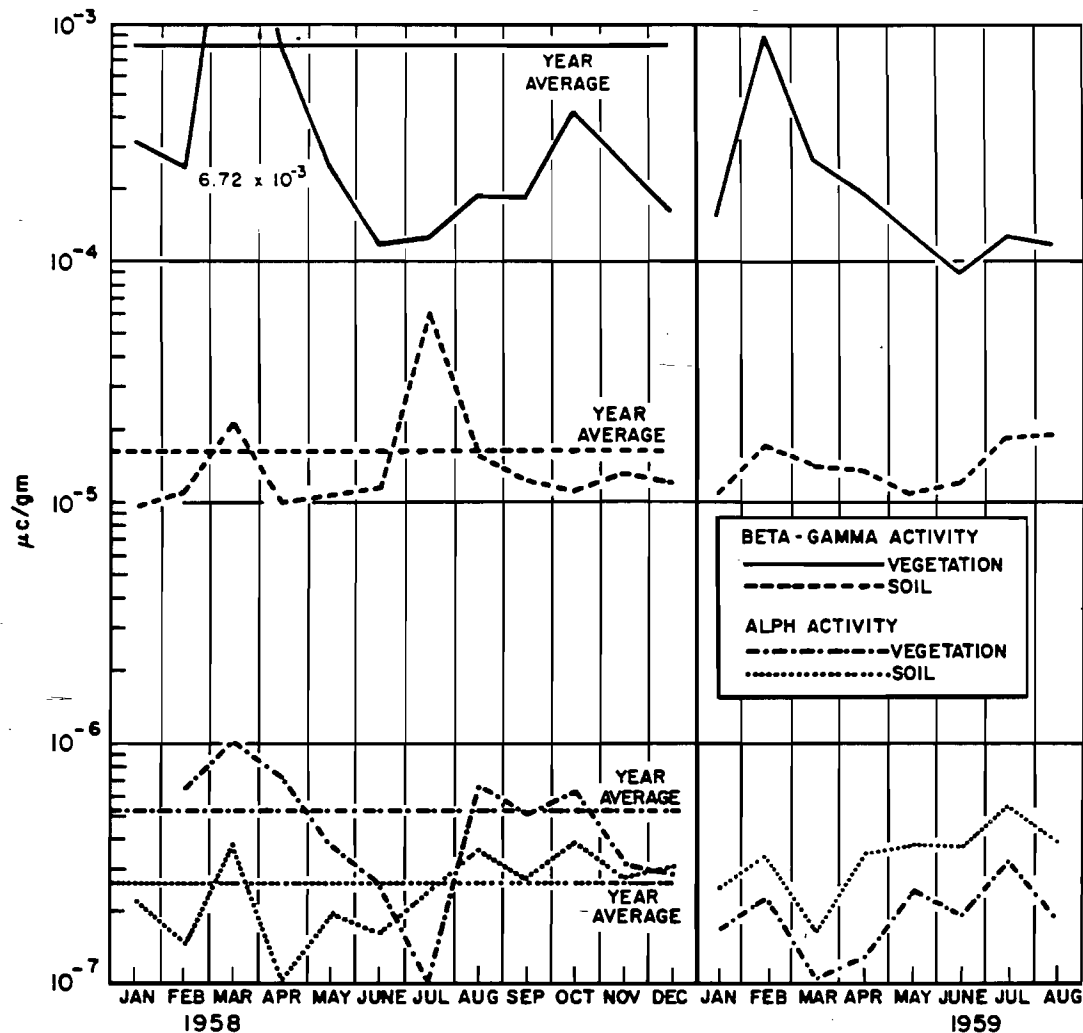


Figure IV-C-4. Environmental Soil and Vegetation Activity
(Lines between points do not represent decay.)

of rain from March 14-31). As evidence of this, a sample of rainfall taken on March 24 yielded a $\beta - \gamma$ activity concentration of $2.98 \times 10^{-6} \mu\text{c/cm}^3$.

The increase noted in the $\beta - \gamma$ activity of vegetation samples taken in October 1958 is attributed to the series of nuclear explosions set off at the Nevada Test Site during the period from September 19 to October 20. This series of detonations included a total of 19 shots, the energy equivalence of which varied from sub-kiloton to about 20 kilotons. The peak in the $\beta - \gamma$ activity in vegetation, as found in February 1959, can be attributed to a rather heavy rainfall in the Santa Susana area, amounting to nearly 2 in. in a six-day period.

Analysis of the water activity data is not so conclusive, due mainly to the relatively small number of samples taken.



TABLE IV-C-11
ENVIRONMENTAL WATER ACTIVITY

1958	Station 2		Station 6		Station 7		Station 11		Overall Averages
	α	β - γ	α	β - γ	α	β - γ	α	β - γ	
January	a	9.1×10^{-10}	a	3.9×10^{-8}	a	1.8×10^{-9}	a	1.4×10^{-9}	
February			a	7.0×10^{-10}				3.0×10^{-9}	
March									
April	$<3.6 \times 10^{-10}$	4.0×10^{-9}			$<3.6 \times 10^{-10}$	6.3×10^{-9}	$<3.6 \times 10^{-10}$	1.7×10^{-8}	
May	3.0×10^{-11}	5.1×10^{-9}			3.0×10^{-10}	8.4×10^{-9}	7.2×10^{-11}	3.8×10^{-9}	
June	3.8×10^{-10}	1.4×10^{-8}	1.0×10^{-10}	5.6×10^{-9}	a	1.8×10^{-9}	a	1.1×10^{-9}	
July	4.6×10^{-10}	4.0×10^{-7}	9.4×10^{-11}	2.5×10^{-9}	1.3×10^{-10}	a	a	1.4×10^{-9}	
August	3.9×10^{-10}	5.0×10^{-9}	2.2×10^{-10}	6.1×10^{-9}	6.2×10^{-10}	3.4×10^{-10}	4.7×10^{-10}	5.0×10^{-9}	
September	a	3.8×10^{-9}	6.9×10^{-11}	4.7×10^{-9}	7.2×10^{-11}	a	1.8×10^{-10}	3.1×10^{-9}	
October	3.0×10^{-10}	9.7×10^{-9}	2.0×10^{-10}	a	8.9×10^{-11}	4.5×10^{-9}	1.5×10^{-10}	a	
November	5.7×10^{-11}	3.0×10^{-9}	4.0×10^{-10}	5.6×10^{-9}	8.1×10^{-12}	2.2×10^{-9}	4.6×10^{-11}	1.6×10^{-8}	
December	3.5×10^{-11}	9.9×10^{-9}	6.3×10^{-10}	2.6×10^{-8}	4.3×10^{-11}	5.2×10^{-9}	2.2×10^{-10}	1.6×10^{-9}	
Average Jan.-Aug.	3.2×10^{-10}	7.15×10^{-8}	1.38×10^{-10}	1.078×10^{-8}	2.85×10^{-10}	3.728×10^{-9}	3.007×10^{-10}	4.671×10^{-9}	2.609×10^{-10} α
Year Average	2.49×10^{-10}	4.55×10^{-8}	2.447×10^{-10}	1.1275×10^{-8}	1.69×10^{-10}	3.8175×10^{-9}	2.14×10^{-10}	5.34×10^{-9}	2.267×10^{-10} β - γ
1959									2.192×10^{-10} α
January	7.96×10^{-11}	3.93×10^{-9}	8.64×10^{-12}	4.61×10^{-9}	8.10×10^{-13}	a	5.53×10^{-11}	1.23×10^{-9}	1.648×10^{-8} β - γ
February	9.72×10^{-12}	1.37×10^{-8}	1.02×10^{-10}	3.24×10^{-8}	a	1.80×10^{-9}	1.17×10^{-10}	2.13×10^{-9}	
March	1.39×10^{-10}	2.35×10^{-8}	a	4.21×10^{-9}	1.70×10^{-11}	1.12×10^{-10}	1.06×10^{-10}	1.68×10^{-9}	
April	a	1.57×10^{-9}	9.66×10^{-13}	7.85×10^{-10}	1.29×10^{-10}	a	a	a	
May	6.78×10^{-12}	9.27×10^{-9}	a	1.89×10^{-9}	a	a	a	a	
June	1.81×10^{-10}	1.18×10^{-8}	4.11×10^{-11}	2.98×10^{-9}	1.45×10^{-11}	1.44×10^{-9}	2.47×10^{-12}	3.21×10^{-9}	
July	6.47×10^{-11}	4.18×10^{-9}	a	6.63×10^{-9}	3.97×10^{-11}	a	1.12×10^{-11}	1.07×10^{-10}	
August	3.63×10^{-10}	1.42×10^{-8}	9.81×10^{-11}	5.35×10^{-9}	1.62×10^{-10}	2.14×10^{-10}	a	1.92×10^{-9}	
Average Jan.-Aug.	1.205×10^{-10}	1.027×10^{-8}	5.016×10^{-11}	7.35×10^{-9}	6.05×10^{-11}	8.915×10^{-10}	5.8394×10^{-11}	1.7128×10^{-9}	7.239×10^{-11} α
									5.0578×10^{-9} β - γ

a = None detected



The activity levels measured by the continuous air monitor (which is of the type that collects activity on a filter paper for a 24-hr period and then counts the β - γ activity collected for a 24-hr period) are briefly summarized in Table IV-C-12.

TABLE IV-C-12
ENVIRONMENTAL AIR ACTIVITY

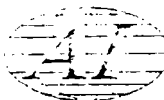
Month	Average β - γ Activity Level ($\mu\text{c}/\text{cm}^3$)
July 1958	$\sim 1 \times 10^{-12}$
September	$\sim 1 \times 10^{-12}$
October	$\sim 1 \times 10^{-12}$ *
November	
February 1959	$\sim 1 \times 10^{-12}$
March to May	$\sim 2 \times 10^{-12}$
June	$\sim 1 \times 10^{-12}$
July	$\sim 7 \times 10^{-13}$
August to September	$\sim 2.5 \times 10^{-13}$

*To October 19; at this time the activity level started to increase, reaching a value of $\sim 10^{-10}$ on October 29; by November 24 the level had decreased to $\sim 3 \times 10^{-12}$.

The marked increase in airborne activity concentration during the mid and late part of October 1958 further substantiates the data recorded by soil, vegetation, and water sampling; the increase being attributable to the nuclear tests being performed at the Nevada Test Site.

Fallout is normally identified by gross decay measurements.

Considering all the environmental data which is available, it appears that SRE operations have not been responsible for the release of any significant quantities of radioactivity to the environs, at least above that normally accompanying periods of rainfall or fallout following nuclear tests.



D. REACTOR PHYSICS

1. Potential Mechanisms of Reactivity Changes

In order to evaluate the causes of the reactivity changes which occurred during operation of the SRE, this section begins with a review of the major potential sources, mechanisms, and magnitudes of reactivity effects in the SRE.

a. Dropping Part of a Fuel Cluster

Two-group perturbation theory was used to calculate the expected reactivity changes resulting from the dropping of a part of a fuel cluster. The reactor parameters were taken from NAA-SR-1517 revised.¹⁰ Because of details of physical construction, it is possible for a fuel cluster to drop a maximum of only 10-3/4 in. At this location, the bottom of the fuel is more than a foot above the bottom of the reflector. It was assumed for this calculation, that no fuel slug melting occurred; that the fuel clusters somehow parted at an intermediate location; and that the bottom portion then dropped essentially intact until it rested at its lower limit of travel. In calculating the fluxes and adjoints, the insertion of the shim rods was taken into account by a windowshade technique. The reactivity change that would result from the central fuel element parting and the bottom portion falling 10-3/4 in. was then calculated by means of the perturbation theory formula. An estimate was made of the flux perturbation caused by the relocation of the fuel. Figure IV-D-1 shows a plot of the reactivity change as a function of the location of the break in the fuel element. This result is for the central fuel cluster, and it is seen that the reactivity change is always negative. However, if a break occurs in the upper half of a fuel element that is very close to a shim rod, it is possible for a positive reactivity to be introduced. This is shown by the dotted curve in Figure IV-D-1. In this case, the fuel drops away from the shadowing effect of the shim rod. An estimate was made of the shadowing effect of a shim rod, and the calculations were adjusted for this effect.

The central-to-average value of the statistical weight in the core is about 1.7. Ten of the elements removed from the core are severely damaged. Their distribution in the core is about average so a radial statistical weight of about 0.6 is appropriate. If the bottom 3 ft of ten clusters had fallen 10-3/4 in., the expected loss in reactivity would be about 0.5%.

Dropping part of a fuel cluster could introduce a positive reactivity step. Suppose that the bottom half of a cluster falls (thereby introducing a negative reactivity change) and that the fuel slugs in the upper half of the cluster

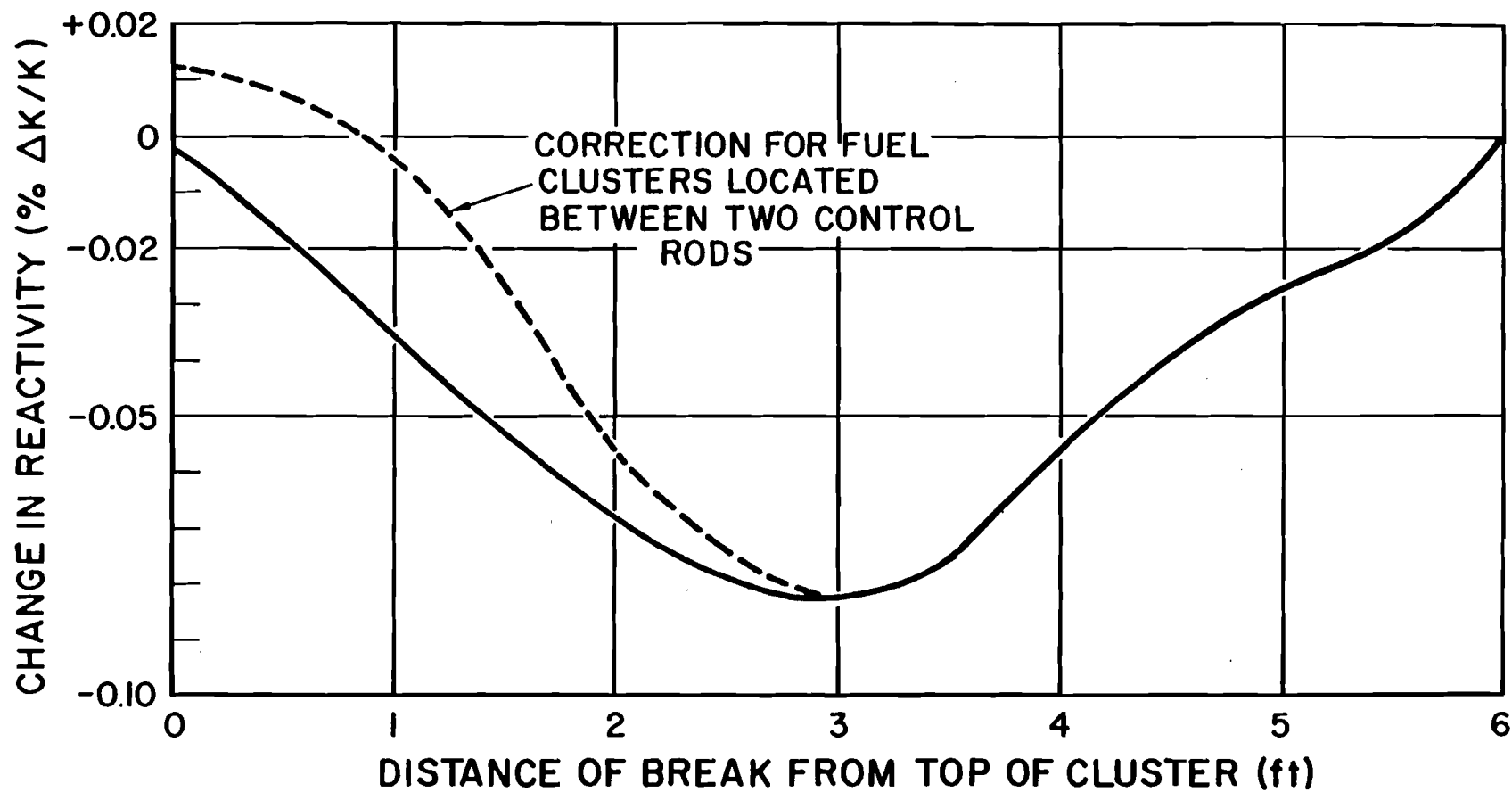


Figure IV-D-1. Reactivity Changes by Partition of Fuel Cluster



remain in their original location. Then suppose that at a later time some of the slugs in the upper portion of the cluster rain down onto the bottom part. From Figure IV-D-1, it is seen that by this means fuel slugs can move from a region of low importance into a region of higher importance, thereby introducing a positive reactivity step. The maximum reactivity step that can be introduced in this manner, by one fuel cluster, is about 0.08%.

b. Doppler Coefficient

The Doppler coefficient has been measured by pile oscillator techniques. This is reported in NAA-SR-3763.¹¹ The value obtained was $-1.1 \times 10^{-5}/^{\circ}\text{F}$. The reactivity change resulting from a change of 400°F in one fuel cluster would be about -0.10% for an average fuel cluster and about -0.17% for the central fuel cluster. Under normal reactor operating conditions, it was found by the pile oscillator method that the metal coefficient has a time constant of about 10 sec.

c. Graphite Coefficient

The graphite coefficient given in NAA-SR-3763¹¹ is $1.7 \times 10^{-5}/^{\circ}\text{F}$ at 600°F moderator temperature. Calculations indicate that this decreases to about $0.56 \times 10^{-5}/^{\circ}\text{F}$ at 800°F . This calculated decrease is due to the change in the cell flux shape as temperature of the graphite increases and to the increase in the thickness of the sodium layer between moderator cans as the temperature of the stainless steel grid plate increases. Pile oscillator experiments show that for normal reactor operating conditions the graphite coefficient has a time constant of about 10 min.

d. Void Coefficient

The void coefficient was calculated by taking into account both the effects of neutron streaming and thermal neutron absorption. Void corrections were calculated for the thermal utilization, the thermal diffusion length at the total migration area. For a void which completely surrounds one of the hexagonal moderator cans (in space normally occupied by moderator coolant) it was found that the effect for a typical moderator can is 0.11% reactivity. The size of the neutron streaming correction was about 1/6 of that due to the neutron absorption. A void which occurs in a process tube gives a smaller effect because of the reduced neutron flux in this area. The result for a complete void in a typical process tube in the core is 0.012% in reactivity. The magnitude



of the streaming correction is about equal but opposite in sign to that for the neutron absorption effect. The change in the effective resonance integral for the uranium was included in calculating the total effect.

e. Gas Bubbles in the Sodium

The effect of gas bubbles uniformly distributed through the sodium was calculated. No neutron streaming correction is applied in this case. It was found that if the density of the sodium is reduced by 5% by the presence of gas bubbles, an increase in reactivity of 0.3% would result. This decrease in density could be caused by one gallon of tetralin present as vapor in the primary sodium. Most of this effect is in the moderator coolant between cans. The presence of hydrogen atoms in the gas bubble would produce a negligible effect on the reactivity because the density of the hydrogen atoms is so small. It was estimated that a concentration of hydrogen atoms of 0.3×10^{20} per cubic centimeter in the above bubbles would contribute about 0.002% to the reactivity.

f. Hydrogenous Plug in the Reactor Core

The density of hydrogen atoms in a hydrogenous plug was assumed to be 0.032×10^{24} atoms per cubic centimeter. The reactivity effect of such a material in the reactor core was calculated by using the MUFT-4 IBM program. It was found that if such material completely surrounds one typical moderator can in the core, an increase in reactivity of about 0.09% would result.

The increase for the complete plugging of a process tube was found to be about 0.008% in reactivity. On the other hand, if the plugging only occurs in between the seven rods of the fuel cluster, the increase in the effective resonance integral of the uranium results in a negative effect. In this case, it was found that a reactivity change of about -0.022% would be introduced by one fuel cluster.

g. Sodium in a Moderator Can

If sodium were to flood a moderator can in the core region, a substantial loss in reactivity could result. An estimate of the magnitude of this effect was made by assuming that 30% of the graphite volume is void and that 2/3 of this volume is flooded with sodium. The reactivity loss which would result



from the flooding from the central moderator can was calculated by perturbation theory and found to be -0.7%. If a moderator can located on the edge of the reactor core were to be flooded, the result would be about 1/2 this large.

h. Nitrogen Gas in Moderator Cans

This would result in a reactivity loss since the absorption cross section of nitrogen is substantially greater than that of helium. It was found that the introduction of 1/5 of an atmosphere of nitrogen at standard conditions into graphite which had about 30% void of space would result in a reactivity loss of about 0.04%, if all the graphite in the reactor were involved.

2. Measured and Calculated Effects

a. Xenon

The reactivity absorbed by xenon as a function of time after a reactor shutdown has been measured and calculated, and these results are displayed in Figure IV-D-2. The calculated reactivity transient was obtained from the product of the thermal utilization and the ratio of xenon to fuel macroscopic absorption cross sections. The thermal utilization as a function of power was obtained from NAA-SR-1517 revised, and the average cross sections as functions of graphite temperature were calculated assuming a Maxwellian energy spectrum. Shim rod calibrations measured in the isothermal reactor and critical shim rod configurations obtained during and after the shutdown were used to evaluate the xenon transient. It was corrected for the reactivity effect caused by the changing temperature distribution in the core using the power and core isothermal temperature coefficients. The latter was measured; the former was estimated from the latter and the fuel temperature coefficient. The 0.1% $\Delta k/k$ discrepancy, shown in Figure IV-D-2, between the measured and calculated transients during shutdown may be due to the unknown temperature effect on the shim rod calibration. The same calculational technique was used to obtain the reactivity absorbed by xenon as a function of time after various step changes in power. The results are shown in Figure IV-D-3. At equilibrium, the reactivity absorbed by xenon is 1.83% at 20 Mw and about 0.3% at 2 Mw.

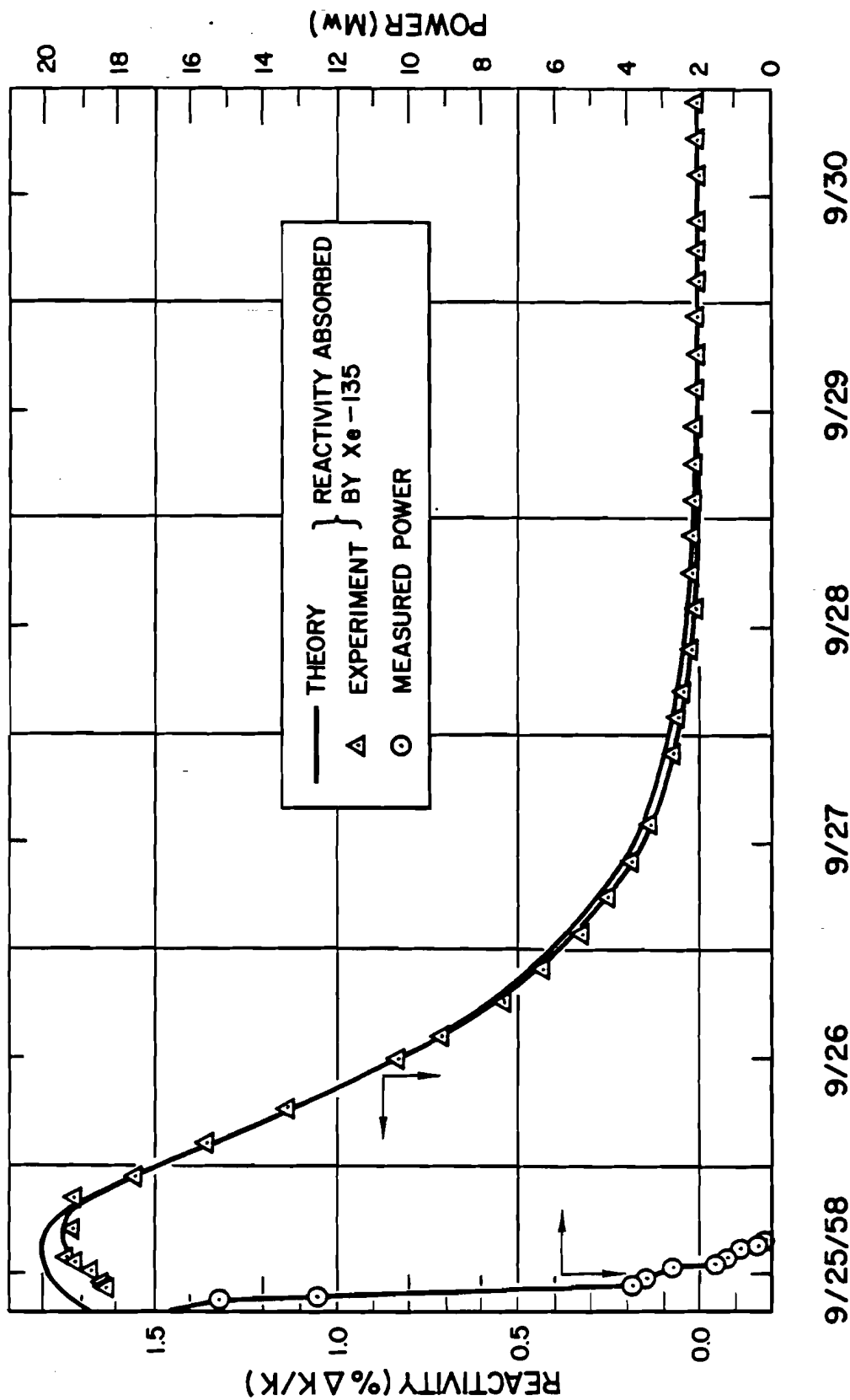


Figure IV-D-2. Reactivity Absorbed by Xenon after Shutdown



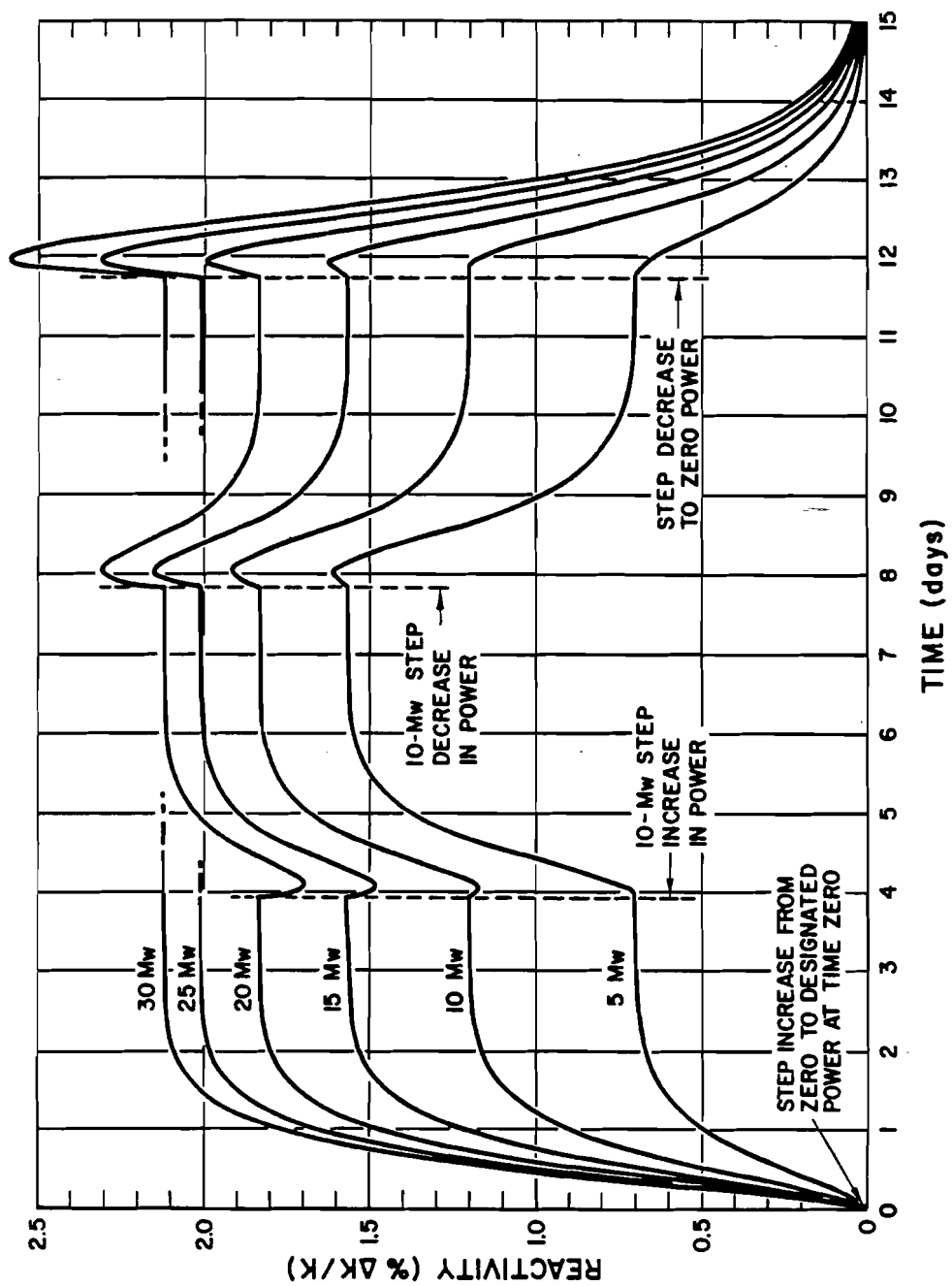


Figure IV-D-3. Reactivity Absorbed by Xenon after Step Changes in Power



b. Temperature

In order to estimate an upper limit of the magnitude of reactivity changes resulting from changing fuel temperatures, the extrapolated temperature profiles shown in Figure IV-A-17 were utilized.

c. Cover Gas Pressure

During run 14, the reactor operators noticed a change in reactivity when the pressure of the cover gas was changed. An increase in pressure appeared to cause a decrease in reactivity. On July 19 and 20 during run 14, some tests were made in an attempt to gather data which would permit interpretation of this effect. Although the results that were obtained are not entirely consistent, they indicate that a pressure coefficient of about -0.02 to -0.03% per psi existed. Other observations made on a different day indicate an effect of this same order of magnitude but differing by a factor of two. The available data do not permit a more precise estimate of this effect.

3. Run 13

Figure IV-D-4 illustrates reactor operating conditions during run 13. Curves are given which show the reactor power level, excess reactivity, reactor inlet sodium temperature, a fuel slug temperature, a fuel channel exit temperature, moderator temperature, and the log mean temperature difference across the heat exchanger. It can be seen that reactor conditions start to change rather significantly starting at about 0900 on May 30. Reactor operating conditions before this time were quite normal. It can also be seen that reactor operating conditions became somewhat worse toward the end of this run.

Although the curves in Figure IV-D-4 do not present all of the available data, they indicate the most significant features of this run. Reactor operating conditions were entirely normal up to about 0900 on May 30, as they were during run 12. The scram shown at 1124 on May 29 was due to improper adjustment of the main primary sodium flow scram point. Recovery from this scram was immediate and the reactor returned to normal operating conditions.

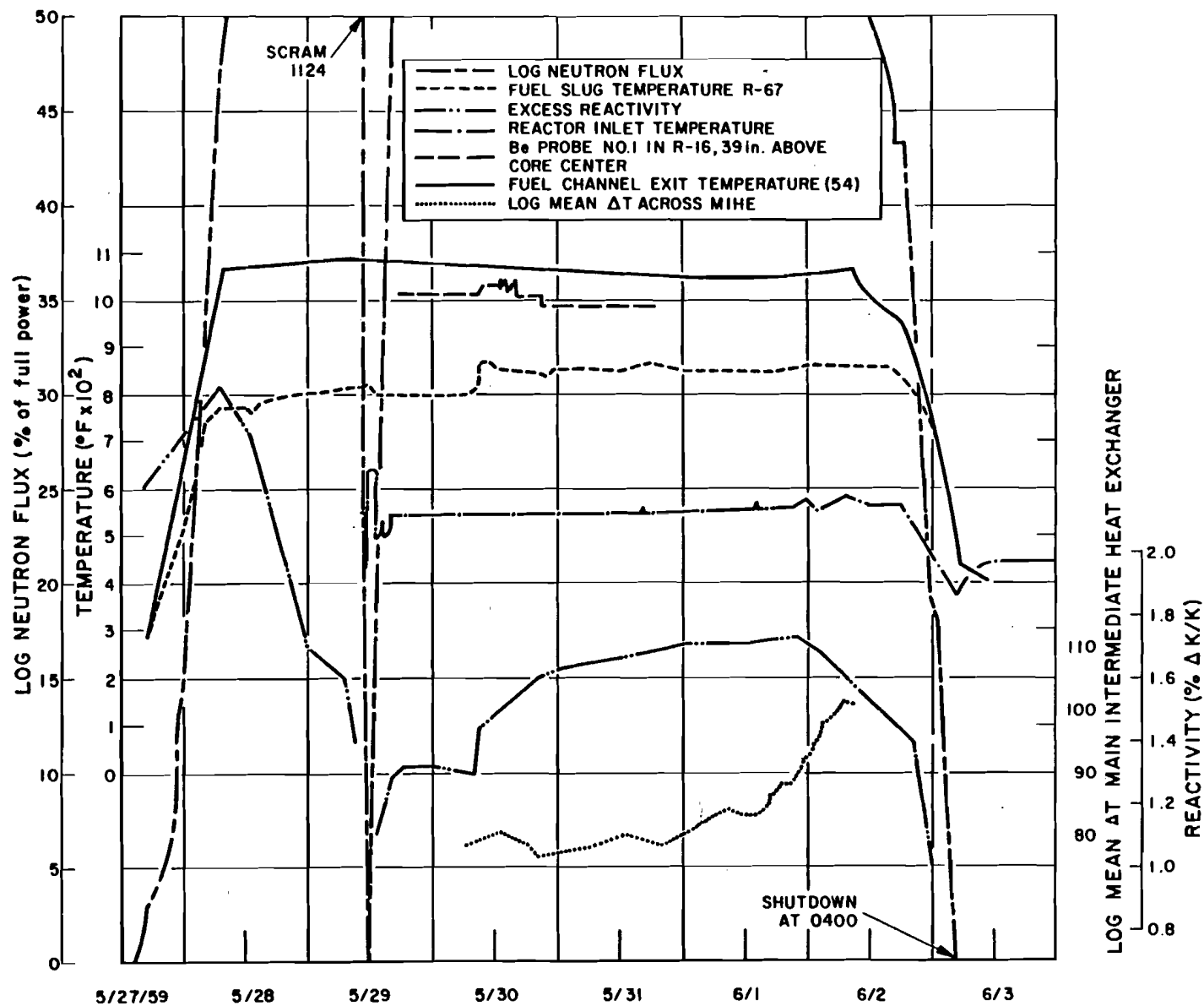


Figure IV-D-4. Reactor Operating Conditions During Run 13



The changes that started to occur at about 0900 on May 30, indicate that abnormal heat transfer and reactivity conditions started to develop at that time. It is suggested that tetralin started to enter the primary sodium then. The 0.3% increase in reactivity that occurred during a period of six hours is difficult to explain (see Table IV-D-1). The observed temperature changes could not account for it. One possible cause is the gradual accumulation of gas trapped between moderator cans. If the sodium surrounding about three moderator cans was displaced, a reactivity increase of about 0.33% would result. The

TABLE IV-D-1

MECHANISMS OF REACTIVITY CHANGES

Mechanism	$\Delta \rho$ (%)	Action Rate
Doppler Effect		
800°F temperature rise in 1 fuel cluster	-0.03 to -0.05	fast
Drop half of 1 fuel cluster	-0.03 to -0.08	fast
Drop 1 entire fuel cluster	-0.005 to 0.014	fast
Accumulation of hydrogenous substance		
Among rods in 1 fuel cluster	0 to -0.02	probably slow
Complete plugging of 1 fuel channel	0.007 to 0.014	
Around 1 moderator can	0 to 0.15	
Sodium Flooding 1 moderator can	0 to -0.7	slow
Moderator temperature coefficient		
180°F temperature rise in		
Entire graphite stock	0.30	slow
One moderator can	0 to 0.01	slow
Small gas bubbles in circulating sodium (5% of the sodium volume)	0.3	slow
Volume increase in a gas bubble trapped between moderator cans. (bubble size equal to Na volume around 1 can)	0 to 0.2	probably slow
Vaporizing sodium in a plugged fuel channel (void creation only)	0.01 to 0.02	fast
Rain of fuel slugs from top part of a parted fuel element onto the bottom part	-0.08 to 0.1	fast
Hydrogen atoms in core	0 to 0.2	slow

drop in reactivity observed at the end of the run when temperatures were reduced supports this type of mechanism, although at the end of run 12 a similar reactivity drop of nearly the same size occurred. This indicates that the reactivity drop at the end of the run cannot be used to support the gas entrapment hypothesis.

Another possible cause to consider is gas bubbles in the primary sodium. A decrease in sodium density of about 5% would be required to cause this much increase in reactivity. Since the effect of these bubbles on the primary sodium pump would probably have been noticed, this cause is not seriously considered. Moreover, it is difficult to see how the gas bubbles would remain in the circulating sodium for such a long time, since the change lasted until the end of the run.

A third possible cause to consider is the gradual accumulation of hydrogen atoms in the core. This could be due to the formation of hydrogenous solids or by formation of zirconium hydride. It was calculated that a typical reactivity increase that would result from a hydrogenous material occupying the entire sodium volume surrounding one moderator can would be about 0.05%. This volume is $1/6 \text{ ft}^3$, so about 0.8 gallons of liquid tetralin would be required to fill this volume. Putting it another way, the hydrogen contained in 0.8 gallons of tetralin deposited in this region of the core would cause a reactivity increase of about 0.05% if uniformly distributed in the 43 cells containing fuel.

If the hydrogen were spread over the entire graphite stack, the reactivity increase would be about 1/3 of this amount or about 0.015%. It therefore appears that it would require the hydrogen contained in from 10 to 20 gallons of tetralin to cause a reactivity increase of the size observed. The gradual increase in reactivity of about 0.1% indicated from May 31 through June 1 could be accounted for by this manner if sufficient hydrogen accumulated in the zirconium during this time.

In summary, the cause of the reactivity increase of 0.3% on May 30 is not known. It probably is related to the tetralin leak.



4. Run 14

Figures IV-D-5a and b illustrates reactor operating conditions during run 14. Curves are given which show the reactor power, reactor inlet temperature, excess reactivity, a fuel slug temperature, graphite temperature (Be probe), and a fuel-channel exit temperature. The time that each reactor scram occurred is also indicated. The reactivity curve has been drawn in a discontinuous manner so as to indicate the time intervals during which the reactor was not operating. Although the curves in these figures do not present all the available data, they indicate the most significant features of this run.

Several features of this chart are noteworthy:

- a) The gradual loss in reactivity of about 1.2% that occurred during the first four days of this run.
- b) The greatest permanent loss in reactivity occurred during the first two days of the run.
- c) There was no permanent reactivity change noted after July 16.
- d) The strong correlation between reactivity and temperatures. (This is particularly striking during the last half of the run although the effect can also be clearly seen at various times during the first half of the run.)
- e) Reactivity fluctuations that occur during the last half of the run are substantial.

There is evidence of fuel channel plugging at the very start of the run. This is shown by the spread in fuel channel exit temperatures and by the large 30°F fluctuations in the moderator delta T. The reactor power was increased just before the radiation level in the high bay area increased sharply on July 12. The significance of this correlation seems to be that some damage to fuel clusters occurred at this time. However, the drop in excess reactivity noted by 1500 on July 13 could have been caused by the falling of parted fuel clusters. Reactivity data just prior to the scram at 2057 is not available, so it is not possible to draw a more definite conclusion.

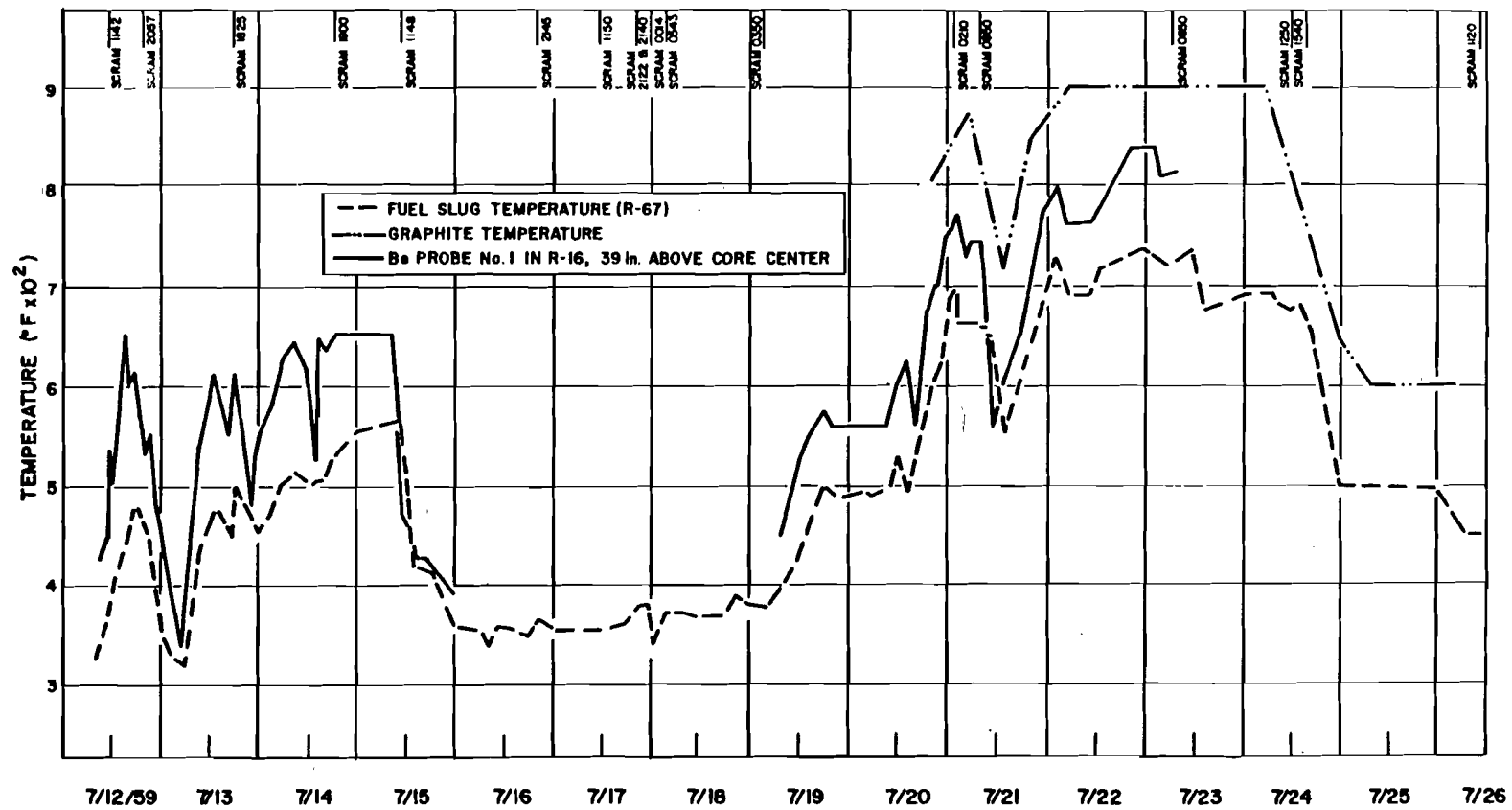


Figure IV-D-5a. Reactor Operating Conditions During Run 14

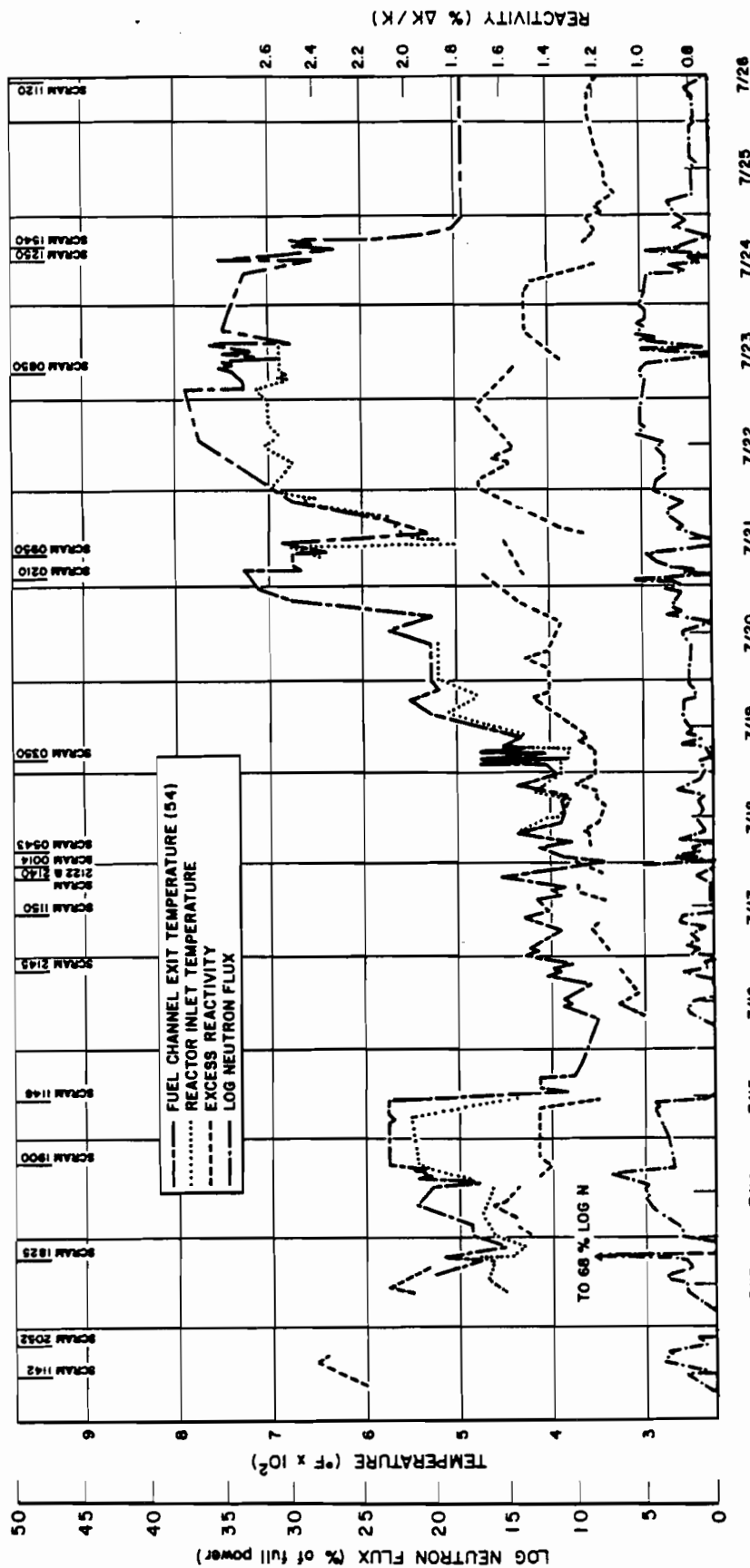


Figure IV-D-5b. Reactor Operating Conditions During Run 14



The gradual loss in reactivity that occurred during the first four days of run 14 was about 1.2% (see Table IV-D-1). Calculations show that the maximum reactivity loss to be expected by dropping the bottom halves of 10 damaged fuel clusters is about 0.5%. Although this could account for about half of the observed effect (if the fuel actually dropped and produced its maximum effect), another explanation must be sought to account for the balance of the effect. Temperature changes are ruled out because the effect persists at the end of the run when the reactor is shut down. Aside from the dropping of parted fuel clusters, the only cause that has been proposed which can account for a large slow loss in reactivity is the gradual flooding of several moderator cans with sodium. The maximum effect expected from flooding one can is a reactivity loss of about 0.7%. The flooding or partial flooding of a few cans could easily account for the entire reactivity loss of 1.2%. It seems impossible to escape the conclusion that at least one moderator can is flooded. The fact that the largest loss occurred on July 13 suggests that part of this loss is due to dropping of damaged fuel clusters. It seems likely that some of the fuel damage occurred during the excursion on July 13.

The correlation between reactivity and temperature has been pointed out. The moderator temperature coefficient is about $1.7 \times 10^{-5}/^{\circ}\text{F}$ while the Doppler coefficient is about $-1.1 \times 10^{-5}/^{\circ}\text{F}$. Thus, a uniform 180°F temperature increase in the core causes a reactivity increase of about 0.1%. A change of 500°F over one third of the core could cause an even greater effect if the hot region is near the center. On the other hand, fuel and moderator temperatures may not have changed proportionately or uniformly because of plugging. If one fuel channel should unplug, causing the temperature of the fuel in that channel to drop by 500°F , the resulting gain in reactivity could be as much as 0.05%.

When the evidence on temperature fluctuation is considered, it is not difficult to account for reactivity fluctuations of the magnitude shown during the last 11 days of run 14. The fact that during this period a temperature dependent trend in reactivity is observed that is somewhat greater than might be expected from temperature changes alone, suggests the possibility that gas was trapped between moderator cans. The observed pressure dependence of reactivity also supports this. Furthermore, since the net increase in reactivity from July 16



to July 26 is insignificant (0.1%), if further damage to fuel elements was occurring during this time due to high temperatures, it was not causing reactivity changes.

5. Power Excursion

a. Reactivity

The power excursion that occurred at 1825 on July 13 was analyzed by means of the AIREK IBM code. In making this analysis, the plan was to first determine what the power trace would have been had the reactor been performing normally taking reactor temperature coefficients and shim rod motions into account. Figure IV-D-6 shows a plot of this result along with the actual power trace as taken from the flux-temperature controller recording instrument. The analysis is started with $T = 0$ at the time of 1728 hours when the reactor was in a fairly steady operating condition. Since the shim rods were being operated in a ganged condition, it was possible to determine quite accurately from the chart of the shim rod 3 motion exactly what changes in control rod positions had been made from this time until the reactor was scrammed. Rod motion was converted into reactivity by means of the shim rod calibration curves which were measured for the reactor. The primary sodium flow was held constant during this entire time interval. The moderator and fuel temperature coefficients which were given earlier (see Table IV-D-1) were used in these calculations. The moderator temperature was obtained from the beryllium probe chart for channel 16. It was assumed that fuel temperature was proportional to the neutron flux. The fuel and moderator temperatures obtained by this manner are, of course, average values. Peak values could be considerably higher if plugging was occurring in process tubes or between moderator cans.

By referring to Figure IV-D-6, it is seen that the main features of the power increase up until 2300 sec are nearly accounted for by normal reactor temperature coefficients and shim rod motions. The total increase in calculated power level at this peak is only 12% less than that actually recorded. In order to estimate the magnitude of reactivity changes required to fit the actual power trace recorded, small step and ramp reactivity insertions were hypothesized and the effects of these insertions calculated using the AIREK IBM Code.



The discrepancy at 2300 sec can be removed by introducing small ramp reactivity changes at the times shown in Figure IV-D-7. An abnormal temperature rise of 20 to 60°F in one moderator can or fuel element could cause reactivity changes of this magnitude. This also shows that the minor fluctuations in the power trace can also be explained by small temperature fluctuations.

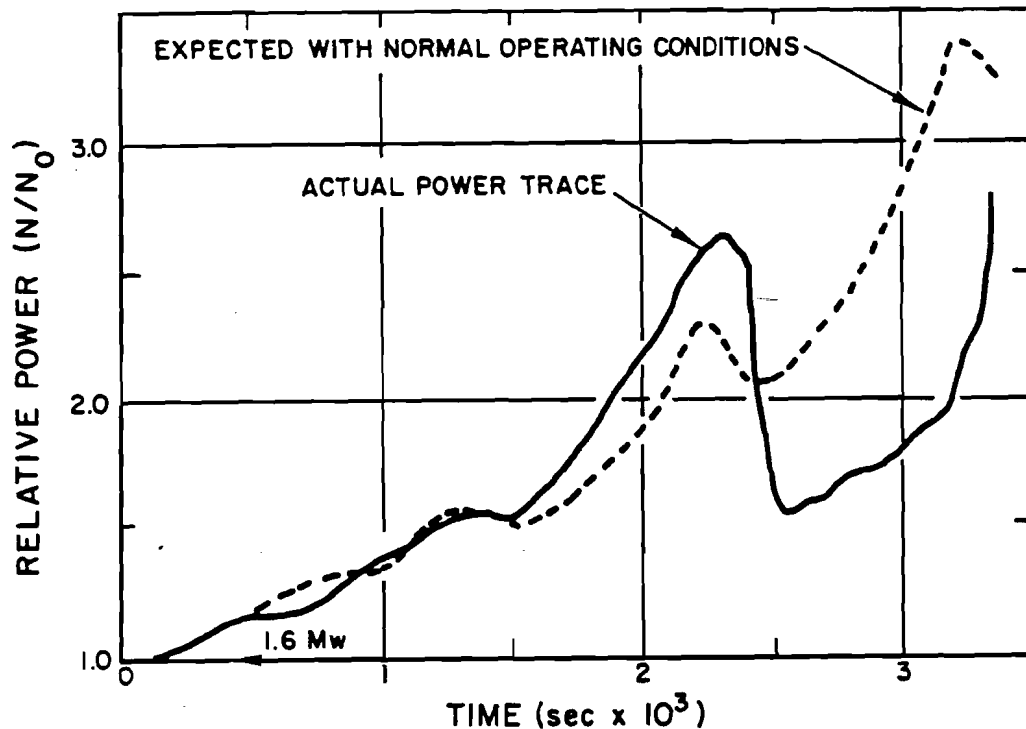


Figure IV-D-6. Machine Calculation I of the Power Excursion

The negative step reactivity of 0.06% introduced at 2400 sec causes the calculated curve to drop with a 75-sec period at its maximum rate of decrease. It can be seen that there is some overshoot. A smaller step of -0.031% produces very nearly the correct reduction in power level but the fastest period reached is only 185 sec. The period recorder shows a minimum period of about 45 sec. This shows that the negative reactivity introduced at this time was about -0.03 to -0.06% rather than -0.3% as had been previously estimated. A fuel temperature increase of 800°F in one fuel channel could cause this reduction in reactivity by means of the Doppler effect. This temperature



increase could be brought about by loss of sodium flow in a channel previously clear. The consequence of this in terms of reactivity effects of boiling sodium and melting fuel are being investigated. A second manner in which a negative reactivity step of the above size could be introduced is to have a fuel cluster part near its center and the bottom portion drop 10-3/4 in. in the reflector.

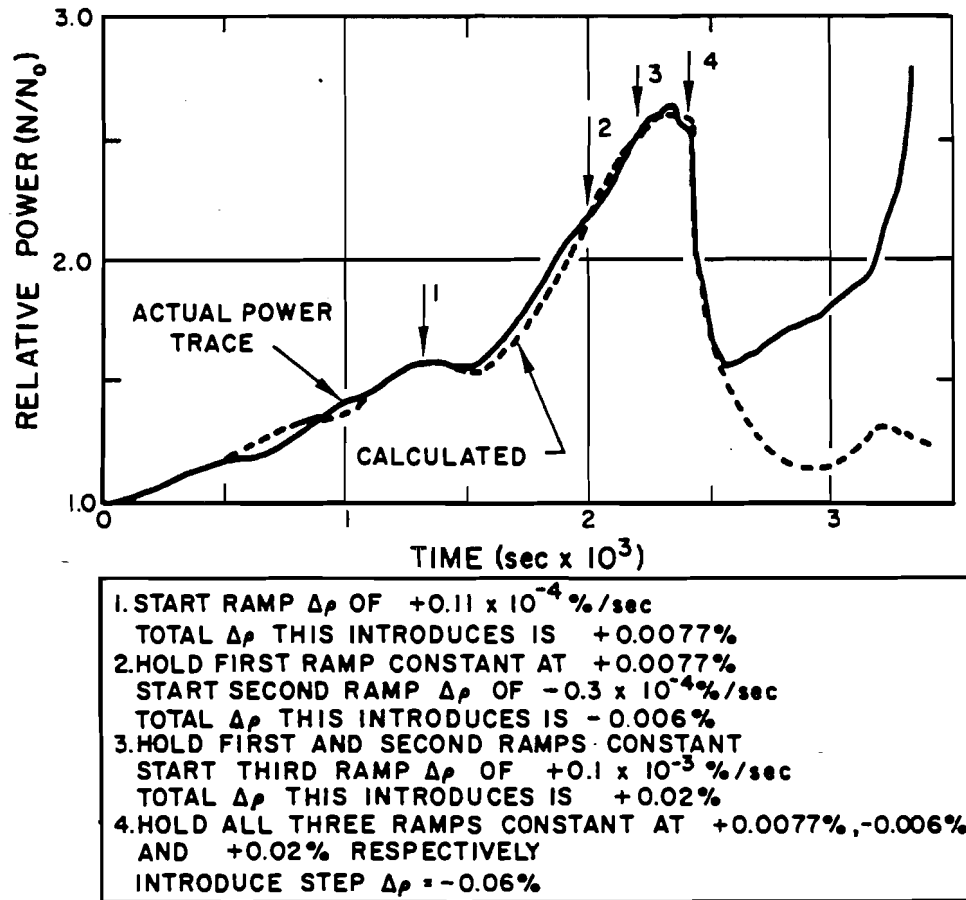


Figure IV-D-7. Machine Calculation II of the Power Excursion

Following the power drop which reaches a bottom at about 2500 sec, there is a slow rise until about 3150 sec. It is believed that shim rod motion and temperature coefficients are sufficient to account for the reactor's behavior during this period. The power trace during this interval can be approximated by means of small step reactivities as shown in Figure IV-D-8. Temperature fluctuations could cause reactivity changes of this magnitude. At 3150 sec, the

reactor power starts to rise at an increasing rate. This increase can be explained by the introduction of a positive ramp reactivity of about 0.002%/sec for the next 150 sec. At 3300 sec, the further increase in the rate of climb of reactor power is noted. The introduction of an additional positive ramp or a positive step in reactivity is indicated. Since the power trace is not linear on a logarithmic scale, the introduction of a ramp appears to be favored. Calculations covering the time interval following 3150 sec are not complete.

Although potential mechanisms for getting reactivity changes of the correct magnitude have been postulated, the mechanism by which the positive reactivities were introduced is not known.

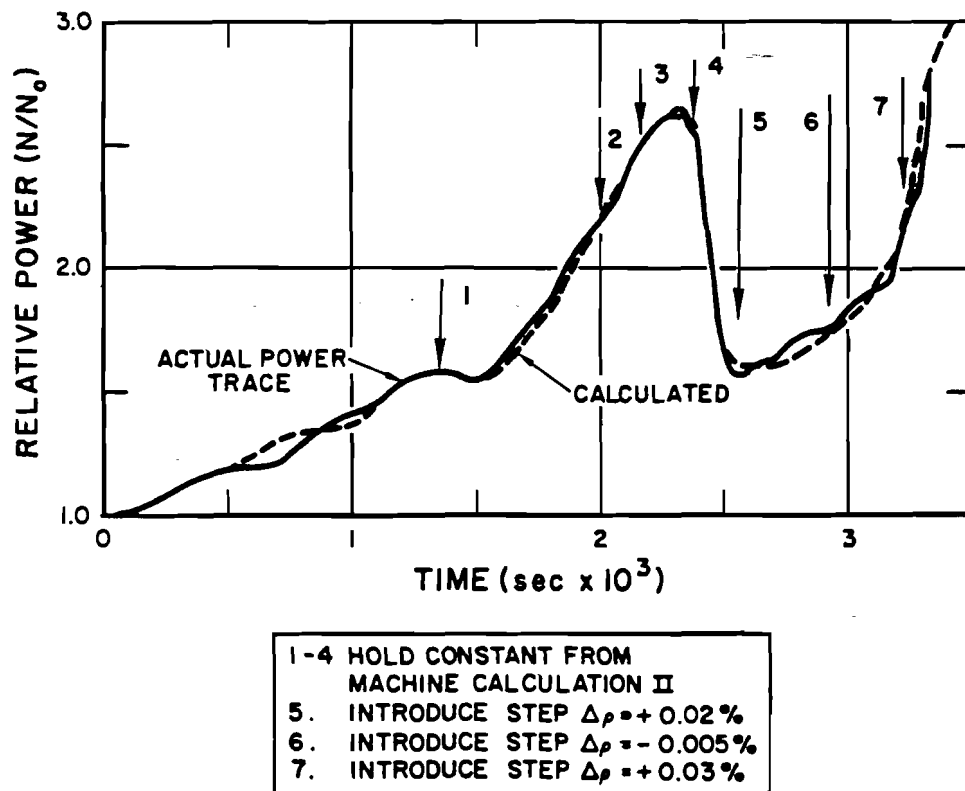


Figure IV-D-8. Machine Calculation III of the Power Excursion



b. Power Release

Due to the many uncertainties in data and in the heat transfer characteristics of the reactor during the period of the positive excursion, it is not possible to calculate accurately the values for fuel and moderator temperatures which could have been reached. However, it is possible to make an estimate of the upper limit of the fuel temperature which could have been reached by use of the log N chart which shows that the power increases from about 4 Mw to about 24 Mw during the last minute of the excursion. If it is assumed that the power increase is exponential, although it is not, the reactor period would be 33.5 sec. The total energy release during this time interval is then found to be 670 Mw-sec of energy. This is an overestimate of the energy released during the last minute before the scram.

The maximum temperature rise in the fuel would occur if there were no heat transfer from the affected section of fuel during and after this excursion. Since this is not realistic, assume that 200 Mw-sec of energy goes into raising the fuel temperature. Assuming the heat capacity of uranium to be 0.035 Btu/lb-°F, the average temperature rise in a fuel cluster so effected is about 850°F. This temperature increase could vary by as much as 50% depending upon the location of the fuel cluster in the reactor core. Moreover, the peak temperature rise, which would occur near the center of the fuel cluster, would be substantially higher than average.

The fuel slug temperatures were indicating about 550°F just before the scram. Based on the above assumptions, temperatures of 1400°F would be reached in the fuel for a short time. If the low heat removal from the fuel extended over a longer period of time, fuel temperatures of 1500°F to 2000°F could result.

If 10 fuel clusters were to suddenly experience a temperature rise of about 900°F, the negative reactivity introduced by this would be about 0.25%. This reactivity loss would not be introduced all at once but gradually as the power rises. The results of the kinetics calculations given in the preceding section take this effect into account.



V. TENTATIVE CONCLUSIONS

The currently active investigation into the causes and results of the severe damage to the first core loading of the SRE has resulted in some conclusions, a few of which are reasonably firm but many quite tentative. As of this writing the fuel has been removed from the core with the exception of the two elements which are stuck in their process channels and the lower sections of the 10 parted elements. The recorded data from the reactor instruments have been examined and evaluated in considerable detail from the beginning of run 8 through run 14. Metallurgical examination has been made of a few samples of the fuel and other components of the reactor where possible. Some chemical analysis has been made of the coolant and its contaminants. Radiochemical analyses have been made of the coolant and gaseous activity. Reactivity effects have been investigated. Some experimental programs have been initiated to examine mechanisms of damage and potential deleterious effects on the reactor system. The conclusions reached are based on these data and on the preliminary examinations completed at this time.

A. CAUSE OF FUEL ELEMENT DAMAGE

The fuel cladding failed as a result of the formation of low-melting iron-uranium alloy. Such alloy has been found in examination of both cladding and spacer wire specimens taken from the region of cladding failure. The diffusion of uranium into the stainless steel to form the alloy was greatly accelerated by local high temperatures which resulted from partial blockage or fouling of the heat transfer surfaces of the coolant passages. Fouling or blockage can be attributed at least in part to the tetralin which leaked into the primary system from the cooling element on the primary pump. It is possible that the presence of low concentrations of sodium oxide and sodium hydride in the coolant may have contributed to the fouling or blockage. Since the solubility of oxide in the sodium increases with temperature, oxide in solution probably would not be precipitated during passage of the coolant up the fuel channel. The actual mechanism of channel blockage is not understood but can, with reasonable certainty, be attributed to the decomposition products of tetralin.



B. TIME OF ELEMENT FAILURE

It seems quite likely that the first cladding failure occurred during the afternoon of the first day of run 14. This conclusion is drawn from the observation that the radioactivity in the high bay area (over the reactor loading face) increased markedly at this time and was almost certainly due to leakage of reactor cover gas into the area. It was believed at the time that a seal had failed on the sodium level probe. It now seems more likely that the leak may have existed for some time and was suddenly noticeable because of the large increase in the radioactivity of the gas.

It is possible, although far from certain, that no fuel elements parted after July 16. This is suggested by the decreasing levels of cover gas activity as well as the lack of any permanent loss in reactivity after this time, as would be expected if the lower section of a fuel element were to drop toward the bottom of the core. It is possible, however, that cladding failure could occur without subsequent dropping of the lower section of the element if the lower section were wedged in the coolant channel. In the area of cladding failure, the uranium temperature was probably well above the design point of 1200°F. The swelling rate of unalloyed uranium is greatly accelerated under these conditions and it is quite possible that the rods or their spacer wires were wedged against the process tube.

C. EFFECT OF THE HIGH TEMPERATURE RUNS

The high temperature runs (runs 12 and 13) bear no known relation to the cladding failures of run 14. This conclusion is supported by the fuel element examinations, including micrometer measurements in the SRE hot cell, between runs. No increase in swelling rate was detected in these measurements. Since the sodium was saturated with carbon during the high temperature runs (from the tetralin leak which occurred prior to run 8), it is possible that the higher temperature increased the rate of carburization of the 0.010-in. -thick fuel cladding. However, the failures have been quite definitely attributed to melting of iron-uranium alloy. Carburization which may have been increased by the high temperature runs apparently was not involved.

D. REACTIVITY CHANGES

General explanations have been postulated for the reactivity changes incurred during run 14, but no definite conclusions can yet be drawn. The slow but sustained loss of reactivity over the first four days of the run might be attributed to failure of a few zirconium process tubes and subsequent leakage of sodium into the graphite moderator, to dropping of the lower section of 10 or possibly 12 fuel elements to a region of lower worth, or to a combination of these. The permanent loss of reactivity, about 1.2%, would occur if 3 or 4 moderator logs were completely saturated.

The loss in reactivity from parting and dropping of the lower section of a single fuel element would be less than 0.1%. It is therefore unlikely that the loss of 1.2% can be attributed solely to dropping of fuel in the fuel channels.

A satisfactory explanation of the power excursion on July 13, the only observed excursion in the reactor's history, is not yet available. The small negative excursion might be explained by the gradual parting and dropping of the lower section of a single element or by the Doppler effect. No rational explanation of the cause of the positive excursion is as yet available. It is hoped that examination of the moderator cans and the location of the lower sections of broken elements will provide this information.

E. CONDITION OF REACTOR AND PRIMARY SYSTEM

Out-of-pile tests on carburization and nitriding of stainless steel, completed since the termination of run 14, would indicate that the piping and components of the primary coolant system are undamaged. The sodium has been found to contain a considerable amount of carbon. The only component of concern is the intermediate heat exchanger which has tubes of 0.058-in. wall thickness and may be partially carburized. The fission-product contamination of the coolant has been measured and does not appear to be a major concern even in the remote event of a major sodium fire. The undamaged fuel elements from the reactor are suspect because of unknown local temperature history. The moderator cans are also suspect because of possible rupture.



F. CONTAINMENT OF RADIOACTIVITY

In spite of major cladding failures to at least 10 of the 43 SRE fuel elements and the subsequent release of fission products to the coolant and cover gas, no hazard was presented to the reactor environs. Some valuable information was obtained on the retention of fission products by the coolant; in particular, it appears that all of the iodine released from the fuel was retained by the coolant. None was detected in cover gas analyses. Data on the radioactivity of the oxide cold trap also indicate that this system may remove some fission products from sodium.

REFERENCES

1. C. Starr and R. Dickinson, Sodium Graphite Reactors (Reading, Mass. Addison-Wesley, 1959)
2. Atomics International Staff, "Hazards Summary for Thorium-Uranium Fuel in the Sodium Reactor Experiment," NAA-SR-3175 (Revised)(July 1, 1959).
3. R. Heusen and E. Kemper, "Effects of Radiation on Tensile Properties of Uranium," HW-41690 (February 9, 1955)
4. R. W. Nichols, "Uranium and Its Alloys," Nuclear Eng. 2 (1957), p 355-364
5. R. S. Neymark, "Rate of Alloying of Metal Fuels with Stainless Steel above 1500°F," Nuclear Congress 89 (April 1959)
6. R. L. McKisson and K. E. Horton, "The Behavior of Tetralin in Liquid Sodium," NAA-SR-1771 (February 1, 1957)
7. J. H. Perry (ed.), Chemical Engineers' Handbook (2nd ed., New York, McGraw-Hill, 1941), p 1167
8. J. G. Gratton, "Solubility of Carbon in Sodium at Elevated Temperatures," KAPL-1807 (June 30, 1957)
9. R. Lyon (ed.), Liquid Metals Handbook, "Na - NaK Supplement," (Government Printing Office, Washington, D.C., 1952) p 7
10. F. L. Fillmore, "Two-Group Calculation of the Critical Core Size of the SRE Reactor," NAA-SR-1517 (July 1, 1956)
11. C. Griffin and J. Lundholm, "Measurement of the SRE Power Coefficients and Reactor Parameters Utilizing the Oscillation Techniques," NAA-SR-3763 (to be published)